THESIS

EXPLORATION OF PASSIVE DESATURATION OF IN PLACE TAILINGS USING WICKING GEOSYNTHETICS

Submitted by

Kendall O. Monley

Department of Civil and Environmental Engineering

In partial fulfillment of the requirements

For the Degree of Master of Science

Colorado State University

Fort Collins, Colorado

Summer 2024

Master's Committee:

Advisor: Joseph Scalia IV

Christopher Bareither
Matthew Ross

ABSTRACT

EXPLORATION OF PASSIVE DESATURATION OF IN PLACE TAILINGS USING WICKING GEOSYNTHETICS

As global demand for metals and critical minerals increases, so too does the production of tailings. Tailings are what is left behind after extraction of valuable metals and minerals from ore, and consist of finely ground rock, water, unrecoverable metals, chemicals, and organic matter. These residuals are managed in engineered facilities that function to both dewater and store tailings, known as tailings storage facilities (TSF). A common assumption is that the water initially contained in TSFs will drain down to an unsaturated condition after deposition of new tailings ceases. However, a review of literature on geotechnical and hydrotechnical conditions of legacy TSFs (TSFs that have stopped receiving tailings) in arid environments illustrates that achievement of unsaturated conditions in internal fine-grained layers may not always occur. As the tailings are deposited, layers of finer and coarser particles are interbedded. This causes the formation of capillary barriers and may ultimately result in finer-grained layers held at near saturation after drain down. These fine-grained layers are more susceptible to liquefaction concerns and can require costly remedial actions to ensure geotechnical stability. Dewatering is the process of removing water from whole tailings and offers benefits including increasing geotechnical stability and recovering stored water. Tailings dewatering may occur prior to or after deposition into a TSF. In this study, I explore in-situ dewatering via use of capillary (wicking) geotextiles, and the effectiveness of the wicking geotextiles. Beaker and column experiments were created to emulate stratigraphy seen in legacy TSFs. Additionally, shrinkage

testing was conducted to compare the final densities and void ratios of samples with and without wicking geotextiles. Column testing reveals the wicking geotextiles accelerated dewatering by 2.8 times the rate of natural drying processes. At the conclusion of testing, the wicking geotextile experiments had reached similar densities and void ratios to control experiments. This novel approach to passively dewatering tailings warrants additional testing.

ACKNOWLEDGEMENTS

This research was made possible by generous support of The Tailings Center. I would like to thank Dr. Joseph Scalia IV and Dr. Chris Bareither for their constant guidance, support, and mentorship throughout this research and my graduate career. I would also like to thank Dr. Ross Matthew for his membership on my committee. Additionally, I would like to thank my partner, family, and friends who have always supported me. I have come to learn that life is not about the journey nor the destination, but rather the people we meet along the way.

TABLE OF CONTENTS

LIST OF FIGURES

LIST OF SYMBOLS

a_s	Area replacement ratio
e	Void ratio
e_c	Critical state void ratio
G_s	Specific gravity of solids
H	Height of capillary rise
k	Hydraulic conductivity
k_{sat}	Saturated hydraulic conductivity
p'	Mean effective stress
w_{opt}	Optimum water content
$Su_{DSM\ col}$	Undrained shear strength of deep soil mixing column
$Su_{Tailings}$	Undrained shear strength of the tailings between the columns
$\gamma_{d,\ max}$	Maximum dry unit weight
θ	Volumetric water content
θ_r	Residual volumetric water content
θs	Saturated volumetric water content
ρ_d	Maximum dry density
ψ	Matric suction
Ψ	State parameter

1. INTRODUCTION

In 2021, 2.8 billion tons of ore and extracted metal were mined globally (USGS, 2022). Global mining needed to satisfy mineral demands has more than tripled since to the mid-1990s, as illustrated for lithium and copper in Figure 1. Simultaneously, easily accessible high-grade ores have already been mined, and thus mineral demand must be met by ever lower ore grades resulting in increased volumes of residuals (Figuerido, 2018). The residual from mined ore, referred to as tailings, consists of ground rock, water, unrecoverable metals, chemicals (used to separate the desired product from the ore), and organic matter. Tailings are then dewatered and stored in engineered facilities, termed tailings storage facilities (TSF).

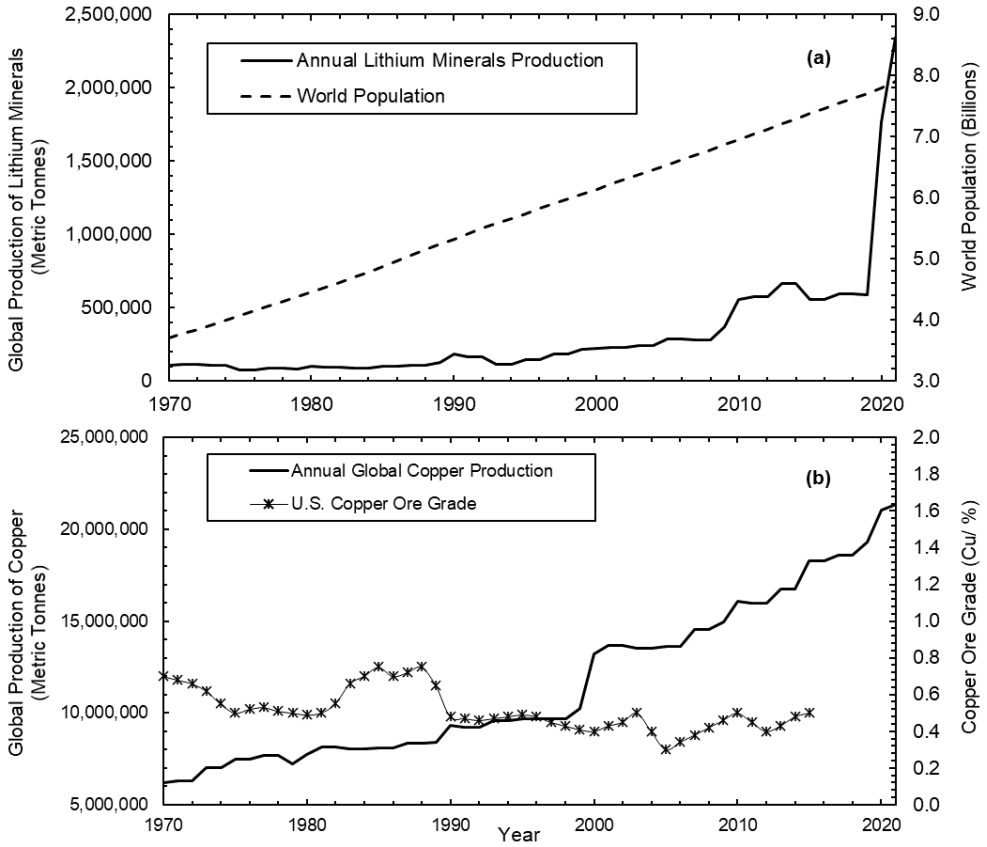

Figure 1 - Global demand for (a) lithium minerals compared to world population and (b) copper compared to average copper ore grade (World Mineral Statistics Data | Statistics & Commodities, 2023) and (World Population by Year - Worldometer, 2023).

Conventional tailings have high water contents and are typically deposited into TSFs from spigots on the perimeter embankment. The deposited tailings are usually in a slurry form. Coarser grained tailings deposit near the spigots while finer grained tailings spread further away from the deposition point. As the tailings are deposited, the water in the tailings begins to drain under gravity and consolidation forces. Over time, the outermost edges of the TSF dry, but due to the heterogeneity of the deposit, water is confined within fine grained tailings pore spaces within the TSF.

There are more than 17,000 TSFs globally with ~40% (~6,800 TSFs) active or currently operational (Spencer et al., 2022). The remaining 60% exist in some form of inactive (mining paused), closure, or post-closure status. Legacy TSFs are often defined as sites "where mining leases or titles no longer exist, and for which responsibility for their rehabilitation cannot be allocated to any individual, company or organization that has undertaken mining activities" Unger (2017). Legacy TSFs include orphaned sites, for which the owner cannot be found, and abandoned sites, where the owner is known but is financially unable or unwilling to carry out clean-up (NOAMI, 2024). The social, economic, and environmental hazards from legacy TSFs are the result of industry practices that often adhered to regulations of the time, however regulations and management have since evolved and adapted. The need for perpetual management of legacy TSFs is an ongoing challenge for the mining industry and society.

Due to a lack of available site data, the geotechnical conditions of legacy sites are often generalized. One frequent assumption is that relatively uniform tailings deposits have undergone, or are in the process of undergoing, drain down of stored water under gravity and are now unsaturated. However, based on reports from legacy tailings facilities in arid (Hardy et al., 2003; Casey et al., 2022) and non-arid environments (Godley and Quaglia, 2023) this assumption may

not be reflective of the state of many legacy TSFs. Instead, these heterogenous tailings often comprise interbedded layers of finer and coarser tailings. Coarser tailings are typically more prevalent near the perimeter (near high-energy deposition points), and finer tailings are more prevalent near the center or rear (away from deposition points). The result is a complex sequence of geotechnical and hydrotechnical characteristics including the presence of numerous capillary barriers that impede desaturation.

Figure 2 is a schematic of the development of saturated fine-grained layers from initial deposition to the final configuration of the TSF. This schematic is supported by the results of the geotechnical characterizations reported by Hardy et al. (2003), Casey et al. (2022), and Godley and Quaglia (2023). Continuous spigotted tailings deposition results in segregation of particle sizes and deposition of newly segregated tailings above previously deposited material results in interbedded layers of fine and coarse tailings. Over time, the tailings will drain excess pore water under gravity, however, as the tailings transition to an unsaturated state, continued drain down of the confined fine grain layers will be impeded. What results is permanent interbedded near-saturated fine grain layers with a potential to liquefy.

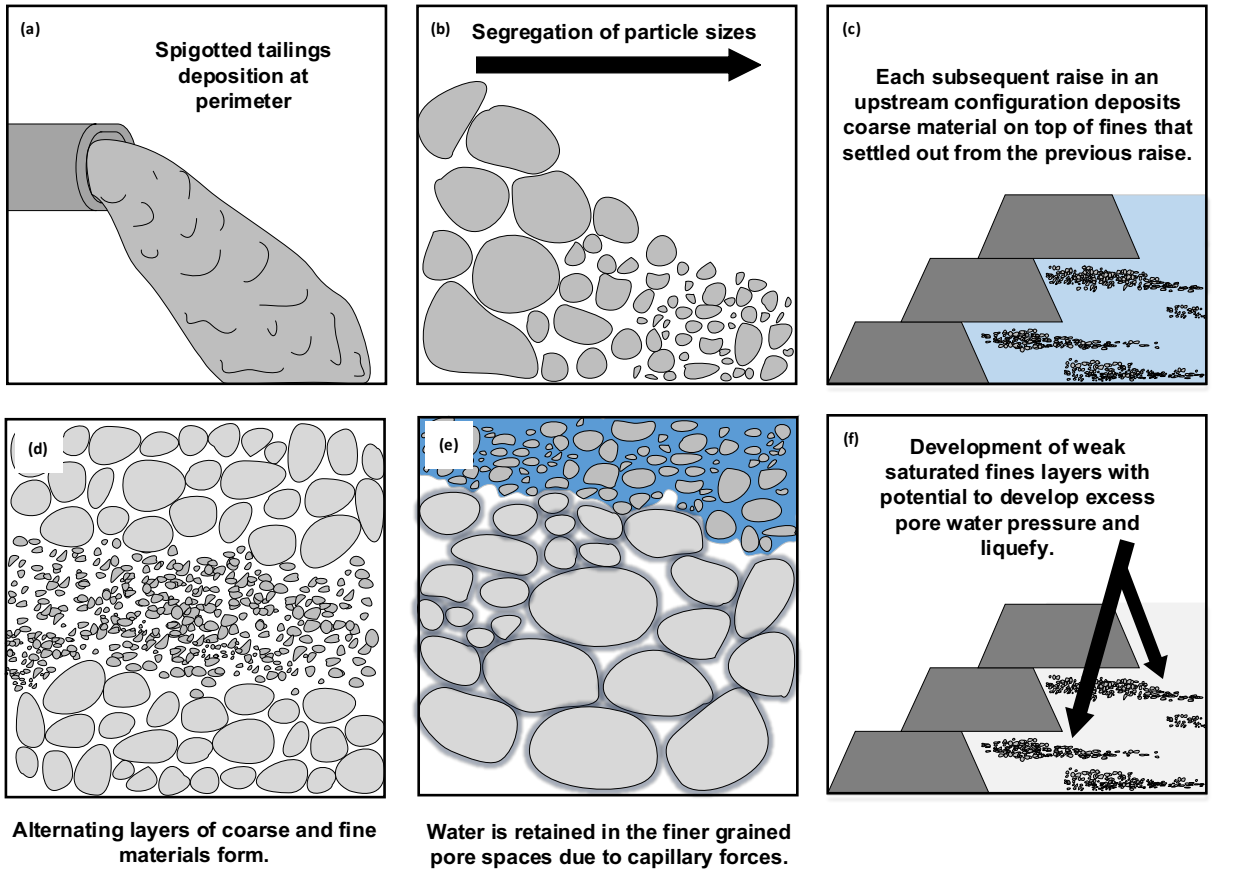

Figure 2 - Schematic progression of TSF construction, drain down, and retention of saturations.

The soil water characteristic curve (SWCC) and the hydraulic conductivity function (HCF) can be used to describe the changing hydraulic properties of the unsaturated soils. The SWCC and HCF describe the relationships between hydraulic conductivity (k), water content (θ), and soil suction (Ψ), and is illustrated in Figure 3 (Fredlund et al., 2012). The upper bound of hydraulic conductivity (Figure 3b) represents the saturated condition and due to the initially higher hydraulic conductivity of the coarser layer drainage first occurs in this layer. The hydraulic conductivity of the coarse grain tailings is greater due to the greater pore sizes of the coarser tailings than the finer tailings. Therefore, the drainage paths are better connected and the

flow throughout is more continuous. The larger pore sizes additionally result in less tortuous drainage paths, further supporting rapid dewatering in saturated conditions.

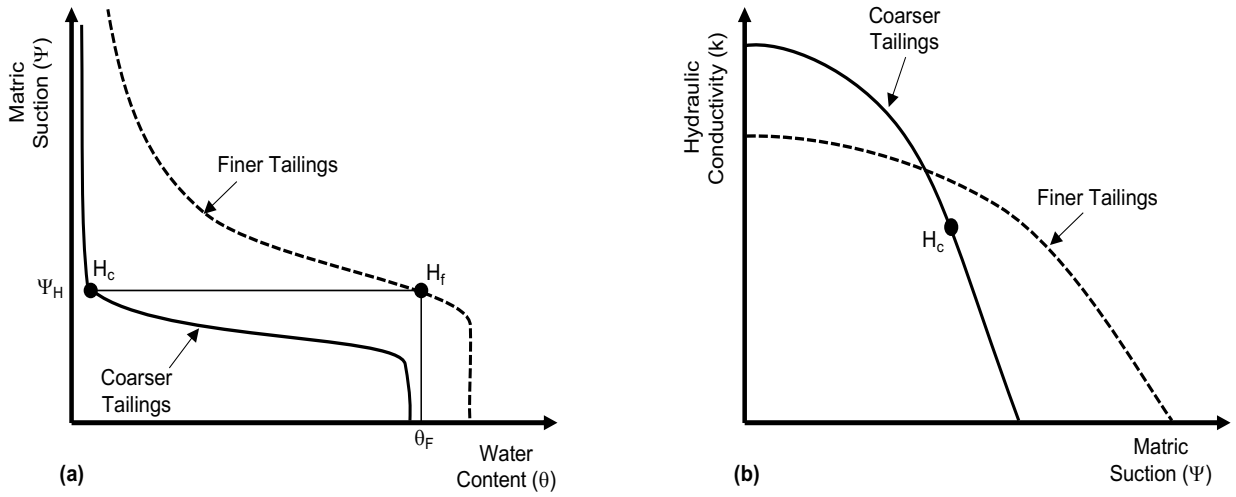

Figure 3 – (a) Soil water characteristic cure (SWCC) and (b) hydraulic conductivity function (HCF) for finer- and coarser- grained tailings (derived from Khire et al, 1999).

Initial gravity drain down occurs due to saturation throughout the tailings. Spigotted tailings deposition and natural segregation of particle sizes produce heterogeneity in the tailings deposit. As both layers begin to desaturate, the suction at the two-media interface is effectively equal. The coarse tailings pores continue to drain more rapidly than the finer tailings pores, and as a result the coarse tailings hydraulic conductivity drops lower than that of the finer tailings. The point at which the coarser soil will stop admitting water can be approximated as the height of capillary rise (H) within the soil. Capillary rise refers to water that exists above the water table, where pore water pressure is equal to zero, in a soil due to surface tension. The height of rise is directly dependent on the pore size distribution of the soil. The inflection point of the coarse tailings curve, denoted H_c in Figure 3b, provides an estimate of the height of capillary rise (Baker and Hillel, 1990). H_c can be translated onto the SWCC, Figure 3a, and the associated suction is denoted Ψ_H. Hydraulic conductivity decreases rapidly after reaching the inflection point value as suction increases due to increased tortuosity and reduced area for flow.

Specifically, water flow is limited to thin films covering the surfaces of the soil particles and in meniscus water bridges at inter-particle contacts. As fine soils desaturate the liquid films become so thin that molecular attraction prohibits liquid movements within the films (Scarfone et al., 2020). The liquid films form due to the hydrophilic nature of water molecules.

Capillary barriers form at the interface of the two homogenous soils of contrasting pore size (i.e., coarse- and fine-grained tailings) and limit the movement of water through the system under unsaturated conditions (Stormont and Anderson, 1999). The result is interspersed near permanently saturated fine-grain layers confined by coarse layers with extremely low hydraulic conductivities.

For sites in arid climates, evaporation of retained water from the uppermost layers is expected, and even heavy rainfall events do not penetrate deep enough into the TSF before evaporation removes infiltrating water (i.e., infiltration of atmospheric precipitation does not lead to deep percolation). Figure 4 reproduces photos of cored samples of tailings in an arid environment. The interbedded fines layers have retained saturations due to the surrounding coarse layers. Samples were collected to correlate cone penetration (CPT) values to field-conditions.

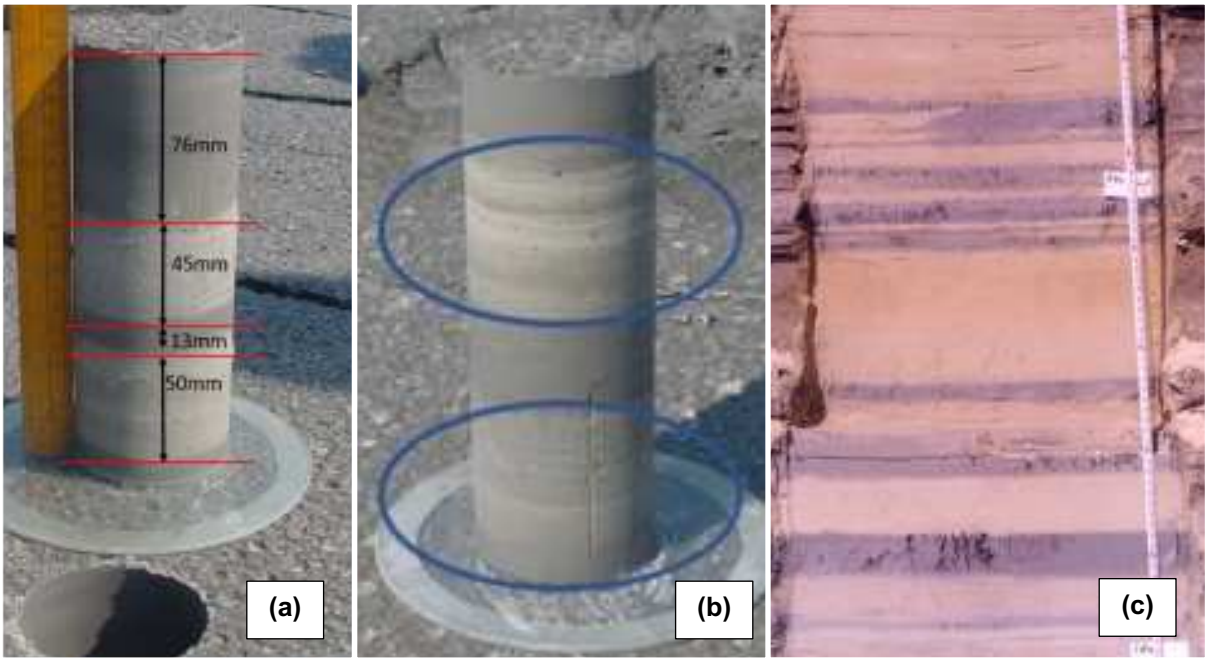

Figure 4 - Layering in hydraulically deposited tailings showing (a) coarse and fine tailings, (b) coarse layers with some fines trapped and (c) tailings profile with thin and thick layers of fine and coarse tailings. Figures (a) and (b) from Rust and Rust (2023) and (c) Vermeulen (2001).

Hardy et al. (2003), Casey et al. (2022), and Godley and Quaglia (2023) report that contrary to collected CPT data, which record negative or zero pore water pressure measurements, legacy TSFs previously assumed to be completely unsaturated, retained confined layers of fine saturated tailings. Retention of saturated, or near-saturated, conditions often elevate geotechnical stability concerns for TSFs, particularly seismic stability and susceptibility to flow liquification. Long-term retention of near-saturated conditions yields conservative assumptions of full saturation and may drive financially costly and environmentally disruptive mitigation efforts. Common industry practice is to assume that tailings are fully saturated until a value less than 60% saturation is reached as described by Cao et al. (2021), who determined that above 60% fine-grained tailings do not have significant variability in the matric suctions and can be assumed to be fully saturated. Banerjee et al. (2022) also describes based on laboratory analysis that in unsaturated fine silty sands liquefaction is possible for degrees of saturation above 60%.

As a solution to long-term retention of saturated layers, tailings dewatering is proposed. Dewatering is the process of removing water from tailings (or soils) to increase the solids content (the percent of solid mass in the whole tailings). Tailings can be dewatered before or after placement in a TSF. The extent to which tailings are dewatered prior to deposition encompasses a spectrum of solids contents (Morrison, 2022):

- conventional (< 40% solids content),
- thickened (40% - 65% solids content),
- paste (65% - 80% solids content),
- or filtered (> 80% solids content).

Dewatered tailings have seen increasing popularity in current mining practice as the process improves "geotechnical stability, reduces the stored water volume, and minimizes the need to introduce new water into the processing circuit" (Furnell et al., 2022). While the upfront costs of dewatered facilities are higher than conventional "slurry" facilities (Carneiro et al., 2018), the investment may be worth the cost due to construction of a potentially more durable and lower risk facility. However, while filtered tailings represent an option for new TSFs, or expansions, remining would be required to implement filtered tailings for an existing facility. Additionally, as of this writing, there is not a technologically viable and economically feasible dewatering solution for large-scale (>100,000 tons per day) tailings production (Nelson, 2023). While some smaller operations have found success with filtered tailings (<40,000 tons per day), there is still more to be understood before mass implementation. With these limitations in mind, new methods for dewatering prior to deposition and in-situ are needed.

Available, in-situ dewatering methods are different than dewatering methods prior to placement. In-situ dewatering methods are typically employed to speed up the time-rate of

consolidation. In-situ dewatering may also free water retained in intersected coarse layers that are confined between capillary barriers and encourage drain down. There are two main categories into which in-situ dewatering methods are divided: active and passive. Active dewatering requires continuous energy or reagent inputs, such as deep soil mixing (Masengo et al., 2019). While passive dewatering operates using low intensity or minimal energy inputs beyond initial installation, such as prefabricated vertical wick drains (Adams et al., 2017). However, both methods are primarily designed around the removal of pore water that is under positive pressures or draining permeable strata. Thus, additional tools are needed for the removal of water retained in fine strata by capillary barriers in TSFs.

Novel capillary geosynthetics have been developed to overcome the problem of capillary barriers in road subbases (Zhang and Connor, 2015; Guo et al., 2021; Lin et al., 2022) but have not been applied to tailings. Broadly, geosynthetics are manufactured synthetic materials used for a wide range of engineering applications. There are several subcategories of geosynthetics. Geotextiles are "used primarily for applications requiring separation, filtration, reinforcement, and drainage" (Shackelford, 2003). Herein, a method to passively desaturate tailings using capillary (wicking) geotextiles is explored. Two concepts are evaluated, initial dewatering prior to subsequent tailings placement, and in-situ dewatering of fines after placement. Laboratory drying experiments with and without two capillary geosynthetic products were conducted on tailings from a North American precious metal mine. Experiments were used to determine the magnitude and rate of dewatering achievable by the wicking geotextiles. The ability of the geotextile to remove both supernatant ponded water as well as pore water from the tailings was assessed in terms of the magnitude and rate of change in solids content, moisture content, and void ratio of the tailing.

2. BACKGROUND

2.1 Historical Methods of TSF Construction

A timeline for the evolution of tailings management is presented in Figure 5.

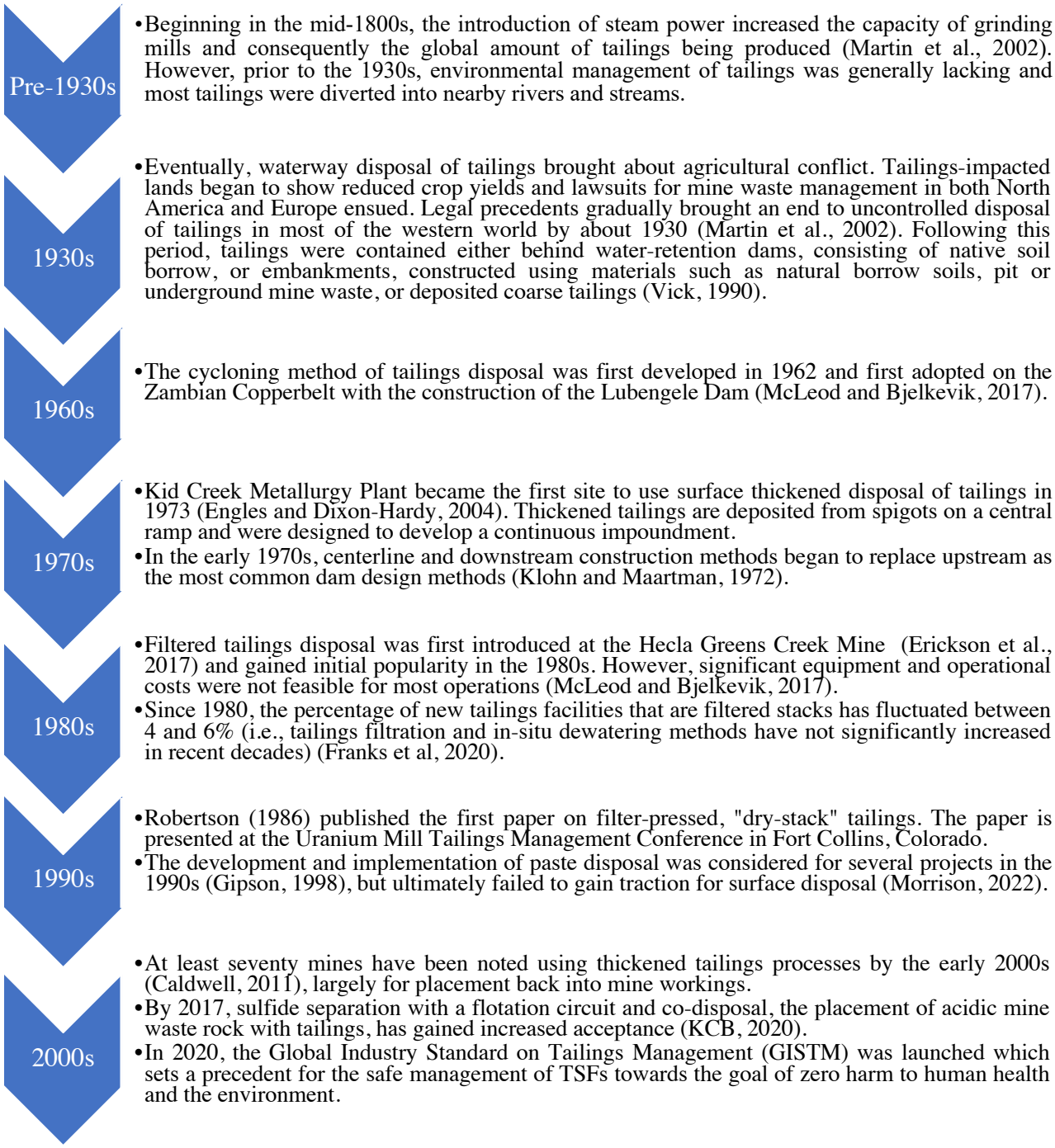

Figure 5 – Tailings management timeline.

A significant take-away from the tailings management timeline (Figure 5) is that tailings deposition within TSFs is nearing 100 years of practice. In these 100 years, there has been progress to develop new or alternative technologies, but these methods have gained minimal traction. The 1970s saw the shift of many new TSFs designs from upstream to centerline/downstream as a response to the problematic behavior identified to be possible with upstream configurations. However, further innovation is needed to prevent tailings management from being purely reactionary.

2.2 TSF Stratigraphy and Hydrology

The predominant method for depositing tailings material into a TSF is via sub-aerial deposition. Due to the high concentrations of water present in tailings, the material is commonly in a mixed semiliquid or slurry form. Slurry material usually is transported with pipelines and discharged via spigots on the embankment of the facility. As the tailings are deposited, natural segregation of particle sizes occurs. The largest particles remain close to the discharge point while the smaller particles flow away from the spigotted tailings beach. Depositional gradients change as the pond is filled and as discharge locations shift. Tailings with high water contents will have free standing water that often form supernatant ponds.

As each dam raise builds atop the previous, and additional tailings are deposited, the increasing weight of new tailings drives primary consolidation. Primary consolidation refers to the dissipation of excess pore-water pressure. This ongoing two-step continuous process, new tailings are deposited - old tailings are consolidated, occurs until the TSF is closed. Deposited tailings produce a heterogeneous stratigraphy composed of layers of fines interbedded with coarser layers. These interbedded layers inhibit vertical flow and dissipation of excess pore pressure throughout the deposit. As the older tailings reach the end of primary consolidation,

where all excess pore water pressure has dissipated, a portion of the confined water within the pore spaces will drain down under gravity. This will occur until the water content of the coarser grained layers becomes significantly less than the finer grained layers and water movement across the two-media system is effectively halted due to the capillary barrier effect.

2.3 Geotechnical Conditions

Understanding the general geotechnical conditions for sites in which data are readily available can help develop a systematic understanding of the conditions and expected behavior of other facilities (e.g., orphan facilities). Investigations of legacy TSFs are focused primarily on assessing the stability of the TSF embankments via geotechnical and hydrotechnical characterization. Sampling and testing results can be used to understand the evolving subsurface conditions throughout a deposit. Typically, site investigations to characterize tailings and foundational native materials include drilling and sampling programs, cone penetration testing (CPT), and laboratory testing. Laboratory testing conducted on retrieved samples may include index, triaxial, direct shear, consolidation (oedometer), Tempe cell (soil-water characteristic curves), and x-ray diffraction. The amount of testing that is conducted is an optimization of time, resources, and characterization.

From a geotechnical perspective, the fines remaining perpetually saturated can be a significant stability concern. Tailings deposited in upstream impoundments, and particularly fine tailings, are generally loose to very loose, contractant during shear, and therefore maybe susceptible to liquefaction due to static and dynamic loading (Martin and McRoberts, 1999). The shear strength of these loosely deposited tailings is assessed and predicted using undrained shear strengths. When a rapid (undrained) increase in the shear strain results in 1) an increase in pore pressure, 2) a corresponding reduction in effective mean stress, and 3) a dramatic reduction in

shear strength, the critical condition of loose materials results, and flow liquefaction may occur (Kalsnes et al., 2017). Contractive tailings are those that maintain the potential for a rapid loading condition to cause the pore water pressures to increase and greatly reduce effective stress. If tailings can be made to release retained water and transition to a dilative and drained state (e.g. due to increased effective stress with removal of positive hydrostatic pore water pressures), the potential for a loading event to cause a failure, or undergo flow liquefaction, is reduced.

Figure 6 and critical state soil mechanics are commonly employed tools to estimate the susceptibility of a material to liquefaction (Schafer et al., 2019). The critical state of a material is the point at which during continuous shearing the material has reached a constant volume. Both dilative (dense) and contractive (loose) materials will move to this state in failure, denoted as the critical state line (CSL). The CSL may be represented by a plot of void ratio (e) versus mean effective stress (p'). The distance between the current in-situ void ratio and the critical state void ratio (e_c) is the state parameter (Ψ) as illustrated in Figure 6 (Jefferies and Been, 2016).

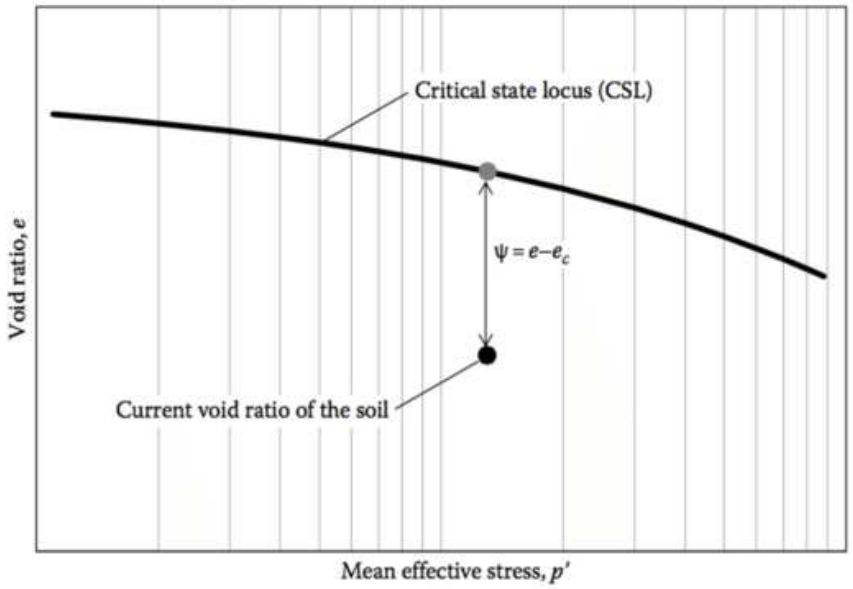

Figure 6 - Definition of state parameter, Ψ, for a dilative tailing (negative state parameter) (Jefferies and Been, 2016).

Laboratory testing to determine the state parameter of tailings and soil are well-proven, but estimation of state parameter in-situ is still limited. Laboratory findings must be applicable to real world behaviors to inform engineering decisions. In-situ experimentation, therefore, is essential to defining tailings geotechnical conditions. However, even state of the art in-situ investigation techniques, such as CPT, are unable to readily determine in-situ strength and tailings liquefaction potential in drained down (partially unsaturated) tailings. Thus, the conservation assumption, of tailings saturation, and associated assumptions are made in-response to address stability concerns of legacy TSFs.

2.3.1 Liquefaction Potential Using Cone Penetration Testing Correlations

Cone penetration testing interpretation methods most frequently used for tailings were first developed for saturated natural soils, as summarized by Robertson and Campanella (1983). These methods may not accurately represent unsaturated, normally consolidated tailings behavior. To date, only a few experimental trials have been conducted on silty or sandy soils to observe the drainage regime that forms between drained, partially drained, and undrained CPT testing (Silva and Bolton 2004; Jaeger et al. 2010; Dejong and Randolph 2012; Dienstmann et al. 2018; Russell, 2022; Ayala et al 2023).

CPT interpretation methods include correlations that connect cone penetration resistance, sleeve friction, and pore pressure at the cone tip to the soil type, state (Ψ), and strength (pre- and post-liquefaction). Correlations for estimating the in-situ state of tailings from CPT data include Plewes et al. (1992), Robertson (2010), Jefferies and Been (2016), and Schafer et al. (2019). These correlations relate a resistance value, coming directly from measurements of driving the cone into the tailings, to the state parameter. Once a state parameter is correlated from in-situ data, the critical state void ratio can be estimated. In unsaturated tailings, suction causes the

particle contact forces to increase above the levels for saturated conditions, resulting in an increase in the effective stress and stiffness of the tailings skeleton (Russell, 2022). The increased strength of unsaturated tailings is beneficial to total TSF stability. However, due to the lack of defined interpretation of the in-situ state parameter to real-world tailings behavior and a limited ability to replicate experimental correlation results, tailings saturations that are reported as 60% or higher, are typically treated as fully saturated. With the assumption that the tailings are saturated, undrained strengths are usually assumed for fine-grained tailings and conservative remedial methods used.

Limited research has been done to better quantify in-situ strength of tailings at near saturation to reduce the current conservative practice of assumed saturation. Tang et al. (2017) aimed to correlate unsaturated soil strength properties and the CPT data interpretation of the effective friction angle. Using CPT soundings and undisturbed samples from near each CPT location Tang et al. (2019) proposed a model that incorporates a more robust stress state using coefficient of earth pressure at rest and over consolidation ratio. The authors found that a more accurate estimation of the friction angle could be developed, compared to traditional approaches that often produce overestimations for the given saturation range but significant reproductions of these results has been limited.

Ulrich and Coffin (2017) present the results of liquefaction analyses of material from a filtered TSF in Latin America. The results of using “bender element testing indicate that the CPT-based liquefaction analysis could not be relied upon due to suction-hardening of the unsaturated tailings.” By comparing the computer analysis to results of the project site investigation, the authors found conflicting liquefaction potential indicators.

Russell et al. (2022) investigated CPTs in two silty tailings, in saturated and unsaturated states. Empirical expressions were found to relate the state parameter to cone penetration resistance when normalized using mean effective stress. The saturations of the tested samples ranged from 0.2 to 0.95 and the data illustrated that the contribution of suction to the effective stress is necessary to correlate CPT results to the wide range of saturations. The cone penetration data may be interpreted once the effects of suction on effective stress are included in the effective stress. The findings from Russell further prove the complexity of necessary data to properly correlate in-situ parameters to CPT values.

Ayala (2023) expanded on CPT interpretation methods by application to sandy silt platinum tailings. Using results from both laboratory and in-situ CPTs, a novel characteristic surface was created that "unifies partial drainage during cone testing within a critical state soil mechanics framework, allowing the use of an approximation equation to smoothly move from drained to undrained regimes and from contractive to dilative responses for the CPT." Saturated samples were used and where partial drainage conditions occurred the state parameter could be inferred using CPT tests. The fulfillment of better defining partially drained tailings behavior to better understand saturations between 60 – 100% is achieved in this research, but the accessibility to replicate results is limited due to necessity of a calibration chamber.

To better understand the complexity of the available correlations of CPT data to the state parameter, an attempt was made to create a step-by-step list of necessary testing, parameters, and assumptions to employ these methods. A simplified list of methods and materials is as follows. The field and laboratory testing regime includes pressure plate or filter paper to develop the water retention curve, saturated drained and unsaturated constant suction triaxial tests to find the suction-dependent shifts of CSLs, collection of undisturbed soil samples, and CPT cone-tip

resistivity readings. Necessary determined parameters include: the in-situ gravimetric water content and void ratio from a recovered sample, and particle size distribution. These parameters can then be extrapolated with estimated material constants (α and Ω) to determine the saturation, air entry- and air expulsion- suctions, and effective stress parameter. Assumptions include the water content from a retrieved sample near the CPT sounding accurately reflects field conditions; application of suction does not change the soil fabric of a loose material; and this method only provides information on the critical state of the tailings sampled i.e., generalizations from results cannot be interpreted onto other tailings.

Although these correlations are actively being developed, the lack of definitive knowledge surrounding in-situ measurement of unsaturated tailings behaviors and complexity of available correlations are not accessible enough to be implemented on an industry scale. Therefore, to decrease the extent to which conservative efforts are taken, the tailings saturations should be reduced by dewatering methods.

2.4 Reasons for Dewatering

The tailings continuum associated with dewatering prior to deposition is shown in Figure 7. Dewatering is the process of removing water from soil or tailings pore spaces. Tailings dewatering has a variety of benefits whether the dewatering occurs prior to or following deposition. Mini-slump cone tests (Suits et al., 2008) were conducted with tailings at varying water contents, including the boundary conditions common for thickened and paste definitions (Morrison, 2022) to provide a visual description of this continuum. Dewatered tailings have a higher solids content paired with a reduced volume of voids in comparison to conventional tailings and can thus be placed in a denser (lower void ratio) state. Denser states are generally associated with dilative tailings as continued shearing will cause an increase in volume (Keaton,

2018). Dilative behaviors are less susceptible to liquefaction than contractive behaviors as excess pore-pressures do not develop during shearing (Molina-Gómez et al., 2021). Additionally, dewatering tailings prior to deposition reduces the amount of water that is transported from the processing plant to the TSF, ensuring greater water recovery, and reducing the total volume of stored material (potentially expanding the TSF capacity).

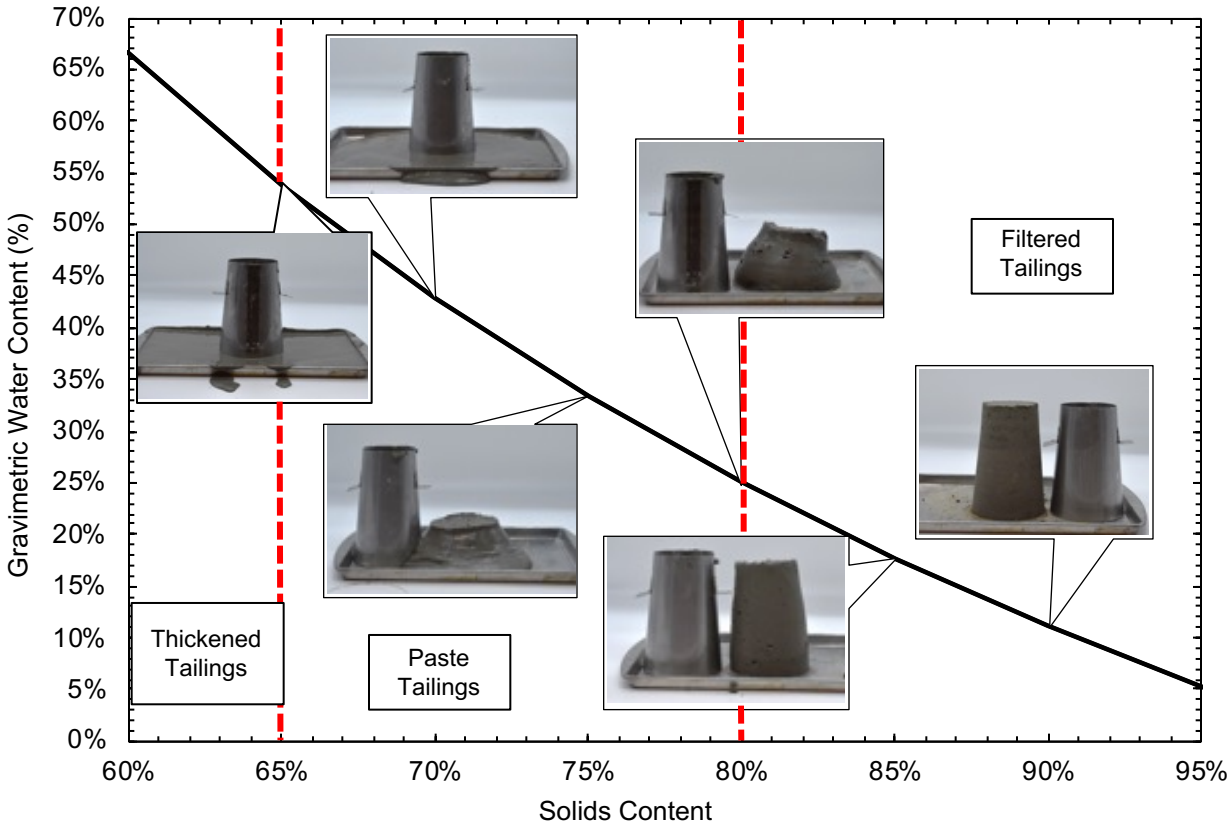

Figure 7 - The tailings moisture content continuum from mini-slump cone testing.

Global initiatives to enhance water stewardship in mining are one driver for tailings dewatering prior to placement. However, this option makes material handling (i.e., transport and placement) more difficult and expensive in comparison to pumping slurry tailings (Carneiro et al., 2018). Additionally, dewatering practices that occur prior to deposition are not a solution for existing (active and legacy) TSFs without significant capitol investments.

Dewatering existing tailings in-situ (i.e., after tailings have been deposited) offers numerous benefits. One advantage of dewatering is the ability to recover stored water more rapidly than natural drain down. Considering that most legacy sites were constructed and operated prior to the modern era of best practices and regulation, significant volumes of water remain within the deposits – trapped due to low hydraulic conductivities and via capillary barriers. Releasing water to be treated and released back into the environment frees this retained water.

Additional benefits of dewatering tailings include the ability to densify the deposit and reduce the likelihood of generating positive pore water pressures during seismic events or other sear events. Conventional in-situ dewatering methods do not desaturate but do decrease the rate of excess pore water pressure dissipation. This, however, indicates that conventional dewatering methods will not appreciably help with overcoming capillary barriers. There is the need for dewatering methods that can remove water in unsaturated conditions.

3. BACKGROUND - AVAILABLE IN-SITU DEWATERING TECHNOLOGIES

There are several available technologies to dewater in-situ tailings. The two main categories into which these technologies are divided are active or passive dewatering. There are few available in-situ dewatering methods and the magnitude of water that can be removed is often limited. Additionally, there are stabilization methods that produce dewatering tailings as an additional, un-intended benefit.

3.1 Active Dewatering Methods

3.1.1 Electroosmosis

Electro-osmotic dewatering has been predominantly used for remediation and construction dewatering, however, the ability to remove water from soils, sediments, and sludges has potential for the mine waste industry. This method extracts water from sludge cake using an electric field, rather than evaporation by heat or a mechanical force, to attract hydrated positively charged ions towards the cathode when the direct current is transmitted to the ground. The ions attach to the hydrated water molecules and establish a constant flow of water through the system (Martin et al., 2019). Casagrande first applied this method in the 1930s, as one of the electrokinetic processes, to direct flow towards the excavation surface and found great success (Yüksek, 2022).

Electroosmosis was initially used for soil improvement and slope stability, but now trial applications in the laboratory and in the field for the dewatering of tailings have begun (Lockhart, 1983; Shang and Mohamedelhassan, 2012; Yüksek, 2022). Disadvantages such as corrosion of the electrodes used in this method and high electricity costs return little support from the mining industry (Yüksek, 2022). Oftentimes, electro-osmosis processes are assisted

with geo-drains or wick drains for the purpose of dewatering. At a large scale, electro-osmotic dewatering of tailings is not a proven technology; further research is warranted.

3.1.2 Seepage Wells

Seepage wells are installed around the perimeter of a tailings embankment to create a cone of depression and reduce the phreatic surface when pumping starts. The cone of depression increases the hydraulic gradient down through the deposit further encouraging downward drainage (*Tailings Info*, 2024.). The effectiveness of the seepage wells depends on the permeability of the tailings and the depth of extraction. Drawing water down through the dam will help to increase the strength and stability of the embankment. While these wells can be effective to a degree, they are expensive to install, and each well must be pumped dry. Seepage wells are targeted at more rapid dissipation of excess pore water pressure and drain down, but do not overcome issues with retained capillary water and capillary barriers.

3.2 Passive Dewatering Methods

3.2.1 Prefabricated Vertical Wick Drains

Prefabricated vertical wick drains (PVD) are geotextile-wrapped plastic tubes with molded channels. The plastic tubes contain a flexible core manufactured of polypropylene and both faces of the core are grooved allowing water to flow unimpeded. The core is wrapped in a geotextile fabric with filtration properties, allowing free access of pore water into the drain. The geotextile wrap also aids in the prevention of piping of fines. For installation, the PVD is fed down through a hollow mandrel. A vibratory or static hammer or static is used to insert the mandrel into the deposit to a given design depth. The hammer is then removed, leaving the wick drain in place (Prefabricated Vertical Drains, 2018).

The decreased travel length of pore water to reach conductive media provided by the installation of PVDs is illustrated in Figure 8. The loss of water translates to a decrease in volume and an increase in the effective stress. Subsequentially the shear strength increases.

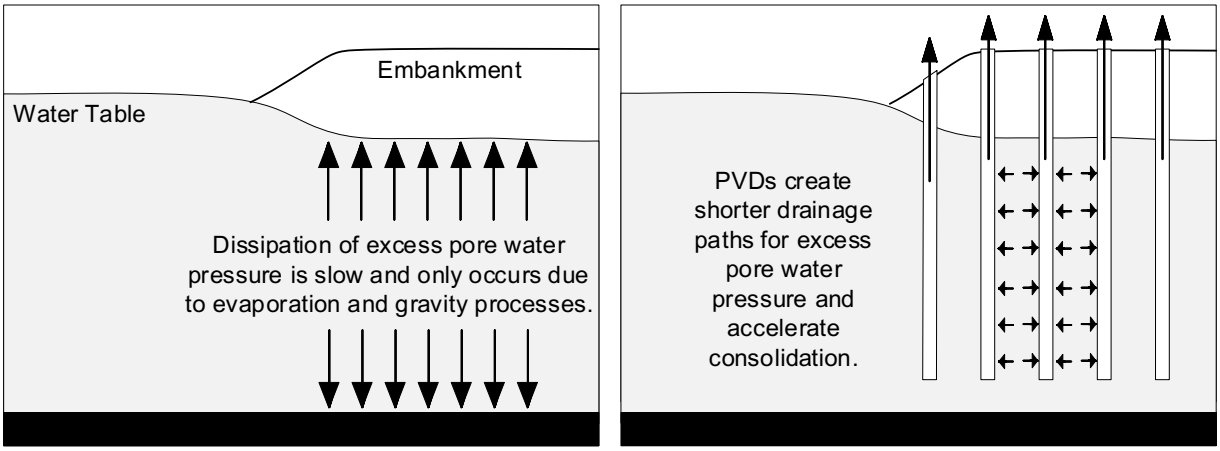

Figure 8 - Prefabricated vertical wick drains (PVD) in the tailings subsurface.

PVDs have been used increasingly in existing TSFs with observable success. The ability for passive dewatering is a significant advance in stabilizing legacy deposits. Adams et al. (2017) conducted a field-scale trial program to demonstrate the ability of wick drains to enhance the dewatering capacity of pumping wells. Vibrating wire piezometers were installed along wick drains cross sections to monitor the pore water pressure and drawdown changes due to improvement efforts. The aquifer beneath the tailings responded quickly and the storativity increased by approximately one order of magnitude due to the wick drains. While PVDs offer great potential to dewater, only excess pore water can be removed and therefore PVDs do not offer desaturation.

3.2.2 Wicking Geotextiles

Wicking geotextiles are a recent advancement designed to remove moisture from roadway embankments or subbases (Lin and Zhang, 2018). The cross-section of the fiber is shown in Figure 9. This geotextile, created from weaving high-tenacity polypropylene filaments

and deep-grooved nylon-wicking fibers, produces a coherent drain by effectively wicking water from soil pores. The diameters of the wicking fibers range from 30 to 50 μm and the width of each groove is between 5 and 12 μm (Zhang and Connor, 2015).

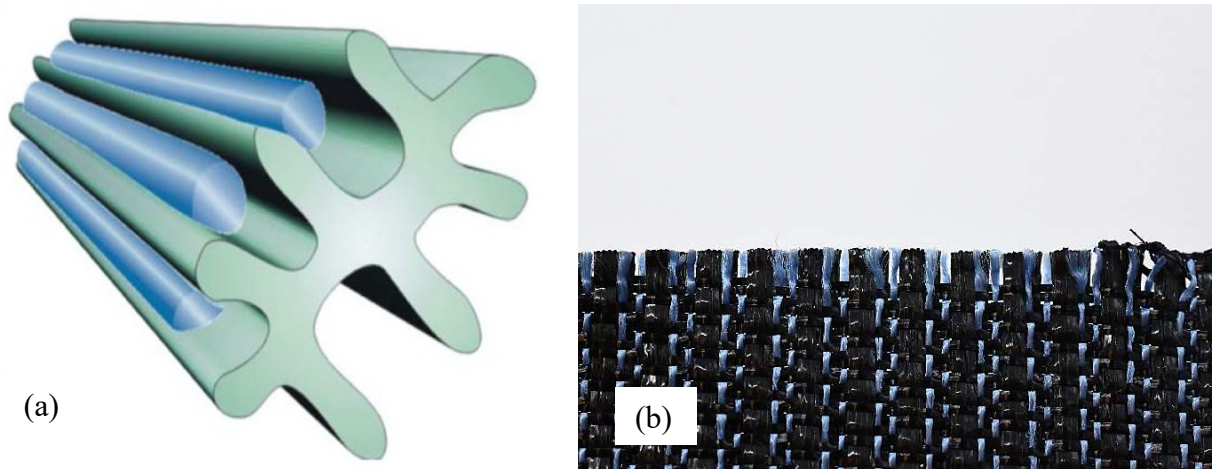

Figure 9 - a) Wicking fiber cross-section (Lin and Zhang, 2018) and, (b) close-up of wicking (blue) fibers.

Unique features of the geotextile include:

1. The wicking fibers have both hydrophilic and hygroscopic properties that provide enhanced lateral drainage along the plane of the geosynthetic. This means that the nylon will pull water from the surrounding soil pores and then provide a conduit for the water to the surface along the inner channels (Tencate, 2022).
2. The rough, woven surface provides a higher friction coefficient than standard geotextiles resulting in greater confinement of fine aggregates (GeoSolutions, 2024).
3. Wicking geotextiles have greater air-entry values, compared to non-wicking geotextiles, allowing for the development of capillary force or suction to remove moisture from soils in unsaturated conditions (Lin et al., 2022).

The geotechnical advantages of wicking geotextiles have been proven in transportation and roadway studies. Guo et al., (2019) summarized the available studies and projects that have demonstrated the effectiveness of the wicking geotextile as a drainage material, the highlights of each study are described subsequently.

Zhang et al. (2014) and Lin and Zhang (2018) estimated that the suction in an unsaturated soil within a pavement system is typically lower than 1000 kPa and the suction induced by the relative humidity in the air (open atmosphere) can be as high as 14 MPa. Due to the relative humidity difference between the geotextile and air, the geotextile can absorb water from the surrounding soil and transport the water to the exposed portion via a large hydraulic gradient within the wicking fibers. Azevedo and Zornberg (2013) performed column capillary model tests on sand and found that the wicking geotextile reduced the moisture buildup formed by a capillary barrier. Zornberg et al. (2017) reported field studies in which the daily water content reduction was evaluated in the soil column from a nearly saturated condition. This study determined that the wicking geotextile was more effective in reducing the water content than the non-wicking geotextile under the same conditions. Additionally, the drainage function of the wicking geotextile continued at a lower water content than the non-wicking geotextile.

The wicking geotextile was produced to move water horizontally out of a roadway subbase to prevent wetting of the road subgrade. The geotextile has proven extremely successful in this field and the ability to remove water from soil layers may transfer to other engineering applications such as tailings dewatering. Assessing the capability to dewater tailings fines is a novel application explored in this research.

3.3 Stabilization Methods with Dewatering Benefits

3.3.1 Deep Soil Mixing

Deep soil mixing (DSM) is a stability method that involves the instillation of columns of cemented material in the tailings deposit by mechanically mixing the in-situ material with a binder agent. The binder agent is most commonly cement or lime and is conducted via a mechanical mixing tool. DSM involves the construction of a grid or series of columns of treated tailings in the deposit for stabilization. The produced columns of material have increased strength, stiffness, and are more uniform (*Keller North America*, 2024). The improvements provided by DSM increase the tailings homogeneity. So, previously discontinuous layers of coarse materials are bridged, and the system acts according to a singular averaged hydraulic conductivity. With increased portions of confined water draining down. DSM may be a viable solution to encourage drain down in some deposits, however, the impacts are localized to where the injections and mixing occur, and the radius of improvement may not be significant.

One example of a successful DSM campaign is Kittilä gold mine in northern Finland as reported by Masengo et al (2019). Prior to DSM installation, CPTs with pore pressure measurements (CPTu), Field Vane Tests (FVT), and tailings samples from boreholes adjacent to the selected CPTus were collected as a base characterization. DSM improvement was conducted to strengthen the soft tailings and extend operational life of the upstream TSF. The achievable amount of ground improvement using DSM was quantified by the increase in undrained shear strength. The undrained average shear strength of the composite material Su_{ave}, tailings plus added dry binder, can be determined using Equation 1:

$$Su_{ave} = Su_{DSM\ col} + (1 - a_S)Su_{Tailings} \quad (1)$$

with a_s = the area replacement ratio; $Su_{DSM\ col}$ = the undrained shear strength of the DSM columns; and $Su_{Tailings}$ = the undrained shear strength of the tailings between the columns. Using Equation 1 and FVT data, the peak undrained shear strength was determined to have increased

from 10-50 kPa, prior to DSM installation, to 51-98 kPa, following DSM installation. CPTu data had also indicated the tailings strength improved from soft to stiff material classification following DSM installation (Masengo et al., 2019). In this instance, water contained within the tailings pore spaces reacted directly with the dry chemical binder and no longer retained an ability to develop excess pore pressure.

3.3.2 Jet Grouting

Jet grouting is a similar method to DSM but instead uses a stream of pressurized fluid to mix in either cement or lime binder to improve the geotechnical characteristics of the tailings. Hill et al. (2015) explains jet grouting as a series of boreholes drilled to target depth, followed by jetting of grout and water into the holes through small diameter nozzles at a high velocity. The high pressure applied by the grout and water results in erosion of the soil as well as mixing of the soil with the introduced grout (Hill et al., 2015). Again, similar to DSM, jet grouting is a localized improvement method and will not produce heterogeneity much further past the direct injection site. However, producing pockets of improved tailings columns may increase the strength and uniformity of the deposit, in directly impacted areas. Where grouting does occur, increasing uniformity of the tailings will produce a more uniform hydraulic conductivity, and thus further encourage uninterrupted drain down. Further drain down may even move the tailings towards dilative behavior.

Hill et al. (2015) describe the use of grouting to improve a legacy TSF that had previously sat dormant for over 50 years in a seismically active region at high elevation. While undergoing remediation, CPT and standard penetration testing (SPT) data identified potentially liquefiable zones in need of improvement. Grouting was selected as the design solution to create shear keys along the toe of the TSF. Grouting proved to be an effective stabilization method and

increased the factor of safety to an acceptable level for the near saturated fine-grain layers during a seismic event.

3.3.3 Bio Cementation

Bio cementation involves the use of microbes to secrete cement-like materials (e.g., calcite) that bind soil particles together. Microbial community-based technologies have been used increasingly in environmental restoration projects by application of various types of microorganisms - including bacteria, algae, and fungi - for the purpose of removing heavy metals from subsurface soils (Mahabub et al., 2023). Bio cementation technology can aid in the remediation and ecological restoration of tailings by improving the physical properties of the tailings, making them more manageable in ecological restoration efforts. The tailings can become less prone to erosion and more suitable for vegetation growth as bio cementation occurs when cement-like materials (i.e., $CaCO_3$) form.

In saturated tailings (Figure 10a), the introduction of microorganisms (Figure 10b) provide cohesion to the tailings particles and effectively bridge or bind the grains together. The stabilized tailings particles following binding are shown in Figure 10c. The colonization of plants and microorganisms within the tailings becomes successful and further aids in the restoration process due to enhanced soil fertility, nutrient cycling, and overall ecosystem development (Mahabub et al., 2023). This potential method for dewatering is relatively novel to the industry and the functional contribution of microorganisms is still being determined.

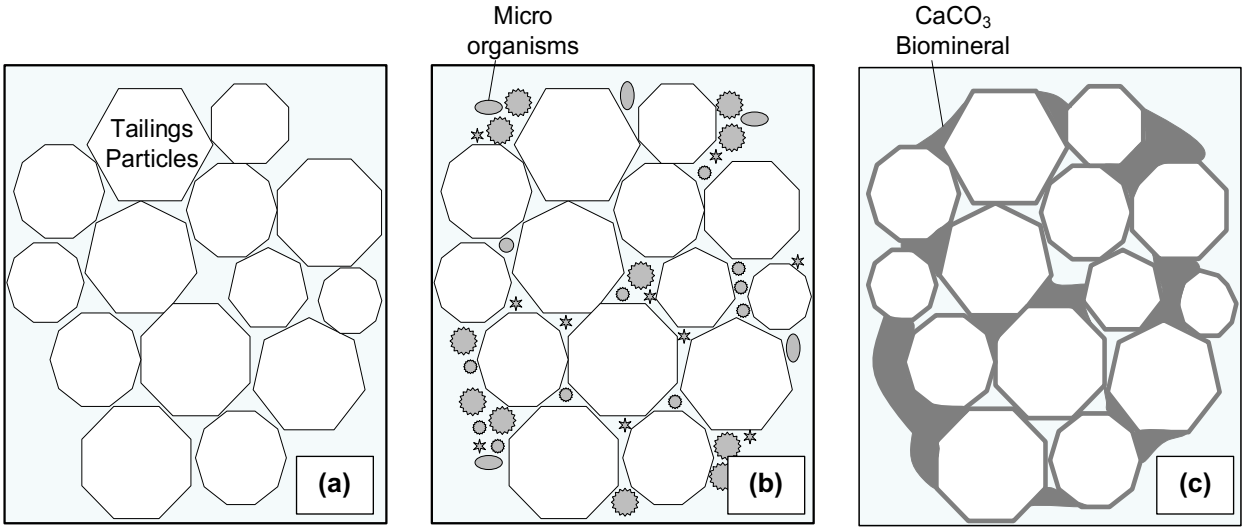

Figure 10 - Bio cementation process occurring inside tailings matrix.

4. MATERIALS AND METHODS

Several series of tests were conducted to assess both the surface water and in-situ capillary water dewatering capabilities of the wicking geotextiles in tailings. Beaker experiments and shrinkage limit testing, at various solids contents, provided surface water dewatering results. Column experiments, in which the tailings were confined between layers of fine and coarse sand, provided in-situ dewatering results. Detailed summaries of the materials and methods used for this research are presented subsequently.

4.1 Material Characteristics

Filtered tailings from a confidential precious metal mine, herein referred to as Mine P, as well as a fine and a coarse sand, were used for testing. Filtered tailings were dewatered at the mine during pilot-scale tests before shipment to Colorado State University. The geotechnical characterization of the tailings is described by Gorakhki et al. (2019) and Aghazamani (2022) and is summarized in Table 1. Properties and characteristics of the tailings include mechanical sieve and hydrometer, Atterberg limits, specific gravity, and standard effort compaction. Based on the properties and characteristics described in Table 1, tailings from Mine P are comparable to average tailings properties.

Table 1 - Summary of physical characteristics and classifications of Mine P tailings (from Gorakhki et al. 2019, and Aghazamani, 2022).

Property/Characteristic	Test Method	Unit	Value
Atterberg limits:	ASTM D4318		
Liquid limit, LL		%	20.9
Plastic index, PI		%	1.3
Classification (USCS)	ASTM D2487		ML
Particle sizes:	ASTM D422	%	
Gravel		4.75 mm – 76.2 mm	0
Sand		0.075 mm – 4.75 mm	35.8
Fines		< 0.075 mm	64.2
Clay		< 2 μm	17.4
Specific gravity of solids, G_s	ASTM D854		2.76
Compaction:	ASTM D698		
Optimum water content, w_{opt}		%	14.2
Maximum dry density, ρ_d		Mg/m^3	1.82

The fine and coarse sands used for testing were completely dried prior to use. The particle side distribution (PSD) for each of the sands and for the Mine P tailings in provided in Figure 11. Both sands and the tailings are relatively uniform and poorly graded.

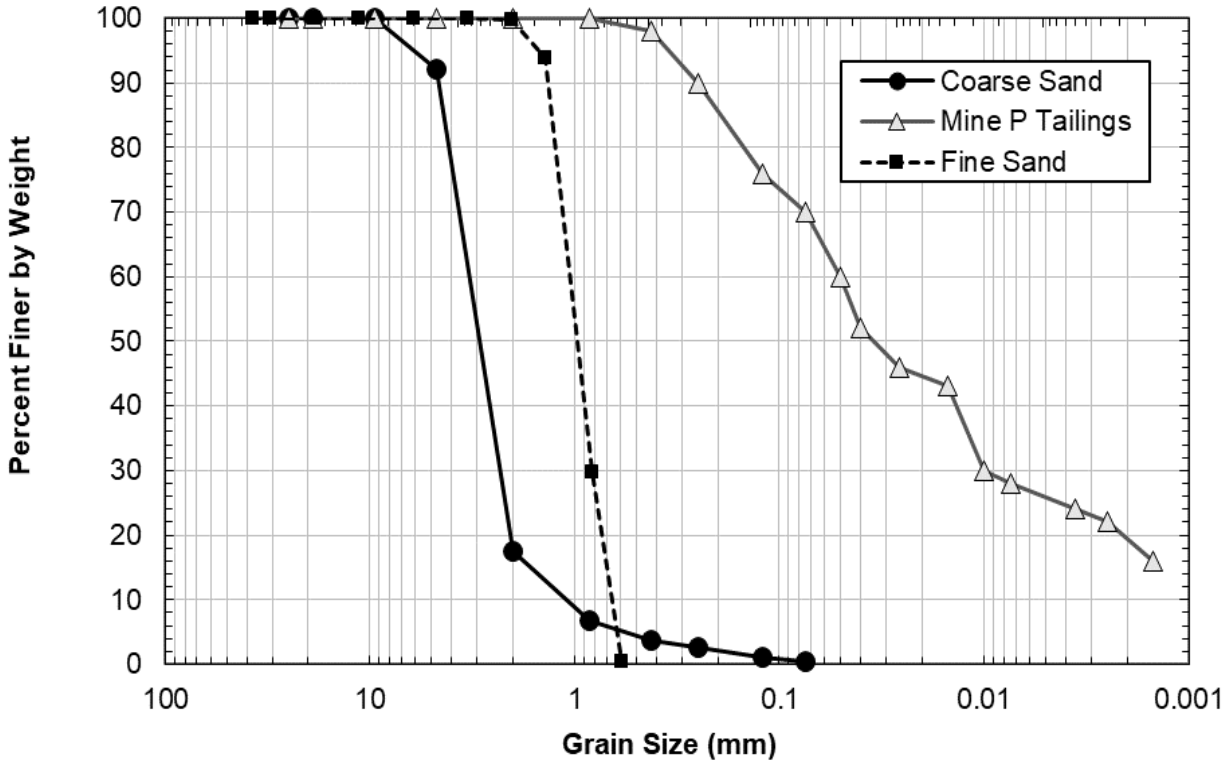

Figure 11 - Particle size distribution for materials testing.

4.2 Geotextile Characteristics

Two capillary geosynthetics were used in this study. Wicking geotextile 1 is a prototype material and wicking geotextile 2 is sold commercially under the name H2Ri by TenCate Geosynthetics (Georgia, United States. The characteristics of wicking geotextiles 1 and 2 are the same and summarized in Table 2.

Table 2 – Mechanical properties of both wicking geotextile 1 and 2.

Mechanical Properties	Test Method	Unit	Minimum Average Value
Wide Width Tensile Modulus (CD)	ASTM D4595	kN/m	77.0
Tensile Modulus @ 2% Strain (CD)		kN/m	15.8
Permittivity	ASTM D4491	s^{-1}	0.4
Flow Rate		L/min/m2	0.1222
Pore Size (050)	ASTM D6767	µm	85
Pore Size (095)		µm	195
			Maximum Opening Size
Apparent Opening Size	ASTM D4751	U.S. Sieve (mm)	40 (0.425)

CD = Cross-machine direction

4.3 Material Preparation

The tailings used in the column experiments were created at 50% solids content (the weight of dry tailings is half of the total weight of the prepared specimen). The tailings used in the shrinkage limit tests were created at various solids contents. The fine sand used in the column experiments was air dried and sieved before addition to the columns. The coarse sand was also completely dried before addition to the columns.

4.4 Column Experiments

Column experiments were created to emulate the previously described stratigraphy observed in legacy TSFs. The final set-ups are shown in Figure 12. The columns were created by depositing layers of varying granular sizes into columns to force the development of capillary barriers. Clear PVC columns were used. Columns were 10.16 cm in diameter and 45.72 cm tall. One end of the column was plastic welded to a square base plate and the interface between the

base plate and the column was additionally sealed with silicone caulk to prevent water loss through the bottom of the system.

The columns were filled with 22.86 cm of dry fine sand. The final surface of the sand layer was leveled. The weight and height of the fine sand layer were recorded.

Mine P tailings were carefully deposited on top of the sand layer to ensure an even distribution of material: a 7.62 cm thick layer of tailings were deposited to a reach a total height of 30.48 cm. For columns that contained some form of geosynthetic, the material was placed in the column after tailings deposition. The weight and height of the tailing layers were recorded. The columns were left to settle for one hour. Due to consolidation, the height of the tailings layers decreased from 7.62 cm to 3.81 cm.

An additional 11.43 cm thick fine sand layer was then placed above the tailings to reach a total height of 38.10 cm. A final 7.62 cm of dry poorly graded coarse sand was deposited on top of the layer of fine sand.

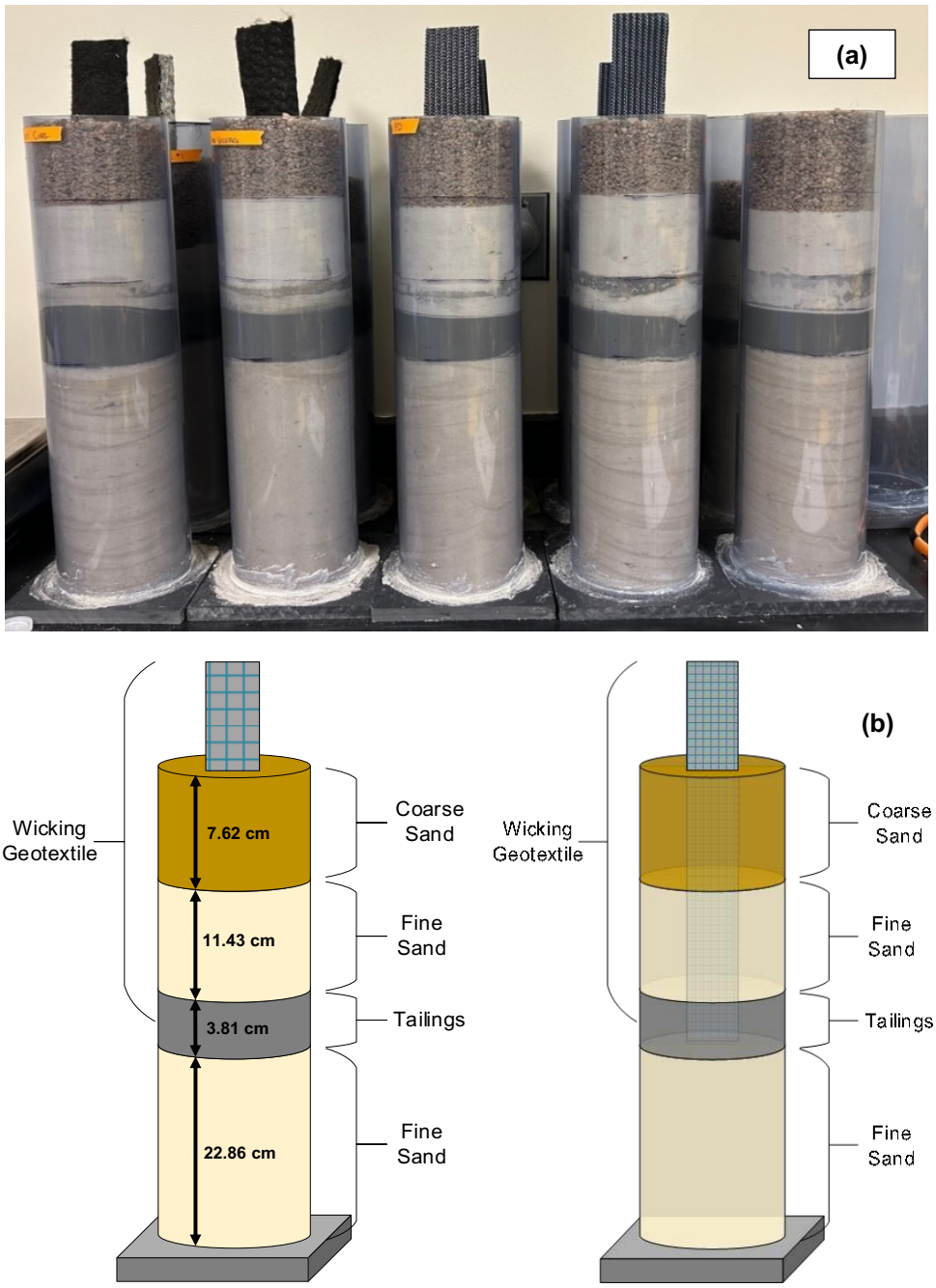

Figure 12 – (a) Tailings columns created at 50% solids contents and (b) columns digital renderings.

The column experiments were weighed at regular intervals to observe water mass loss. The change in solids contents corresponding to the new total masses were determined at regular intervals. Phase diagrams were created for the initial conditions of the tailings layer and updated as the water mass changed. Determining updated solids contents was done by subtracting the

water mass loss from the initial water mass of the tailings while assuming no change in solids mass. The solid mass divided by the new total mass produces a changed solids content. Similarly, the new water mass can be divided by the new total mass to determine a change in water content.

4.5 Shrinkage Limit Testing

Shrinkage limit tests were conducted in accordance with ASTM D4943 (2018) to determine if the wicking geotextiles dewatered to a greater extent than natural processes. The shrinkage limit test produces completely dry samples for which the dewatering capability of the wicking geotextile can be assessed in terms of final density and void ratio. Water was added to completely dry Mine P tailings to achieve solids contents of 50%, 60%, and 70%. In total, 36 shrinkage rings were filled with tailings material. Each variable being assessed was conducted in triplicate so that an average void ratio measurement could be produced. The inside band and bottom edges of the shrinkage rings were coated with a petroleum-based lubricant so that the samples could be easily removed following drying. A small amount of pressure was applied to secure the ring to a square of parafilm. The mass of the shrinkage ring and parafilm were recorded.

The shrinkage test setup is shown in Figure 13. Tailings were carefully deposited into each ring. The rings were filled, and excess tailings were removed to ensure a level sample. The ring plus wet soil masses were determined and recorded. Small strips of the non-wicking geotextile, wicking geotextile 1, and wicking geotextile 2 were inserted into the wet tailings. The total mass and volume changes of these rings were compared against a control in which no geotextile was inserted.

After one week of drying, the tailings samples were visually dry. The change in visual appearance of the tailings puck is illustrated in Figure 14. At this point, the samples were removed from the rings and the masses were recorded. The inside volume of each specimen shrinkage ring was determined and recorded. The samples were weighed regularly following initial observations until no change in mass was recorded. At the test conclusion, the volume of the tailings puck was determined using the dispersed water method, due to desiccation cracking that had formed in the geotextile samples. The differences in the initial void ratio and solids content were compared against the final void ratio and solids content values.

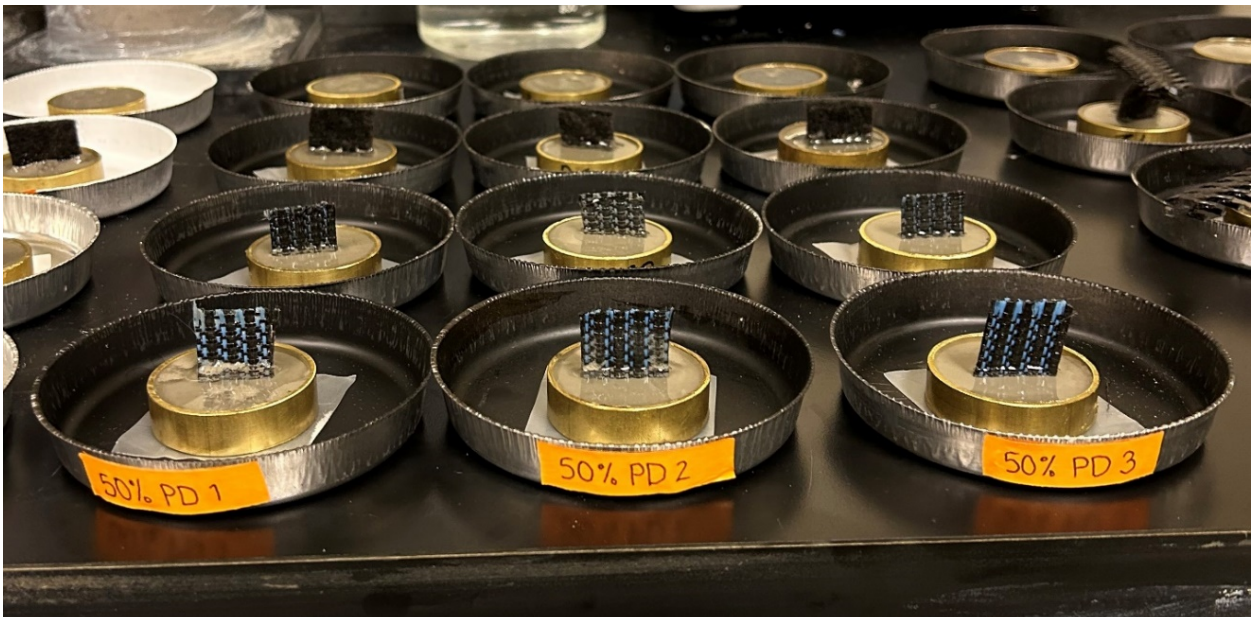

Figure 13 - Shrinkage testing, prior to drying, for tailings samples at 50% solids content.

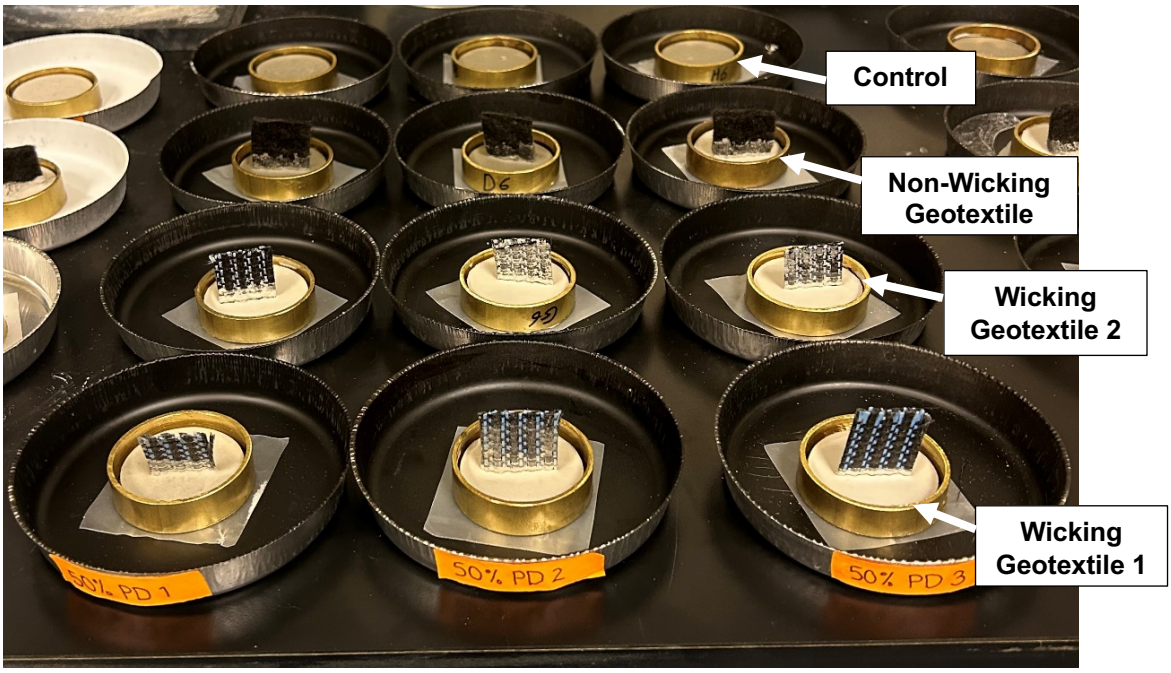

Figure 14 - Shrinkage testing at test conclusion for tailings samples at 50% solids content.

4.6 Volumetric Displacement Method

The volumetric displacement method, ASTM D7263-21, is the standard method for laboratory determination of density of soil specimens. Method A (*Water Displacement*) was used. This method was employed following complete drying of the tailings specimen from shrinkage testing. Shrinkage testing produces small tailings pucks for which volumes can be estimated using a caliper device. However, because the samples with geotextiles experienced desiccation cracking, the wax coating and water displacement method was used.

4.7 Beaker Experiments

Beaker experiments were conducted to assess the ability of the wicking geotextiles to remove freestanding and near surface water from tailings. Three series of beaker experiments were conducted: tailings created at 30%, 40%, and 50% solids contents. A total weight of 400 g of wet tailings was used. Tailings were deposited into each of the 12 300-mL beakers and strips of either wicking geotextile 1, wicking geotextile 2, or non-wicking geotextile were inserted into

the beakers. A control with no geotextile was also assembled. The mouths of the beakers were covered with plastic wrap, and the plastic wrap was secured with tape. A 4 cm slit was cut into the plastic cover to allow the geotextiles to reach the outside atmosphere.

Figure 15 shows a frontal view of the wicking geotextile 1 beakers at various solids contents, immediately following initial construction. The beakers were weighed at regular intervals to observe mass loss changes. After 24 days of observation, the plastic wrap was removed, and the beakers were placed in the fume hood to air dry completely.

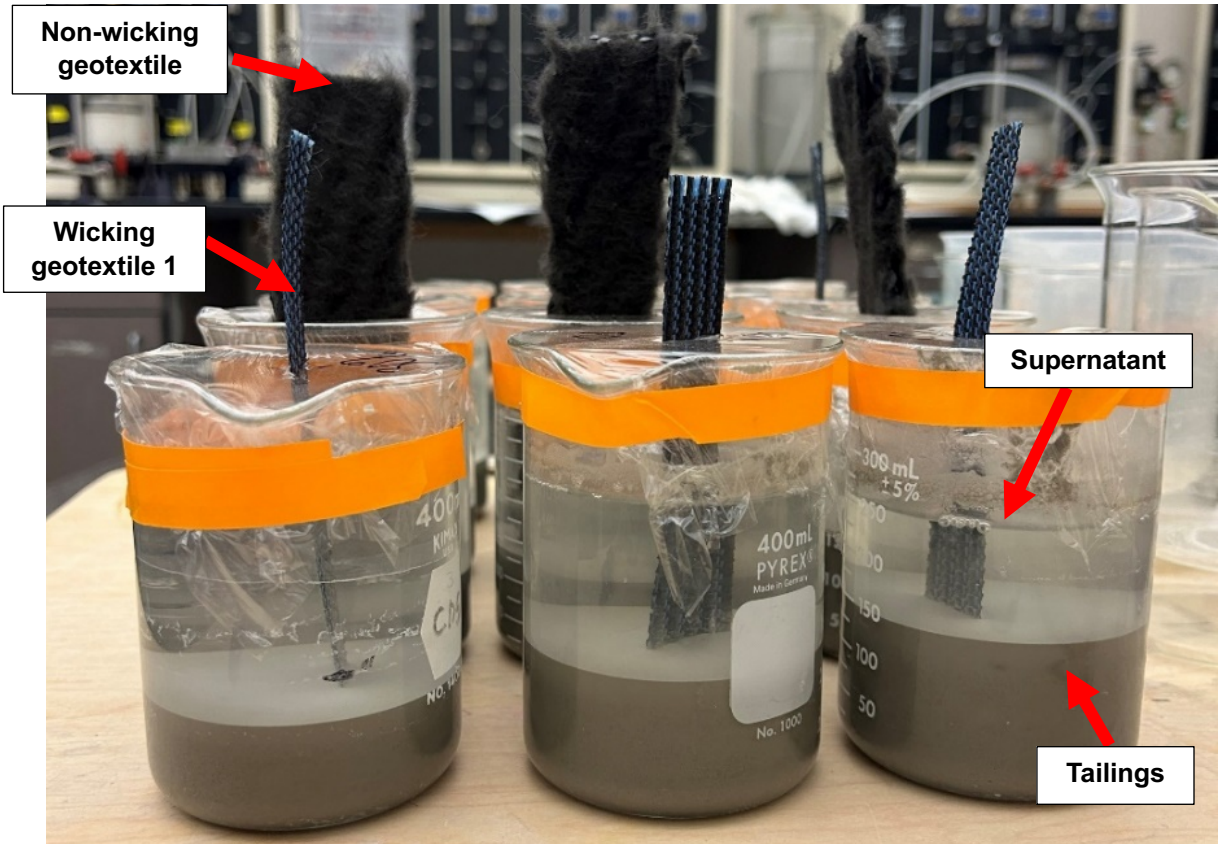

Figure 15 – 300 mL tailings beaker experiments at various solids content frontal view.

5. RESULTS

5.1 Suction Potential of Wicking Geotextile

The van Genuchten (1980) equation was used to calculate the volumetric water contents of the fine sand and tailings:

$$\theta = \theta_r + (\theta_s - \theta_r)\left[\frac{1}{1+(\alpha\psi)^n}\right]^m \quad (2)$$

where θ_r is the residual volumetric water content, θ_s is the saturated volumetric water content, α is inversely related to the air entry value, n controls the slope of the SWCC, $m = 1 - n^{-1}$. The van Genuchten (1980) equation was also used to calculate the unsaturated hydraulic conductivities of the fine sand and tailings:

$$K_r = \left(\frac{\theta-\theta_r}{\theta_s-\theta_r}\right)^P \left[1 - \left(1 - \left(\frac{\theta-\theta_r}{\theta_s-\theta_r}\right)^{\frac{1}{m}}\right)^m\right]^2, \quad P = -2 \quad (3)$$

where K_r is the relative hydraulic conductivity, and P is a fitting parameter, usually considered -2 for fine soils. Fitting parameters to Equations 2 and 3 are provided in table 3.

Table 3 - SWCC parameters for the tailings and fine sand.

Parameter	Value	
	Fine Sand	**Tailings** at **95% $\gamma_{d,\,max}$**
θ_r	0.01	0.004
θ_s	0.206	0.339
α (kPa^{-1})	0.833	0.013
n	3.449	1.421
m	0.710	0.296
k_{sat} (m/s)	1.2x10^{-3}	2.3x10^{-9}

*Tailings parameters provided by Aghazamani (2022).

The SWCCs and HCFs of the wicking geotextile 2, provided by Lin et al. 2016, and for the tailings and fine sand is displayed in Figure 16. The suction potential of the geotextile can be viewed in two parts: the geotextile surface, and the inter-yarn drainage path (the deep grooves that have an average spacing of 5 microns to 12 microns). Air and soil particles cannot easily infiltrate the drainage path due to the small openings. When the suction is less than 200 kPa, water movement from the surrounding soil into the geotextile multichannel is assumed due to greater unsaturated hydraulic conductivity of the geotextile. The transmissivity of the geotextile surface decreases significantly within the suction range of 45 kPa to 200 kPa, but the deep grooves remain saturated and continuously wick water into the atmosphere due to the gradient pressure difference (Lin et al., 2016). As the tailings are drying and dewatering the unsaturated hydraulic conductivity of the wicking geotextile 2 is greater than that of the tailings up to a suction of around 1000 kPa. Beyond this point, the hydraulic conductivity of the wicking geotextile drops off significantly, and the drainage efficiency is therefore dramatically reduced. The suction potential of the wicking geotextiles was not reassessed in this study, but based on previous findings, the estimated working range of the geotextile is up to 1000 kPa of suction. For Mine P tailings, a suction of 1000 kPa translates to a saturation of 28%. This is a saturation reduction of 70% beyond the capillary barrier effect of the fine sand, which resulted in retention of a saturation of 98% within the tailings layer.

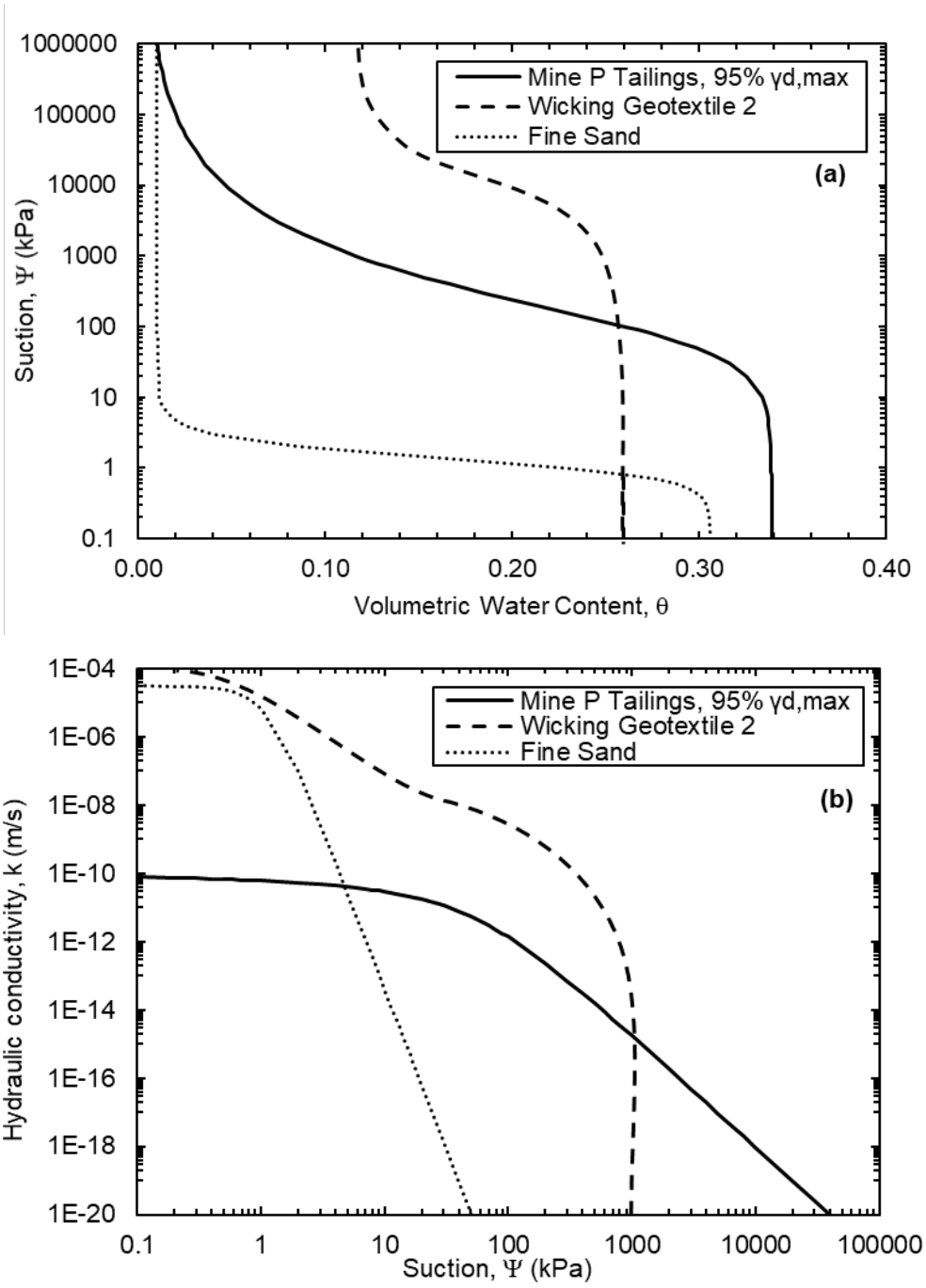

Figure 16 – (a) Drying SWCC and (b) HCF curves for the fine sand, tailings, and wicking geotextile 2.

5.2 Magnitude of Drying and Dewatering

5.2.1 Column Experiments

The percent total water mass removed of the total initial water mass for each column at experiment deconstruction are presented in Figure 17. The wicking geotextiles removed water

from the tailings layer to a greater extent by test conclusion (80 days) than natural evaporation or gravity processes as shown by the control column. At the conclusion and deconstruction of the columns, the wicking geotextile 2 had removed 48% of the water in this column, while the control column had only lost 19% water.

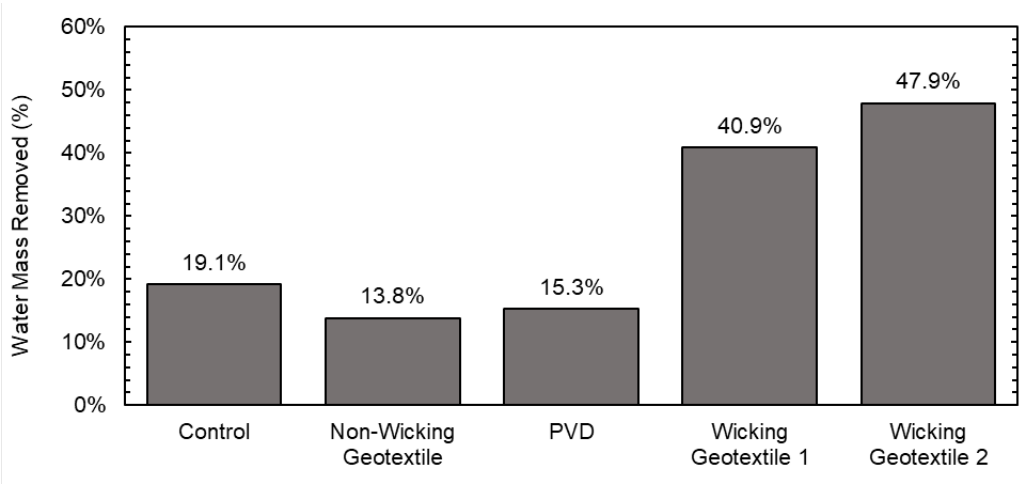

Figure 17 - Percent water mass removed in column tests.

To support the water loss values calculated throughout the testing period, water content samples were taken from the columns at the end of testing. The final water contents observed in Figure 18 were collected from the midpoint of the tailings layer and averaged across three points at the same depth.

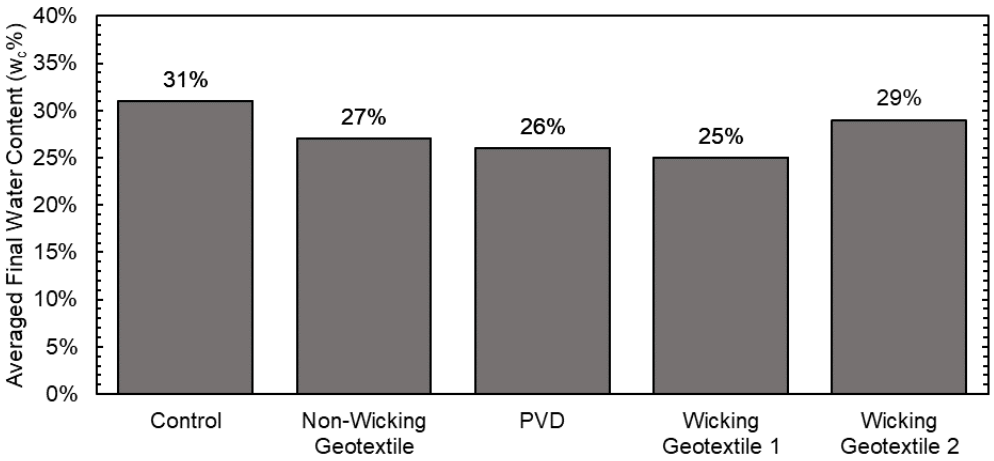

Figure 18 - Water content samples from the midpoint of the tailings layer within the columns.

The final water contents for each mid layer were similar. However, the wicking geotextile columns were observed losing more mass than the other columns during 80 days of testing. Therefore, water content samples were also taken in the layers above and below the tailings to observe where the water moved to.

Figure 19 presents a graphical representation of the water contents seen throughout the layering of the columns. As was visually observed, water from the tailings layer moved into the fines layer below during test construction. Gravimetric water content samples taken near the midpoint of the lower fine sand layer in the wicking geotextiles column had 0% moisture. While in the control and non-wicking columns water contents varied between 5 and 9%. This is indicative of the geotextile's ability to pull water back into the tailings layer to move the water to the atmosphere. Some movement of moisture into the fine sand layer above the tailings can be observed in all the columns, but further movement was impeded by the coarser grained sand. In all columns with a geotextile very little moisture (1-3%) was recorded above the fine-sand-tailings interface. The wicking geotextile columns show water mostly retained within the tailings layer.

The column experiments were created to evaluate the ability of the wicking geotextiles to remove water from the tailings. The wicking geotextiles first aid in dewatering excess pore water similarly to PVDs (Lin and Zhang, 2018). Once all excess pore water pressure is removed, the wicking geotextiles transition to unsaturated dewatering. The wicking geotextile effectively bypasses the capillary barriers introduced by the coarser sand as water moves within the inner yarn drainage path to the exposed end: creating a continuous conduit for dewatering. Water is directly removed from the tailings to the atmosphere. Beyond dewatering the tailings, the wicking geotextiles are effectively creating a vacuum that pulls up the water that previously

drained into the lower fine sand layer during column construction (as supported by the w_c% samples = 0%).

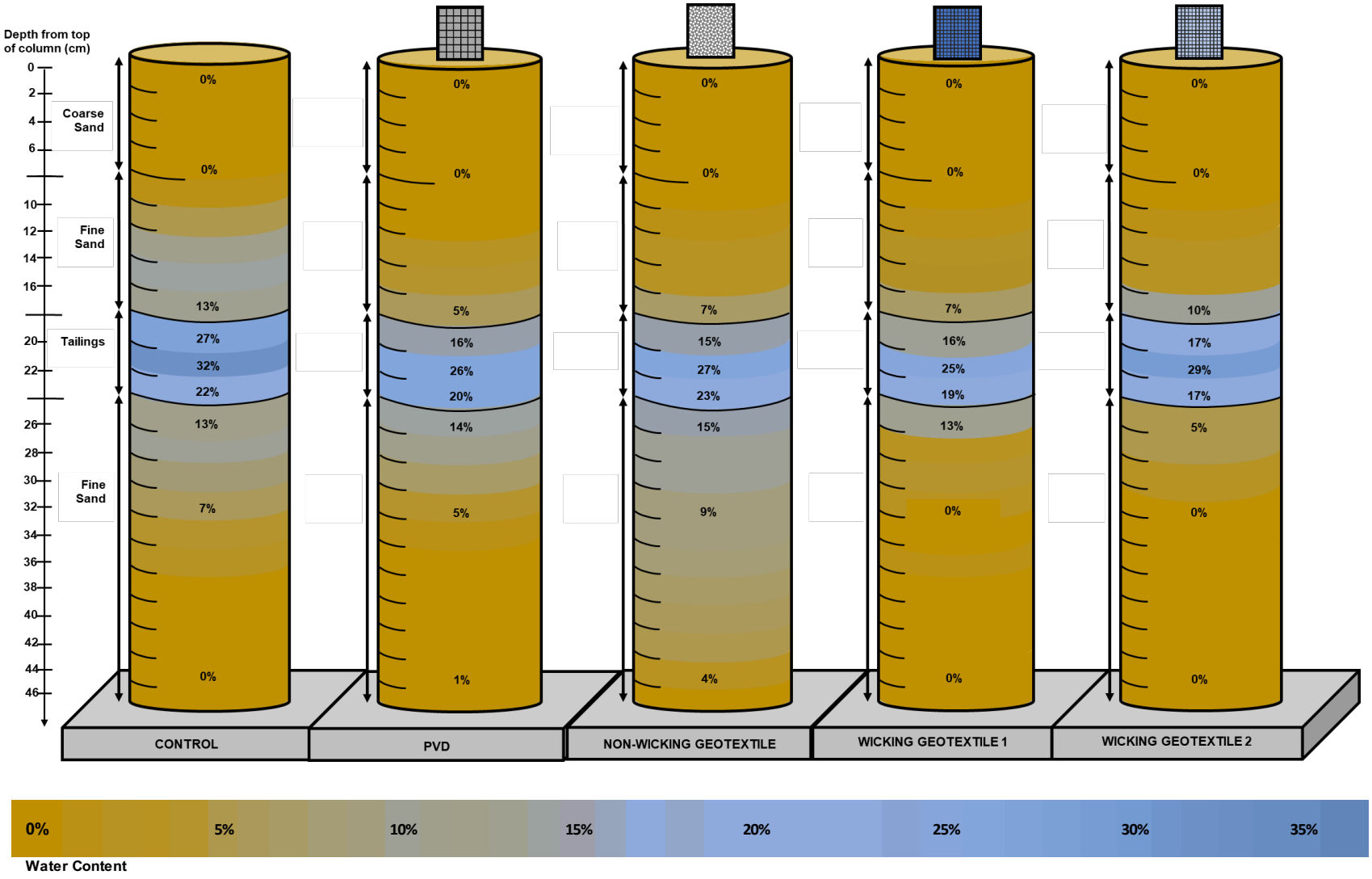

Figure 19 - Column experiments schematics representing water content samples versus depth.

5.2.2 Shrinkage Tests

The final averaged densities for the tailings samples from shrinkage limit testing are displayed in Figure 20. The initial, final, and change in void ratios for the tailings samples are presented in Table 4. The results from the shrinkage ring testing demonstrate that the densities and void ratios of the samples, with or without a textile, reach similar magnitudes once completely dried. The samples used in the shrinkage testing rings were so small that visual observance of which samples dried faster was not possible. Shrinkage testing was therefore only used to assess the magnitude of dewatering that can be achieved by the wicking geotextile.

Two observations of the final densities are a dip in the 60% solids content samples and a general decline in the 50% solids content samples from the control to the wicking geotextiles. These phenomena may be explained by recognizing sources of error in testing. The volumetric displacement method used for determination of final volumes is sensitive and the scale may report different submerged masses dependent on the small differences in the suspended positioning of the sample. Additionally, if the wax seal does not perfectly enclose the sample, small amounts of water may infiltrate, causing an incorrect mass to be determined.

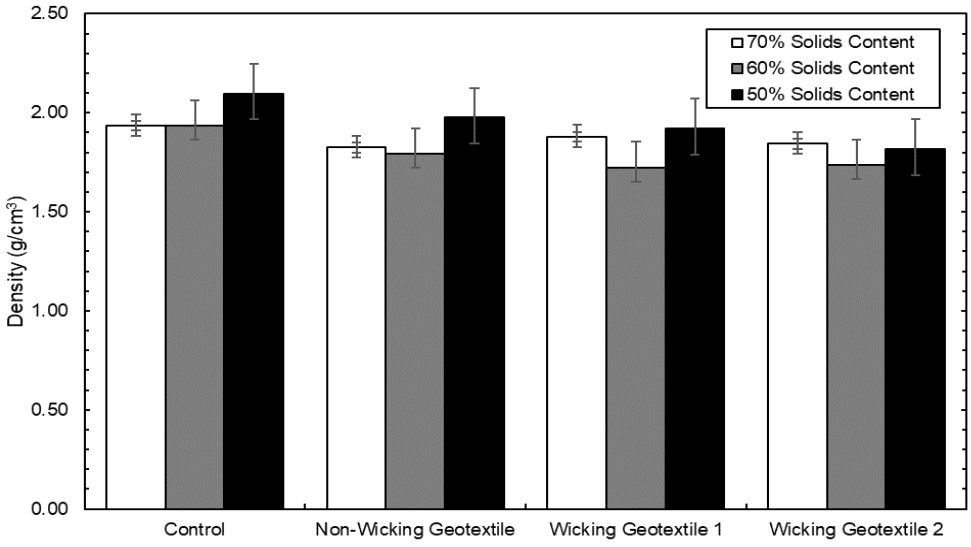

Figure 20 - Final density values from shrinkage ring and submersion method testing.

Table 4 - Void ratio values for tailings samples at various initial solid contents.

70% Solids Content											
Control			Non-Wicking Geotextile			Wicking Geotextile 1			Wicking Geotextile 2		
Initial	Final	Change	Initial	Final	Change	Initial	Final	Change	Initial	Final	Change
1.14	0.37	0.76	1.14	0.44	0.69	1.14	0.41	0.74	1.14	0.43	0.71

60% Solids Content											
Control			Non-Wicking Geotextile			Wicking Geotextile 1			Wicking Geotextile 2		
Initial	Final	Change	Initial	Final	Change	Initial	Final	Change	Initial	Final	Change
1.77	0.36	1.41	1.77	0.54	1.22	1.77	0.34	1.42	1.77	0.45	1.32

50% Solids Content											
Control			Non-Wicking Geotextile			Wicking Geotextile 1			Wicking Geotextile 2		
Initial	Final	Change	Initial	Final	Change	Initial	Final	Change	Initial	Final	Change
2.65	0.23	2.42	2.65	0.40	2.25	2.65	0.36	2.29	2.65	0.45	2.20

5.3 Rate of Drying and Dewatering

5.3.1 Beaker Experiments

The tailings beakers were observed steadily drying until day 24 as the plastic wrap coverings were removed and the beakers were placed in a fume hood to finish drying. The cumulative percentage of initial water mass loss is plotted in Figure 21. In all three series, both wicking geotextiles can be observed dewatering more rapidly than the non-wicking and control beakers. On day 7, both wicking geotextile beakers, across all three series, had removed nearly all the supernatant water and the water loss then transitioned to pore dewatering. The control retained supernatant ponded water until the plastic wrap was removed. The effect of accelerated drying is illustrated by the slope spikes observed in all experiments in Figure 21. At test

completion, all beakers effectively dried out to completion with or without the wicking geotextile aid. This is indicative that the wicking geotextiles cannot dewater surface or freestanding water to a greater extent than natural processes, but they can reach a drier state more rapidly.

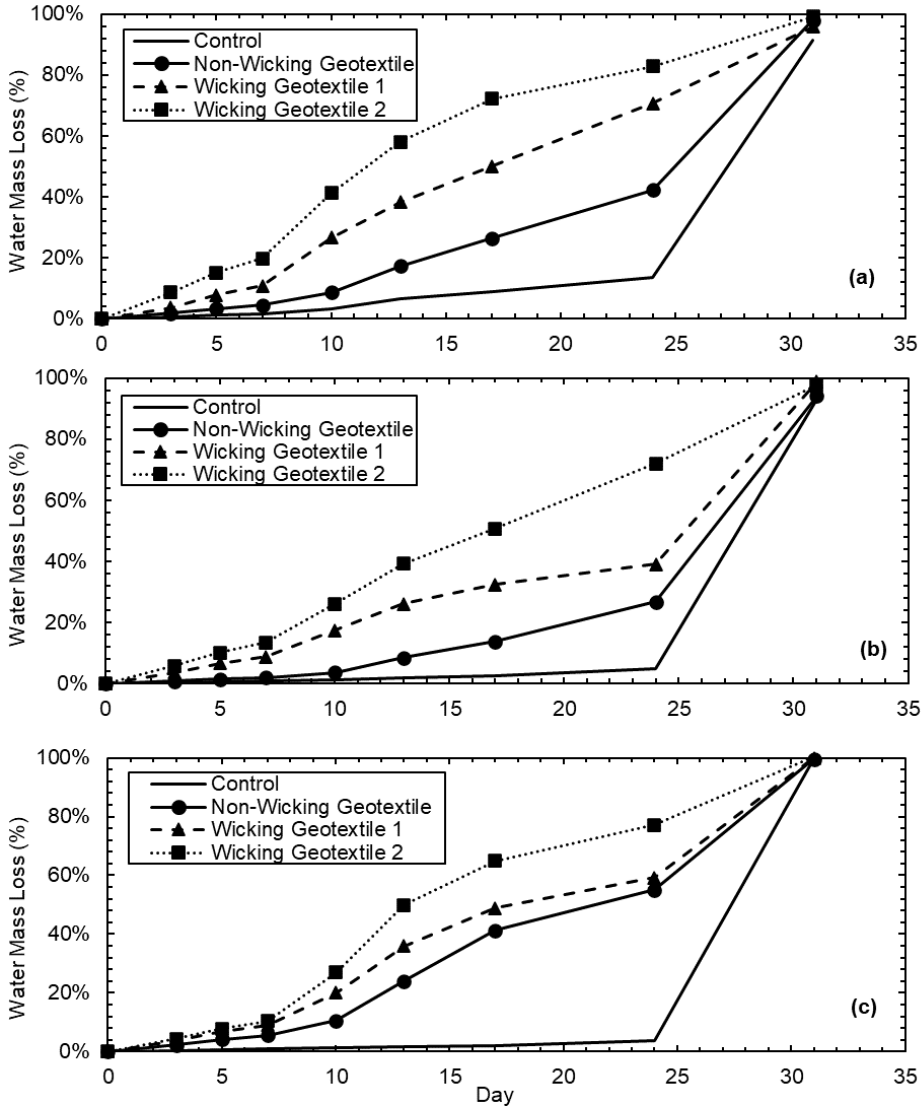

Figure 21 - Percent water mass loss for beaker experiments at (a) 50% (b) 40% and (c) 30% solids contents.

In addition to observing the cumulative mass loss of the beakers, the cumulative change in solids contents were determined at regular intervals. The magnitude of solid content change is illustrated in Figures 22 and 23. The rate of dewatering occurring in each series of the wicking geotextile beakers was directly dependent on the initial solids content. Initially the 50% solids

content wicking geotextile beakers dewatered more rapidly than the 40% and 30% series. However, at day 13, the 30% wicking geotextile beakers began to remove more water than the 40% and 50% beakers. This is likely due to the transition of the greater solids content beakers from surface dewatering to pore water dewatering. At test completion, day 31, all beaker experiments are observed reaching an equally dried state regardless of initial solids content or geotextile addition.

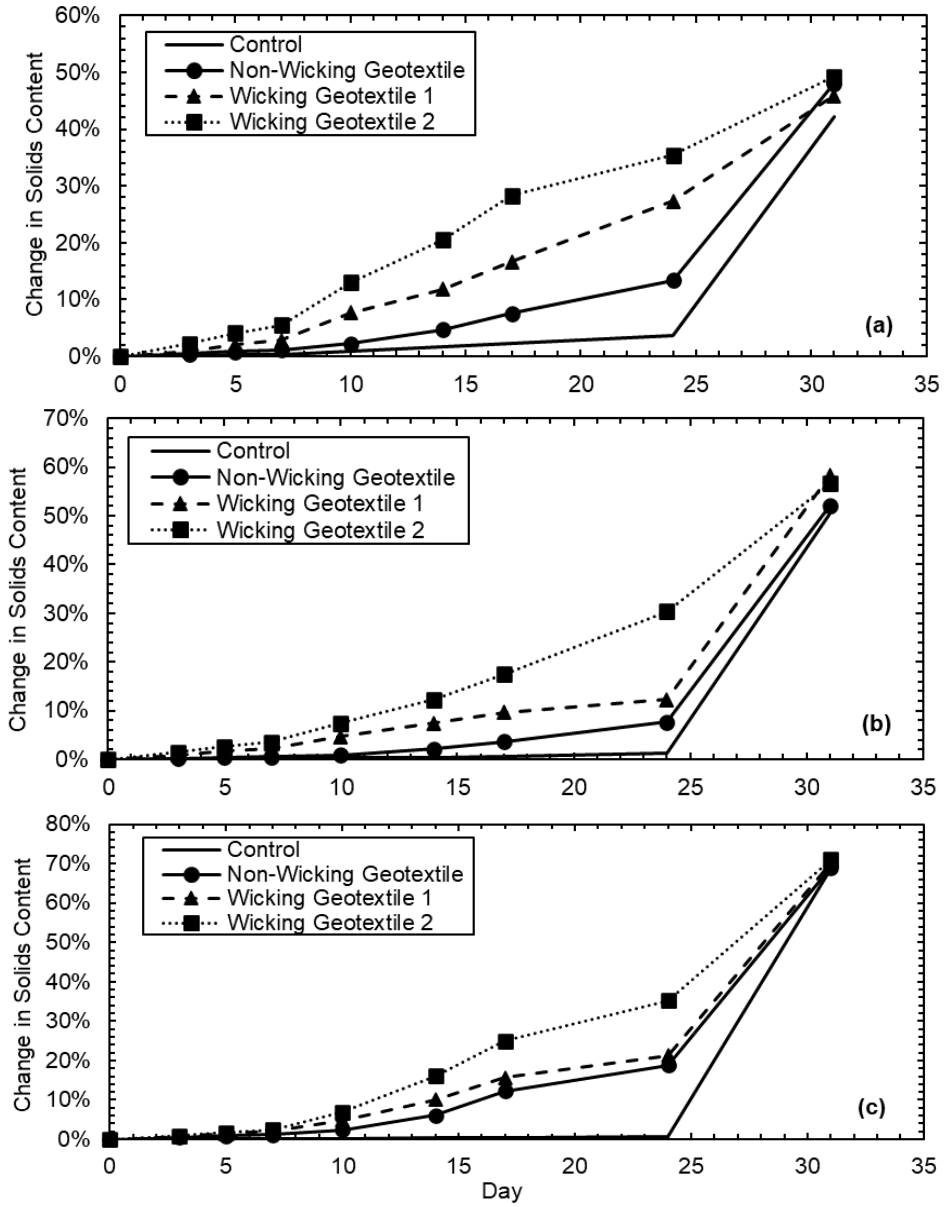

Figure 22 - Change in solids content for beaker experiments at (a) 50% (b) 40% and (c) 30% solids contents.

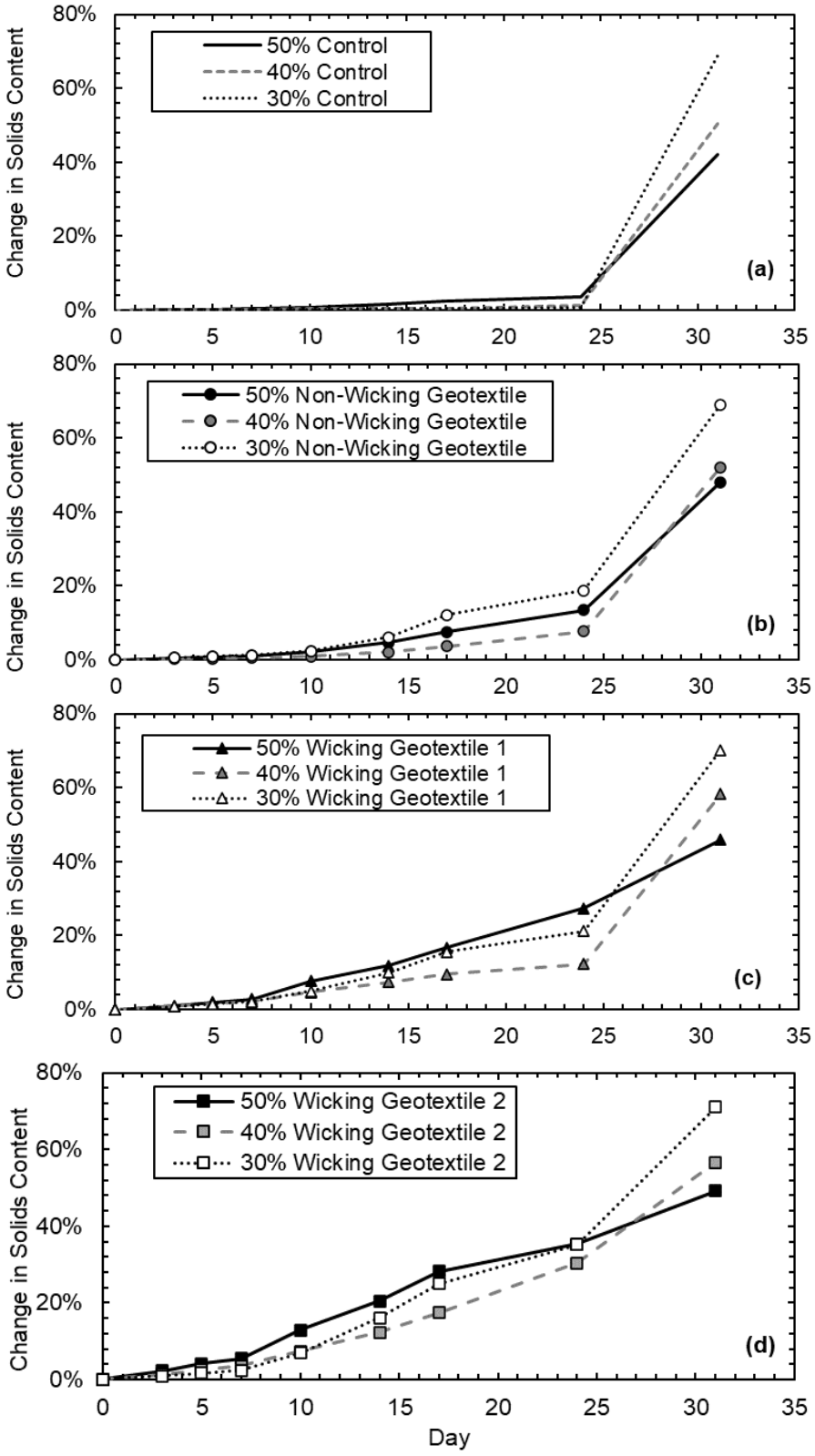

Figure 23 – Change in solids content for (a) control (b) non-wicking geotextile (c) wicking geotextile 1 and (d) wicking geotextile 2 beaker experiments.

By day 24 of allowing the beakers to dry,

- the 50% solids content wicking geotextile 2 had removed 6 times as much water mass as the control,
- the 40% solids content wicking geotextile 2 had removed 15 times as much water mass as the control,
- and the 30% solids content wicking geotextile 2 had removed 20 times as much water mass as the control.

The 50% wicking geotextile 2 had reached a filtered tailings state, the 40% had reached a paste tailings state, and the 30% reached the lower boundary of the paste tailings state. Extrapolated slopes show that:

- the 50% control beaker would have needed a minimum 141 additional days to reach the lower paste boundary of dewatering,
- the 40% control beaker would have needed a minimum 483 additional days to reach the lower paste boundary of dewatering,
- and the 30% control beaker would have needed a minimum 1009 additional days to reach the lower paste boundary of dewatering.

5.3.2 Column Experiments

After 80 days of allowing the columns to sit under the fume hood and weighing at regular intervals, the average rate of water removal per day for each of the columns was assessed, these values are illustrated in Figure 24. The water mass removed in grams per day of the wicking

geotextile 2 was 2.1 g/day, while the control was 0.8 g/day, less than half of the rate of the wicking geotextile.

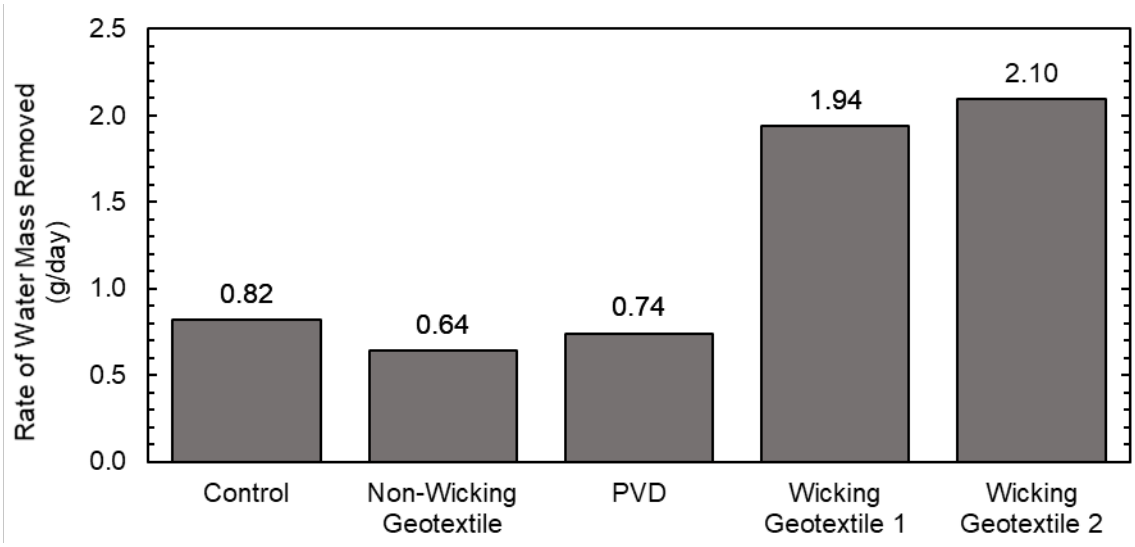

Figure 24 - Rate of water mass removed from the tailings columns per day.

The temporal evolution of wicking geotextile dewatering rates is shown in Figure 25. Throughout the entirety of testing, both wicking geotextiles maintained a higher water mass loss rate than the other non-wicking geosynthetics as well as the control.

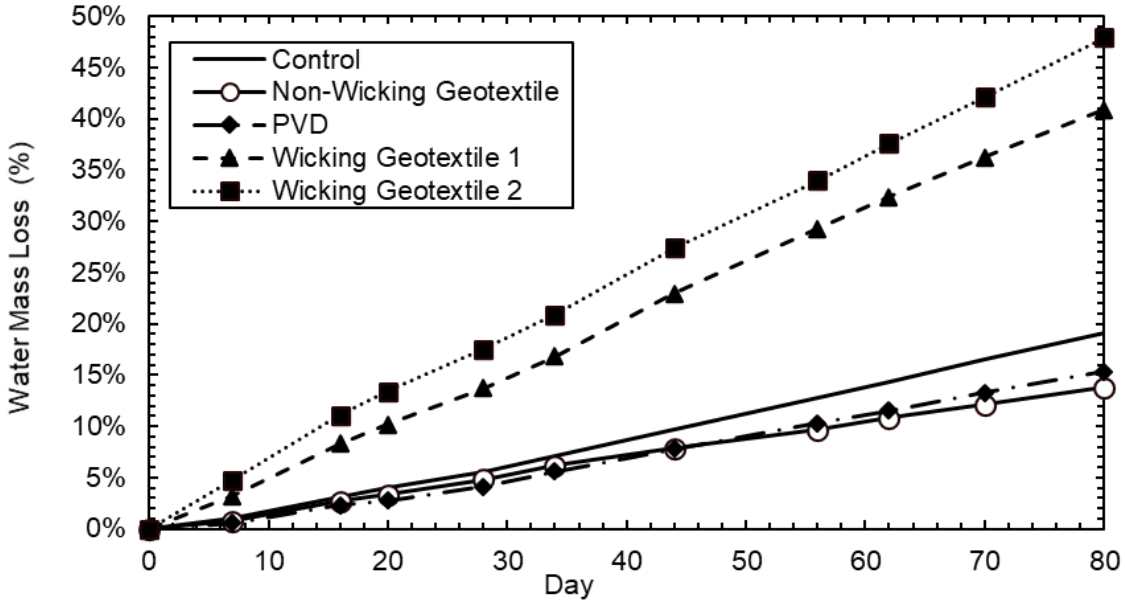

Figure 25 - Averaged percent water mass loss for the tailings column experiments.

The change in solids contents of the columns were calculated at regular intervals and these values are plotted in Figure 26. Although some water was initially observed percolating into the lowest fine sand layer upon initial construction, the amount of water was not determined and change in solids content of the columns was therefore made with the assumption that water loss was occurring directly in the tailings from the initial solids content of 50%. At the conclusion of columns testing, the wicking geotextiles had removed more than twice as much water than the control columns. The wicking geotextile 1 reached a solids content of 61.4% and the wicking geotextile 2 reached a solids content of 68.5%. This indicates that the wicking geotextile 2 tailings had transitioned to the paste form of the dewatering continuum: this transition occurred near day 65 as shown in Figure 25. The wicking geotextile 2 can be assumed to reach a filtered tailings state given an additional 40 days of dewatering. The control columns reached a solids content of 55.4% and due to the less than 1 g of water mass loss per day extrapolated data predict an additional 120 days of drying would be necessary to reach the lower end of the paste boundary and 275 days to reach the lower filtered boundary. However, some water moved into the fine sand layers above and below the tailings, and therefore, only the samples collected at the conclusion and deconstruction testing reflect actual solids contents.

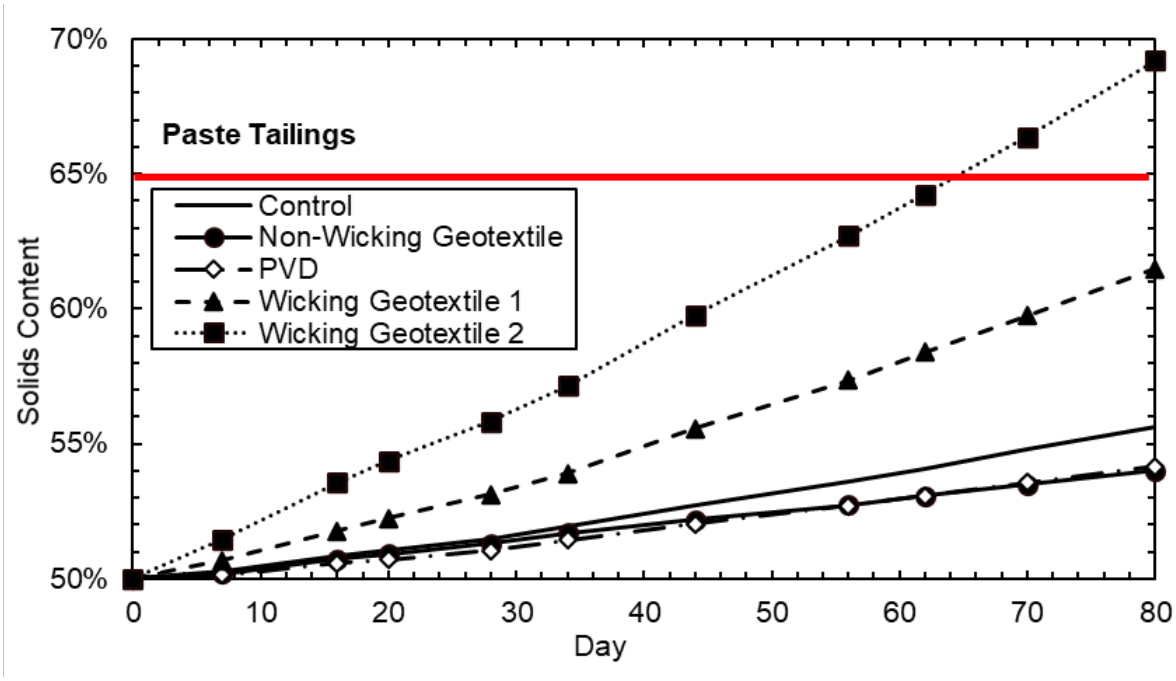

Figure 26 - Dewatered paste boundary surpassed by wicking geotextile 2.

5.4 Radial Zone of Influence of Wicking Geotextiles

As the tailings columns were deconstructed, gravimetric water content samples were collected at radial distances away from the tailings, as well as throughout the layers. In each column, the minimal variability (± 1%) in the gravimetric water content of the samples indicated water content to be independent of the distance from the geotextile. Therefore, the radial capability of the geotextiles exceeds the radius of columns used. Future testing should include larger diameters columns to better assess the radial wicking capabilities.

6. DISCUSSION

6.1 Magnitude of Drying and Dewatering

Assessing the magnitude of drying and dewatering achievable by the wicking geotextile was conducted to determine if transitioning the tailings from an undrained to drained state is possible. Dewatering beyond the 60% conservative threshold, practiced by industry, would indicate achievement of this transition. In the case of the column experiments, by day 80, between 41 – 48% of the initial water mass had been removed by the wicking geotextiles. The removal of this magnitude of water and achievement of a solids content above 80% has moved the tailings into the filtered tailings dewatering boundary. These interim results produced contradictory to the magnitude of dewatering capable by the wicking geotextiles. Due to the rapid dewatering occurring in the wicking geotextile columns, the assumption was that the tailings were at lower water contents than the tailings in the other columns. However, final water content samples showed relatively uniformity between all the columns.

To assess the maximum extent of the tailings dewatering with and without the geotextile aid, the tailings beaker experiments and shrinkage ring testing results were assessed. Overall, these tests produced the best data to assess the magnitude of dewatering capability of the wicking geotextile. Ultimately, all samples (with or without some form of geotextile) lost similar magnitudes of water, reached similar void ratios, and similar densities. Therefore, the wicking geotextiles are not believed to have the capability to increase the final dry density of surficial or exposed tailings. Although the geotextile does not dewater to a greater extent or produce a higher density material compared to natural drying processes – the geotextile can achieve desired results

faster. Additionally, the wicking geotextiles showed potential to overcome capillary barriers that formed in the column experiments and greatly impeded natural water loss via evaporation.

6.2 Rate of Drying and Dewatering

The rate of drying and dewatering due to the introduction of the wicking geotextiles into the tailings slurry was assessed. The ability of the wicking geotextile to accelerate dewatering and therefore reduce the consolidation period was assessed in both the beaker and column experiments. Envisioned implementation of wicking geotextiles are shown in Figures 27 and 28. Figure 27 displays dewatering occurring while the mine is operational and therefore both surface and pore water dewatering will be accelerated by the wicking geotextiles. Figure 28 displays dewatering that would occur in a legacy TSF in which the geotextiles would need to be installed following TSF closure.

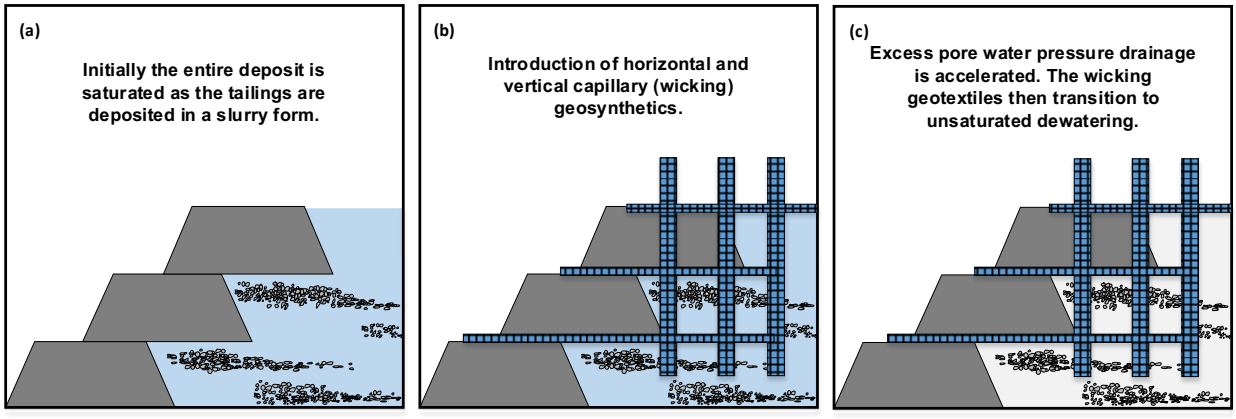

Figure 27 – (a) Operational TSF at full saturation with the (b) installation effects of horizontal and vertical wicking geotextiles to (c) accelerate excess pore water drainage and unsaturated dewatering.

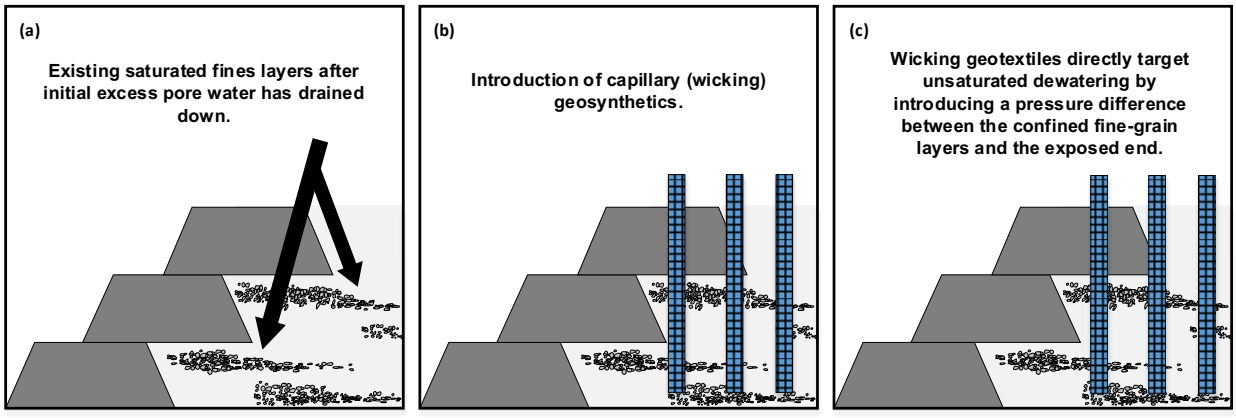

Figure 28 – (a) Closed TSF with no excess pore water pressure and saturated fine layers representing (b) installation effects of vertical wicking geotextiles to (c) aid in unsaturated dewatering.

In both scenarios, the wicking geotextiles theoretically aided in unsaturated dewatering and increased the consolidation rate of the tailings deposit. Accelerated drying during placement emulates filtered tailings deposition and densifies the freshly deposited tailings. Accelerated drying in-situ implies the ability to overcome capillary barriers. Both the beaker and column experiments illustrated clear achievement of faster rates of drying induced by the geotextiles. These experimental results support the final schematics and the conclusions that increased tailings consolidation rates are expediated by the introduction of wicking geotextiles.

6.3 Overcoming Capillary Barriers

The wicking geotextile creates a capillary continuum from the fine-grained tailings layer to the atmosphere. The columns water-content schematics displayed the wicking geotextiles removing water directly from the tailings layer and transferring the water to the atmosphere, overriding the capillary barriers formed by the fine grain and coarse grain sand. However, since this series of columns was deconstructed prior to an asymptote being reached, a definitive statement on the capillary dewatering success of the wicking geotextile cannot be made. Additional long-duration testing has been started concurrent to the finalization of this document. The ability of wicking geotextiles to remove both excess and non-excess pore water out of

tailings is a novel characteristic. Dewatering excess pore water pressure would decrease the pressure existing within the system; then transitioning to non-excess, or hydrostatic, dewatering may aid in desaturating to a degree where overly conservative estimates of strength are not needed. At the time of writing this, no known passive methods of dewatering are available to remove capillary non-excess pore water beyond gravity drainage. This renders the capabilities of existing passive methods, such as PVDs, relatively futile for legacy TSFs in which water is already retained by capillary barriers.

6.4 Potential Advantages and Disadvantages of Passive Dewatering

Passive dewatering is a low cost and energy effort way to increase the stability of a TSF. Due to the methods operating relatively independently, without additional energy or reagent input, following initial installation, the operation and maintenance efforts are reduced in comparison to active dewatering. However, a significant disadvantage of passive dewatering is that all currently available methods have a limited working range and will not remove water beyond that point. The effectiveness of each passive dewatering method can be estimated to find the lifespan and capability, and in turn, the practicality of installation. Additionally, initial installation of passive dewatering methods poses danger. In the case of PVD installation, pushing the hollow mandrel into the ground may cause pore water pressure to increase in sensitive deposits, due to the vibratory nature of the machinery. If the dispersed saturated layers generate enough pore water pressure, a series of localized liquefactions ensue and may evolve into a global deposit failure.

Installation of wicking geotextiles may look like that for PVDs. This is a conundrum, as the purpose of passive dewatering is to eventually create a more stable landform by reducing the total risk of liquefaction. However, liquefaction concerns of a deposit can be reduced if the

tailings behavior is deemed dilative rather than contractive. This represents an additional research challenge.

A significant advantage of dewatering using wicking geotextiles is the ability to move the tailings behavior from undrained and contractive to drained and potentially dilative, by overcoming capillary barriers. Wicking geotextiles have a working range of desaturation up to a suction of 1000 kPa. For Mine P tailings, this corresponds to a saturation of 28%. The fine tailings transition from a saturation of 98% due to the capillary barrier effect of the fine sand to below the 60% threshold for assuming drained behavior. The wicking geotextile reduces the water content of the tailings by an additional 20% and the saturation by 70%. This additional reduction would be beyond the filtered tailings dewatered boundary.

Dewatering tailings stabilizes the deposit and strengthens the material to decrease the estimated liability. Dewatering is viewed as a continuum based on solids content boundaries. Transitioning conventional tailings to a thickened or paste state in-situ is an additional benefit of the wicking geotextiles. The column and beaker experiments confirmed the wicking geotextile's ability to reach these continuum boundaries much earlier than what could be achieved by natural processes. The stated advantages and disadvantages of the wicking geotextiles should be considered in future research of the capabilities of passive dewatering methods.

6.5 Recommended Next Steps

The capability of the wicking geotextiles to dewater tailings in-situ is a novel application and further research should be conducted to support the findings of this research. In addition to creating another round of column tests to further assess the wicking geotextiles dewatering capability, there are a few recommended next steps:

- Determining how high the wicking geotextiles can lift water from a ponded source or from within an in-situ capillary layer to assess the working range of depths.
- Reassessing the ASTM mechanical properties of the original wicking geotextile design and the newer geotextile design to support previous characterizations.
- Extended testing on the tailings in contact with the wicking geotextile, after the testing period is concluded, to determine if the assumption that the wicking geotextile is transitioning the tailings from an undrained to drained state is correct.
- Conducting a field pilot test to evaluate effectiveness under real-world conditions. Laboratory testing cannot always provide accurate representations of field behavior and field behavior is essential to understand real-world conditions.
- Determining optimal deployment strategies and spacing of wicking geotextiles in a physical setting.
- Conducting a cost-benefits analysis to explore the feasibility of using wicking geotextiles in place of PVDs. Since PVDs are the current state of practice for passive in-situ dewatering, PVDs provide a baseline for comparison.

7. SUMMARY AND CONCLUSION

The magnitude of impact associated with attempting to mitigate liquefaction concerns of legacy TSFs is not well defined. However, stability concerns must be addressed. Review of available literature and geotechnical characterization data on the legacy case studies showed that fine-grain saturated layers may often exist in the center of a TSF even in extremely arid climates. Essentially, a completely dried crust forms across the entire surface of the tailings deposit due to historic drain down and evaporation of the uppermost layers. The center of the TSF experiences initial drain down of excess pore water, but eventually reaches a point where the formation of capillary barriers at the interfaces of coarser- and finer- grain tailings impedes further desaturation. The fine grain layers continue to drain down but at rates so incredibly slow that legacy TSFs closed over 100 years ago still display fully saturated fines layers.

Dewatering of legacy TSFs is a viable path to increasing the general strength and stability of the deposit and reduce liquefaction potential. Dewatering of tailings prior to deposition is an increasingly evaluated method in tailings and several methods of dewatering are available. Dewatering is conducted to various water contents and therefore is understood as a continuum. Reviewing the general past 100 years of tailings management practice, the development of technology to dewater already place tailings appears to receive less industry and research focus.

Some in-situ dewatering methods are available and are of common practice. However, existing dewatering methods, such as PVDs, can only remove excess pore water pressure from saturated tailings. No currently available methods can dewater tailings in unsaturated conditions by overcoming existing capillary barriers.

As a potential solution to dewatering beyond excess porewater pressure, use of a wicking geotextile is proposed. This wicking geotextile has been used in pavement but is a novel approach to dewatering tailings. To assess the geotextile potential, column testing was conducted that simulated in-situ legacy TSF stratigraphy. Column tests used fine-grain sand to confine the water held within the initially slurry tailings. Throughout the testing period, the wicking geotextiles were observed dewatering at a rate 1.5 – 2 times faster than the control. At the end of the 80-day testing period, the columns were deconstructed, and gravimetric water content samples were collected. The water content samples taken from the midpoint of the tailings layer ranged between 25 – 31% for all columns, with the control having the highest moisture content and the wicking geotextile 1 having the lowest moisture content.

Additionally, shrinkage ring testing was conducted to determine the dried void ratio of tailings with different solids contents with and without the wicking geotextiles. Across all samples, the final void ratio ranged between 0.32 – 0.46, with corresponding densities of 1.98 – 1.80 g/cm^3. To support the conclusions of shrinkage ring testing, beaker experiments explored the surficial dewatering capabilities of the wicking geotextiles. Beakers at varying solids contents (50%, 40%, and 30%) showed that the wicking geotextiles dewater at rates 2 – 3 times that of natural processes, however, given enough time, all samples will dewater to completion.

The following conclusions are extracted from this study:

- Reviewed legacy TSF characterization data show that interbedded layers of near saturated fines exist within the tailings. These fine layers desaturate on the magnitude of hundreds to thousands of years, and therefore as they currently exist may pose liquefaction concerns.

- Wicking geotextiles can accelerate water removal from the tailings up to 2.8 times the rate of natural dewatering processes as illustrated by column and beaker tests. These results highlight that incorporation of capillary geosynthetics is a potential method to enhance the rate of evaporative drying of exposed tailings.
- However, for exposed evaporative drying, shrinkage ring tests show that the geotextiles and the control reach a similar void ratio and density after complete drying.
    - An initial solids content of 50% averaged a final density of 1.87 g/cm^3.
    - An initial solids content of 60% averaged a final density of 1.80 g/cm^3.
    - An initial solids content of 70% averaged a final density of 1.95 g/cm^3.
- The wicking geotextiles have potential to overcoming in-situ capillary barriers by creating continuous conduits for moisture removal in tailings. The SWCCs and HCFs show that the wicking geotextiles have a working range up to 1000 kPa of. The column experiments show that water within a confined tailings layer can be wicked to the surface via the inner-yarn drainage path of the wicking geotextile, bypassing coarse-grained capillary barriers.
- Wicking geotextiles have been used in pavement design to prevent water migration further into the subgrade. Use of wicking geotextiles is a novel approach to finding a solution to strengthening and stabilizing legacy TSFs via passive dewatering.

To further assess the practicality of using wicking geotextiles in the field, repeat testing should be done to support previously defined geotechnical properties. Testing would include generations of the SWCC for the geotextile, to assess the unsaturated hydraulic conductivity and

associate working suction ranges. Additionally, a field pilot test should be conducted alongside a cost of installation analysis.

REFERENCES

Adams, A., Friedman, D., Brouwer, K., and Davidson, S. (2017). Tailings Impoundment Stabilization to Mitigate Mudrush Rise. *85th Annual Meeting of International Commission on Large Dams*.

Aghazamani, N. (2022). *Unsaturated fluid flow and volume change behavior of filtered tailings* [PhD, Colorado State University]. https://hdl.handle.net/10217/235334

ASTM D422-63. (2007). "Standard test method for particle-size analysis of soils," West Conshohocken, PA, www.astm.org, DOI: 10.1520/D0422-63R07E02.

ASTM D2487-11. (2011). "Standard practice for classification of soils for engineering purposes (unified soil classification system)," West Conshohocken, PA, www.astm.org, DOI: 10.1520/D2487-11.

ASTM D4318-10. (2014). "Standard test methods for liquid limit, plastic limit, and plasticity index of soils," West Conshohocken, PA, PA, www.astm.org, DOI: 10.1520/D4318-10.

ASTM D698-12. (2014). "Standard test methods for laboratory compaction characteristics of soil using standard effort (12400ft-lbf/ft^3 (600 kN-m/m^3))," West Conshohocken, PA.

ASTM D854-14. (2014). "Standard test methods for specific gravity of soil solids by water pycnometer," West Conshohocken, PA, www.astm.org, DOI: 10.1520/D0854-14.

ASTM D4943-18. (2018). "Standard test method for shrinkage factors of cohesive soils by the water submersion method," West Conshohocken, PA, www.astm.org.

ASTM D4491/D4491M-20. (2020). "Standard test method for water permeability of geotextiles by permittivity," West Conshohocken, PA, www.astm.org.

ASTM D6767-21. (2021). "Standard test method for pore size characteristics of geotextiles by capillary flow test," West Conshohocken, PA, www.astm.org.

ASTM D4751-21a. (2021). "Standard test methods for determining apparent opening size of a geotextile," West Conshohocken, PA, www.astm.org.

ASTM D4595/D4595M-23. (2023). "Standard test method for tensile properties of geotextiles by the wide-width method," West Conshohocken, PA, www.astm.org.

Ayala, J., Fourie, A., and Reid, D. (2023). A Unified Approach for the Analysis of CPT Partial Drainage Effects within a Critical State Soil Mechanics Framework in Mine Tailings. *Journal of Geotechnical and Geoenvironmental Engineering*, *149*(6), 04023036. https://doi.org/10.1061/JGGEFK.GTENG-10915

Azevedo, M., and Zornberg, J. (2013). Capillary barrier dissipation by new wicking geotextile. In: Panamerican Conference on Unsaturated Soils, pp. 20–22.

Baker, R. and Hillel, D. (1990). Laboratory tests of a theory of fingering during infiltration into layered soils. *Soil Science Society of America Journal*, *54*, 20–30.

Banerjee, A., Puppala, A., and Hoyos, L. (2022). Liquefaction Assessment in Unsaturated Soils. *Journal of Geotechnical and Geoenvironmental Engineering*, *148*(9), 04022067. https://doi.org/10.1061/(ASCE)GT.1943-5606.0002851

Caldwell, J. and Van Zyl, D. (2011). Thirty Years of Tailings History from Tailings & Mine Waste. *Proceedings Tailings and Mine Waste 2011*.

Cao, B., Tian, Y., Gui, R., and Liu, Y. (2021). Experimental Study on the Effect of Key Factors on the Soil–Water Characteristic Curves of Fine-Grained Tailings. *Frontiers in Environmental Science*, *9*. https://www.frontiersin.org/articles/10.3389/fenvs.2021.710986

Carneiro, A., Fourie, A., Jewell, R., and Fourie, B. (2018). A conceptual cost comparison of alternative tailings disposal strategies in Western Australia. *Australian Centre for Geomechanics,* 439-454. https://doi.org/10.36487/ACG_rep/1805_36_Carneiro

Casey, J., Chambers, R., and Eng, P. (2022). Characterizing Tailings Behavior at the San Manuel Copper TSFs Part 1: In-situ and Laboratory Geotechnical Techniques. *Proceedings of the 26th International Conference on Tailings and Mine Waste*, 652–653.

Davies, M. (2011). Filtered Dry Stacked Tailings – The Fundamentals. *Proceedings Tailings and Mine Waste 2011*.

Dejong, J. and Randolph, M. (2012). Influence of partial consolidation during cone penetration on estimated soil behavior type and pore pressure dissipation measurements. *Journal of Geotechnical and Geoenvironmental Engineering, 138*, 777–788. https://doi.org/10.1061/(ASCE)GT.1943-5606.0000646.

Engels, J. and Dixon-Hardy, D. (2004). Tailings disposal - Today's storage of high volumes of waste from mines. *JKMRC Conference 2004*, Brisbane, Australia: 13.

Erickson, B., Butikofer, D., Marsh, A., Friedel, R., Murray, L., and Piggott, M. (2017). Filtered Tailings Disposal Case History: Operation and Design Considerations Part I – KCB. *International Conference on Tailings and Mine Waste*. https://klohn.com/technical-papers/filtered-tailings-disposal-case-history-operation-and-design-considerations-part-i/

Figueiredo, J., Vila, M., Matos, K., Martins, D., Futuro, A., Dinis, M., Góis, J., Leite, A., and Fiúza, A. (2018). Tailings reprocessing from Cabeço do Pião Dam in Central Portugal: A kinetic approach of experimental data. *Journal of Sustainable Mining, 17*(3), 139–144. https://doi.org/10.1016/j.jsm.2018.07.001

Franks, D., Stringer, M., Baker, E., Valenta, R., Torres-Cruz, L., Thygesen, K., Matthews, A., Howchin, J., and Barrie, S. (2020). Lessons from tailings facility data disclosures. *Towards Zero Harm - A Compendium of Papers Prepared for the Global Tailings Review*, 84–109.

Fredlund, D., Rahardjo, H., and Fredlund, M. (2012). *Unsaturated Soil Mechanics in Engineering Practice*. Wiley. https://books.google.com/books?id=jWFK5UgUG0IC

Furnell, E., Bilaniuk, K., Goldbaum, M., Shoaib, M., Wani, O., Tian, X., Chen, Z., Boucher, D., and Bobicki, E. (2022). Dewatered and Stacked Mine Tailings: A Review. *ACS ES&T Engineering*, *2*(5), 728–745. https://doi.org/10.1021/acsestengg.1c00480

Gipson, A. (1998). Tailing disposal – the last 10 years and future trends. *Proceedings of the Fifth International Conference*, 127–138.

Godley, D. and Quaglia, G. (2023). Deconstruction of an Upstream Raised Tailings Storage Facility: Project Design and Execution. *Proceedings of Tailings and Mine Waste 2023.* Vancouver, BC.

Gorakhki, M., Bareither, C., Scalia, J., and Jacobs, M. (2019). Hydraulic Conductivity and Soil Water Retention of Waste Rock and Tailings Mixtures. *Geo-Congress 2019.* 41–50. https://doi.org/10.1061/9780784482148.005

Guo, J., Han, J., Zhang, X., and Li, Z. (2019). Evaluation of moisture reduction in aggregate base by wicking geotextile using soil column tests. *Geotextiles and Geomembranes*, *47*(3), 306–314. https://doi.org/10.1016/j.geotexmem.2019.01.014

Hardy, J., Lindstrom, R., Bingham, L., Fuller, A., and Krohn, C. (2003). Characterization and design of the old dominion remedial action plan. *National Meeting of the American Society of Mining and Reclamation and the 9th Billings Land Reclamation Symposium,* 329–352.

Hill, J., Kolz, J., Gerondale, A., and Fisher, D. (2015). Improvement of geotechnical and environmental conditions of mine tailings facilities by pre-fabricated vertical drains and jet grouting. *Proceedings Tailings and Mine Waste 2015.* Vancouver, BC.

Jaeger, R., Dejong, J., Boulanger, R., Low, H., and Randolph, M. (2010). "Variable penetration rate CPT in an intermediate soil." *In Proc., 2nd Int. Symp. on Cone Penetration Testing (CPT10)*. Huntington Beach, CA.

Jefferies, M. and Been, K. (2016). Soil Liquefaction: A Critical State Approach. CRC press, Boca Raton.

Kalsnes, B., Jostad, H., Nadim, F., Hauge, A., Dutra, A., and Muxfeldt, A. (2017). Tailings Dam Stability. In M. Mikos, B. Tiwari, Y. Yin, and K. Sassa (Eds.), *Advancing Culture of Living with Landslides*. Springer International Publishing. 1173–1180. https://doi.org/10.1007/978-3-319-53498-5_133

Keaton, J. (2018). Dilatancy. In P. T. Bobrowsky and B. Marker (Eds.), *Encyclopedia of Engineering Geology*. Springer International Publishing. 231–232. https://doi.org/10.1007/978-3-319-73568-9_91

Khire, M., Benson, C., and Bosscher, P. (1999). Field Data from a Capillary Barrier and Model Predictions with UNSAT-H. *Journal of Geotechnical and Geoenvironmental Engineering*, *125*(6), 518–527. https://doi.org/10.1061/(ASCE)1090-0241(1999)125:6(518)

Klohn, E. and Maartman, C. (1972). Construction of Sound Tailings Dams by Cycloning and Spigotting. *Proceedings of the 1st International Tailing Symposium, October 31-November 3, 1972*. Tucson, Arizona.

KCB. (2020). *History of Tailings Dam Design*. https://klohn.com/blog/history-of-tailings-dam-design/

Lin, C. and Zhang, X. (2018). Laboratory Drainage Performance of a New Geotextile with Wicking Fabric. *Journal of Materials in Civil Engineering*, *30*(11), 04018293. https://doi.org/10.1061/(ASCE)MT.1943-5533.0002476

Lin, C., Zhang, X., and Han, J. (2016). Development of a Design Method for H2Ri Wicking Fabric in Pavement Structures. *Center for Environmentally Sustainable Transportation in Cold Climates*. https://scholarworks.alaska.edu/handle/11122/10398

Lockhart, N. C. (1983). Electro-osmotic dewatering of fine tailings from mineral processing. *International Journal of Mineral Processing*, *10*(2), 131–140. https://doi.org/10.1016/0301-7516(83)90038-8

Maghous, S. and J. Dejong. (2018). Piezocone penetration rate effects in transient gold tailings. *Journal of Geotechnical and Geoenvironmental Engineering 144* (2): 04017116. https://doi.org/10.1061/(ASCE)GT .1943-5606.0001822.

Mahabub, S., Alahi, F., and Al Imran, M. (2023). Unlocking the potential of microbes: Biocementation technology for mine tailings restoration — a comprehensive review. *Environmental Science and Pollution Research*, *30*(40), 91676–91709. https://doi.org/10.1007/s11356-023-28937-4

Martin, L., Alizadeh, V., and Meegoda, J. (2019). Electro-osmosis treatment techniques and their effect on dewatering of soils, sediments, and sludge: A review. *Soils and Foundations*, *59*(2), 407–418. https://doi.org/10.1016/j.sandf.2018.12.015

Martin, T. and McRoberts, E. (1999). Some considerations in the stability analysis of upstream tailings dams. *Tailings and Mine Waste '09, Proceedings 13th International Conference On Tailings and MineWaste*.

Martin, T., Davies, M., Rice, S., Higgs, T., and Lighthall, P. (2002). Stewardship of Tailings Facilities. *Mining, Minerals and Sustainable Development*, *20*.

Masengo, E., Julien, M., Lavoie, P., Lepine, T., Nousiainen, J., Saukkoriipi, J., Piekkari, M., and Karvo, J. (2019). Enhancement of contractive tailings using deep soil mixing technique at Kittilä min. *Sustainable and Safe Dams Around the World.* 3396–3409. https://doi.org/10.1201/9780429319778-306

McLeod, H., and A. Bjelkevik. (2017). Tailings Dam Design: Technology Update (ICOLD Bulletin). *Proceedings of the 85th Annual Meeting of International Commission on Large Dams, July 3-7, 2017.* Prague, Czech Republic: Czech National Committee on Large Dams.

McPhail, G., Ugaz, R., Garcia, F., Paterson, A., Fourie, A., and Reid, D. (2019). Practical tailings slurry dewatering and tailings management strategies for small and medium mine. *Australian Centre for Geomechanics.* 235–243 https://doi.org/10.36487/ACG_rep/1910_15_McPhail

Molina-Gómez, F., Ferreira, C., and Cordeiro, D. (2021). An integrated interpretation of SCPTu for liquefaction assessment in intermediate alluvial deposits in Portugal. *Proceedings of the 6th International Conference on Geotechnical and Geophysical Site Characterization*.

Morrison, K. (2022). Tailings Management Handbook: A Life-Cycle Approach. The *Society for Mining, Metallurgy & Exploration.* https://www.smenet.org/productdetail?productid=27873533

Nelson, P. (2023). New Directions for Tailings Management. *Proceeding of Tailings and Mine Waste 2023, November 5 – 8, 2023.* Vancouver, BC.

NOAMI | National Orphaned/Abandoned Mines Initiative. (n.d.). Retrieved December 7, 2023, from https://abandoned-mines.org/en/

Plewes, H., Davies, M., and Jefferies, M. (1992). CPT based screening procedure for evaluating liquefaction susceptibility. *Proceedings of the 45th Canadian Geotechnical Conference, Toronto Ontario.* Toronto, ONT.

Prefabricated Vertical Drains (PVD). (2018). Keller Middle East. https://www.kellerme.com/expertise/techniques/prefabricated-vertical-drains-pvd

Robertson, A. (1986). Mine waste disposal: An update on geotechnical and geohydrological aspects. *Geotechnical and Geohydrological Aspects of Waste Management: Proceedings of the Eighth Symposium,* Fort Collins, CO. Colorado State University. 31–50.

Robertson, P. (2010). Evaluation of Flow Liquefaction and Liquefied Strength Using the Cone Penetration Test. *Journal of Geotechnical and Geoenvironmental Engineering, 136*(6), 842-852.

Robertson, P and Campanella, R. (1983). Interpretation of cone penetration tests – Part I (sand). *Canadian Geotechnical Journal, 20*(4): 718-733.

Russell, A., Vo, T., Ayala, J., Wang, Y., Reid, D., and Fourie, A. (2022). Cone penetration tests in saturated and unsaturated silty tailings. *Géotechnique*, 1–15. https://doi.org/10.1680/jgeot.21.00261

Rust, E., and Rust, M. (2023, November 5). Determination of the Degree of Saturation above the Water Table from CPTu Probing in Tailings. *Proceedings of Tailings and Mine Waste 2023*.

Scarfone, R., Wheeler, S., and Lloret-Cabot, M. (2020). Conceptual hydraulic conductivity model for unsaturated soils at low degree of saturation and its application to the study of capillary barrier systems. *Journal of Geotechnical and Geoenvironmental Engineering*, *146*(10), Article 10. http://eprints.gla.ac.uk/223568/

Schafer, M., Dugie, M., An, R., and Wightman, A. (2019). State Parameter Estimation by CPTu Interpretation for Liquefaction Susceptibility—A Comparison of Methods. *Geo St. John's 2019.*

Shackelford, C. (2003). Geoenvironmental Engineering. In R. A. Meyers (Ed.), *Encyclopedia of Physical Science and Technology (Third Edition)* (pp. 601–621). Academic Press. https://doi.org/10.1016/B0-12-227410-5/00879-6

Shang, J., and Mohamedelhassan, E. (2012). Electrokinetic Dewatering of Eneabba West Mine Tailings: A Laboratory Experimental Study. *Soft Ground Technology.* 346–357. https://doi.org/10.1061/40552(301)27

Silva, M. and Bolton, M. (2004). Centrifuge penetration tests in saturated layered sands. *Proceedings ISC-2 on Geotechnical and Geophysical Site Characterization*.

Spencer, D., Bareither, C., Scalia IV, J., Hatton, C., and Ward, K. (2022). Characterizing tailings professional labor demand. *Mining Engineering*, *74*(277), 16–16.

Stormont, J., and Anderson, C. (1999). Capillary Barrier Effect from Underlying Coarser Soil Layer. *Journal of Geotechnical and Geoenvironmental Engineering*, *125*(8), 641–648. https://doi.org/10.1061/(ASCE)1090-0241(1999)125:8(641)

Stormont, J. and Morris, C. (1998). Method to Estimate Water Storage Capacity of Capillary Barriers. *Journal of Geotechnical and Geoenvironmental Engineering*, *124*(4), 297–302. https://doi.org/10.1061/(ASCE)1090-0241(1998)124:4(297)

Suits, L., Sheahan, T., Malusis, M., Evans, J., McLane, M., and Woodward, N. (2008). A Miniature Cone for Measuring the Slump of Soil-Bentonite Cutoff Wall Backfill. *Geotechnical Testing Journal - GEOTECH TESTING J*, *31*. https://doi.org/10.1520/GTJ101487

Tailings.info ▪ Water Management Considerations for Conventional Storage. (n.d.). Retrieved October 18, 2023, from https://tailings.info/technical/water.htm

Tang, C., Borden, R., and Gabr, M. (2017). Approach for Estimating Effective Friction Angle from Cone Penetration Test in Unsaturated Residual Soils. *Journal of Geotechnical and Geoenvironmental Engineering*, *143*(11), 04017087. https://doi.org/10.1061/(ASCE)GT.1943-5606.0001799

TenCate. (2022). *Mirafi® H2Ri Woven Geosynthetic*. PDF.

Ulrich, B. and Coffin, J. (2017). Characterization of Unsaturated Tailings & its Effects on Liquefaction. *Proceedings of the Twentiy-first International Conference on Tailings and Mine Waste, 5-8 November 2017.* Banff, AL.

Unger, C. (2017). Legacy Issues and Abandoned Mines. Mining in the Asia-Pacific. The Political Economy of the Asia Pacific. O'Callaghan, T. and Graetz, G. (eds). *Springer International Publishing.*

U.S. Geological Survey. (2022). Mineral commodity summaries 2022: U.S. Geological Survey, 202 p., https://doi.org/10.3133/mcs2022.

Vick, S. (1990). Planning, Design, and Analysis of Tailings Dams. *BiTech Publishers LTD*. https://doi.org/10.14288/1.0394902

World mineral statistics data | Statistics & Commodities | MineralsUK. (n.d.). Retrieved December 7, 2023, from https://www2.bgs.ac.uk/mineralsuk/statistics/wms.cfc?method=searchWMS

World Population by Year—Worldometer. (n.d.). Retrieved December 7, 2023, from https://www.worldometers.info/world-population/world-population-by-year/

Yüksek, S. (2022). Electroosmotic Dewatering of Iron Ore Tailings: A Laboratory Study to Improve Geotechnical Properties. *Advances in Civil Engineering*, *2022*, e7662997. https://doi.org/10.1155/2022/7662997

Zhang, X., Presler, W., Li, L., Jones, D., and Odgers, B. (2014). Use of wicking fabric to help prevent frost boils in Alaskan pavements. *ASCE J. Mater. Civil Eng. 26* (4), 728–740.

Zhang, X. and Connor, B. (2015). Evaluate H2RI Wicking Fabric for Pavement Application—Year 2. *Pacific Northwest Transportation Consortium.* https://scholarworks.alaska.edu/handle/11122/10380

Zornberg, J., Azevedo, M., Sikkema, M., and Odgers, B. (2017). Geosynthetics with enhanced lateral drainage capabilities in roadway systems. *Transportat. Geotech. 12*, 85–100.

APPENDIX A – TANK EXPERIMENTS SUPPLEMENTAL DATA

A.1 MATERIALS AND METHODS

Tank experiments were created to emulate the previously described stratigraphy commonly seen in legacy TSFs. This was done by depositing layers of varying granular sizes into the tank above the tailings layer to force the development of capillary barriers. The columns created for this research are based on preliminary results from the tanks.

The tank experiments were the first assessment of the abilty of the wicking geotextiles to dewater tailings. To begin the assessment, three single-layered tanks were created: the control, the wicking geotextile 1 (updated design), and the wicking geotextile 2 (original design). Both geotextiles proved to be more efficient at removing water in comparison to the control after 1 week and therefore inspired a second series of tank experiments. This second series was created with alternating layers of fine and coarse materials. To further assess the capability of the wicking fibers, a woven non-wicking tank was created in addition to the three from the first series. For both series, Mine P tailings were deposited into the bottom of the tank to a height of 7.62 cm and left to settle for one hour. For tanks that contained some form of geosynthetic strip, the material was placed in the tank after tailings deposition and tape was used to keep the textiles upright. The arrangement of strips is shown in Figure A.1.

Two stratigraphies were generated for the tank experiments. The first, Figure A.1a, contained alternating layers of fine and coarse material above the tailings. The second, Figure A.1b, contained a single layer of coarse and a single layer of fines overlaying the tailings. The weights and heights of each layer were recorded. The tanks were weighed at regular intervals to

observe mass loss due to wicking or evaporation of water. The solids contents corresponding to the change in total masses were determined at regular intervals as well.

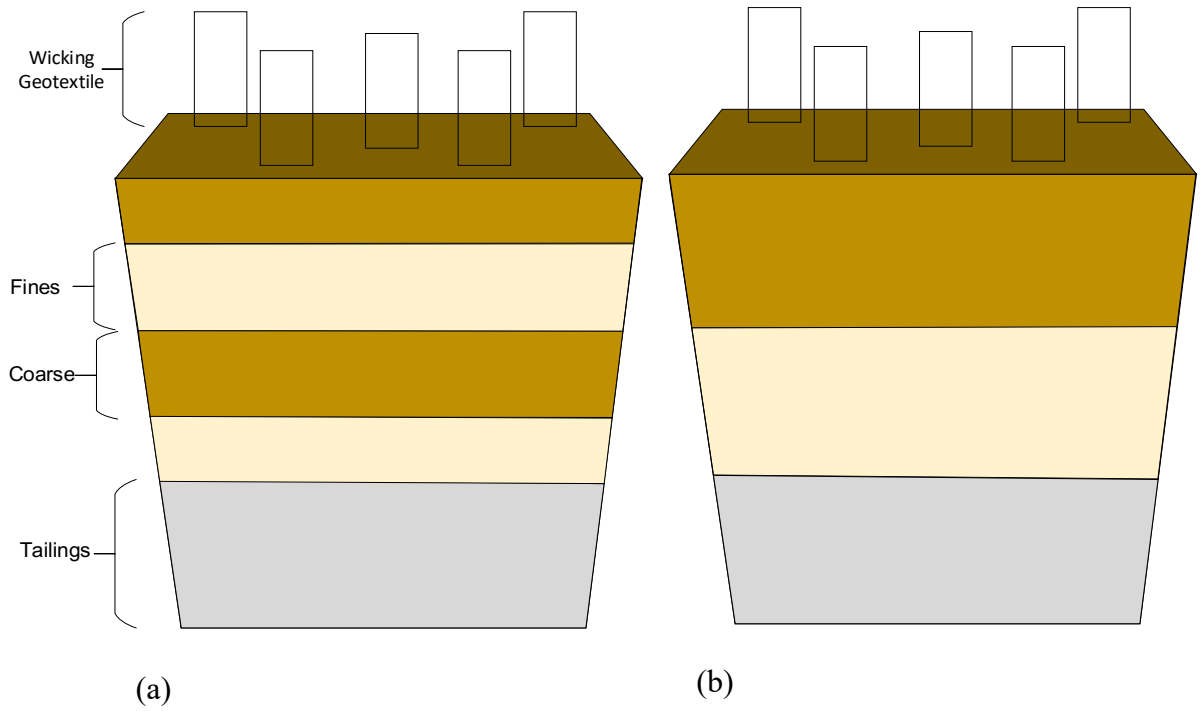

Figure A.1 – (a) Double-layered and (b) single -layered tank experiment configurations.

A.2 RESULTS

A.2.1 Magnitude and Rate of Drying and Dewatering

The assumption upon initial construction of the tank experiments was that the control tailings would reach an asymptote of water loss, due to retained water in the unsaturated tailings layer, and therefore no change in mass would be observed in the tank weight after a certain period of drying. However, after 120 days of drying, all tanks were observed still losing water mass consistently and a plateau had not been achieved, as can be seen in Figure A.2. Therefore, the consistent rate of water mass loss per day, across all tanks, provided sufficient support in the decision to conclude testing at an estimated 1-2 grams of mass loss per day. The equilibirum established across the tanks can be viewed around Day 80 in Figure A.3. The updated assumption is that the tanks would have continued to lose all initial water mass given sufficient time.

The wicking geotextile tanks can be observed dewatering more rapidly than the non-wicking and control tanks. Before reaching a similar rate of dewatering, as noted in Figure A.2, the wicking geotextiles were removed 2 to 4 times as much water mass as the control per day. So, although the tanks reached a similar void ratio and saturation at test completion, the wicking geotextiles achieved a drier state earlier.

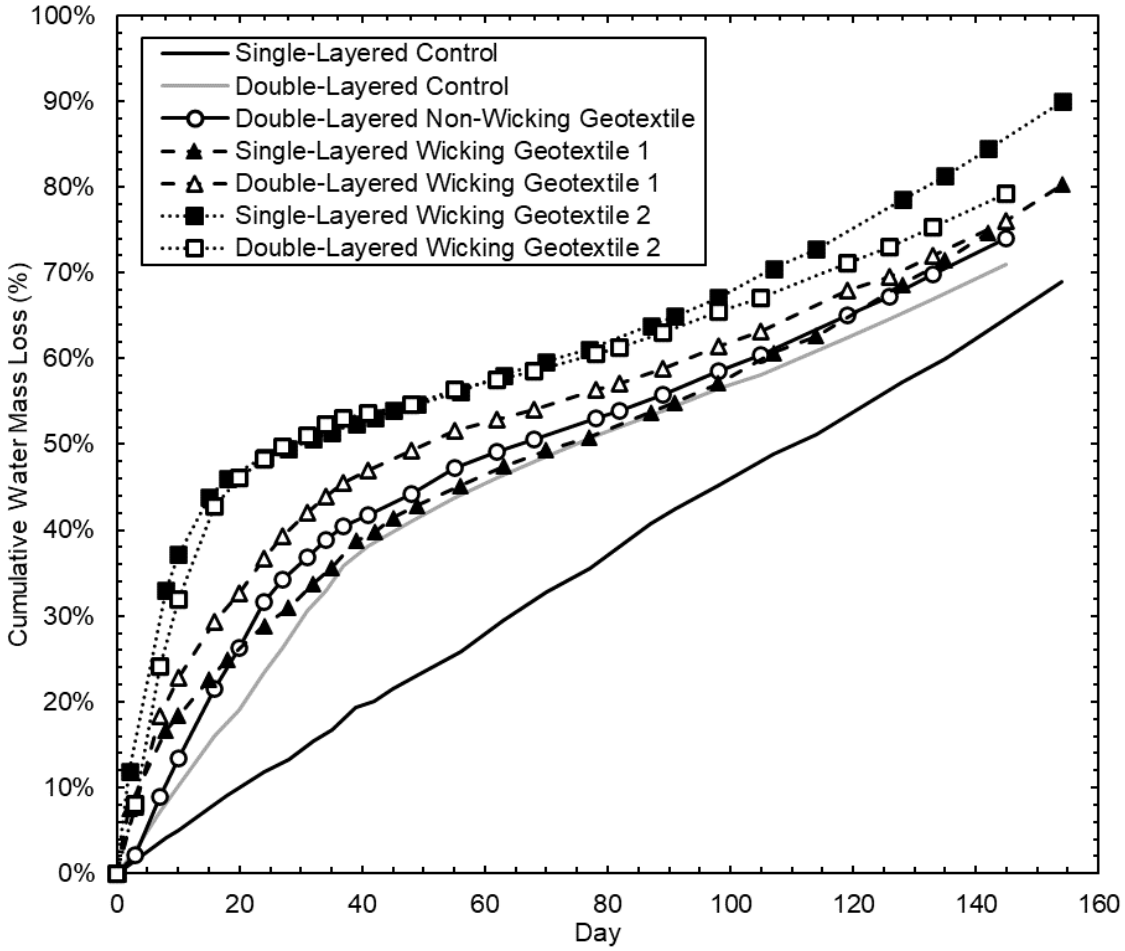

Figure A.2 – Single-layered and double-layered tank experiments cumulative water mass losses.

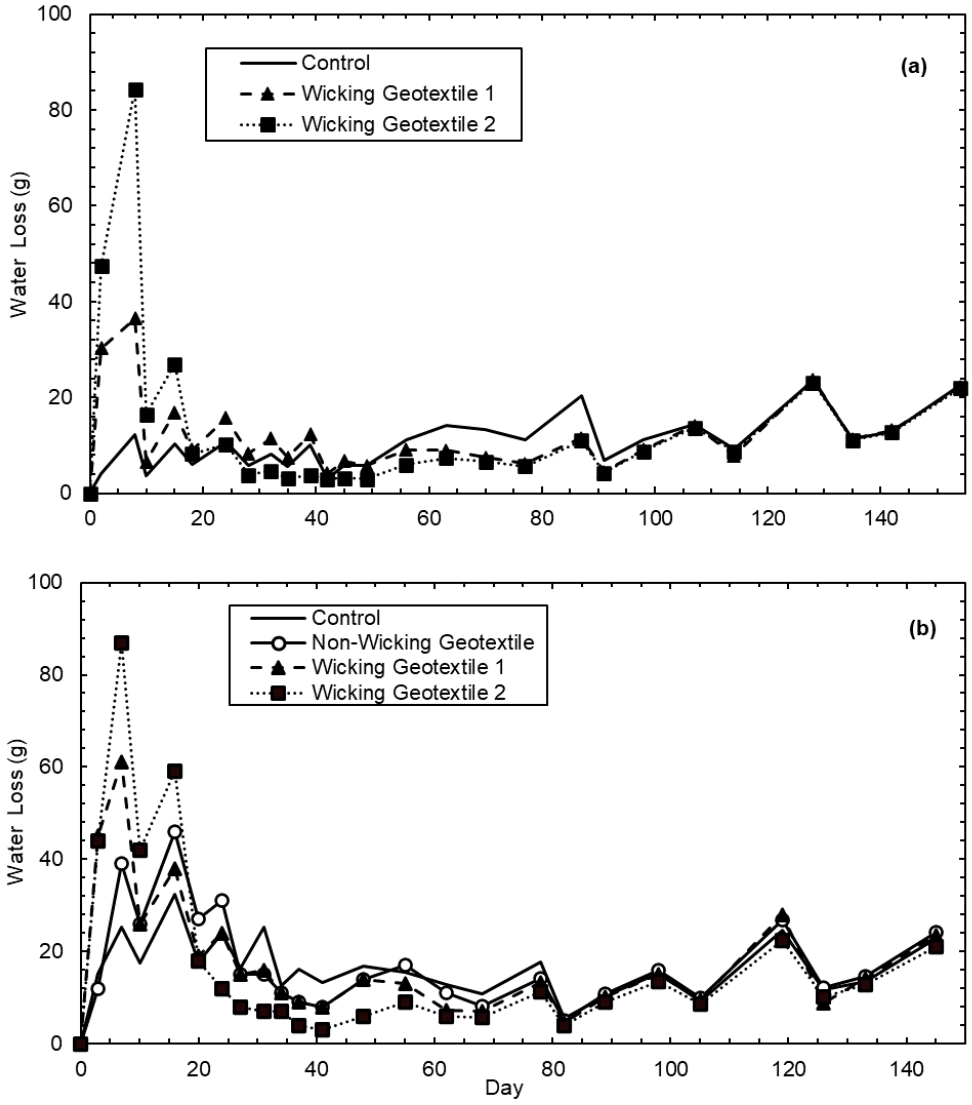

Figure A.3 – (a) Single-Layered and (b) double-layered tank experiment daily water mass losses.

The wicking geotextiles removed a greater magnitude of water from the tailings layer than natural evaporation or gravity processes as observed in the control tank by the conclusion of testing. The percentages of total water mass removed from the initial water mass for each tank are displayed in Figure A.4. These values were determined at the conclusion and deconstruction of the tanks. The single-layered geotextiles removed between 11 and 21 percent more water than the control. The double-layered geotextiles removed between 5 and 8 percent more water than the control. This can be attributed to the fact that a thicker layer of coarse material produces a

stronger capillary barrier and greater impedance of flow, and therefore less water can be removed via evaporation processes.

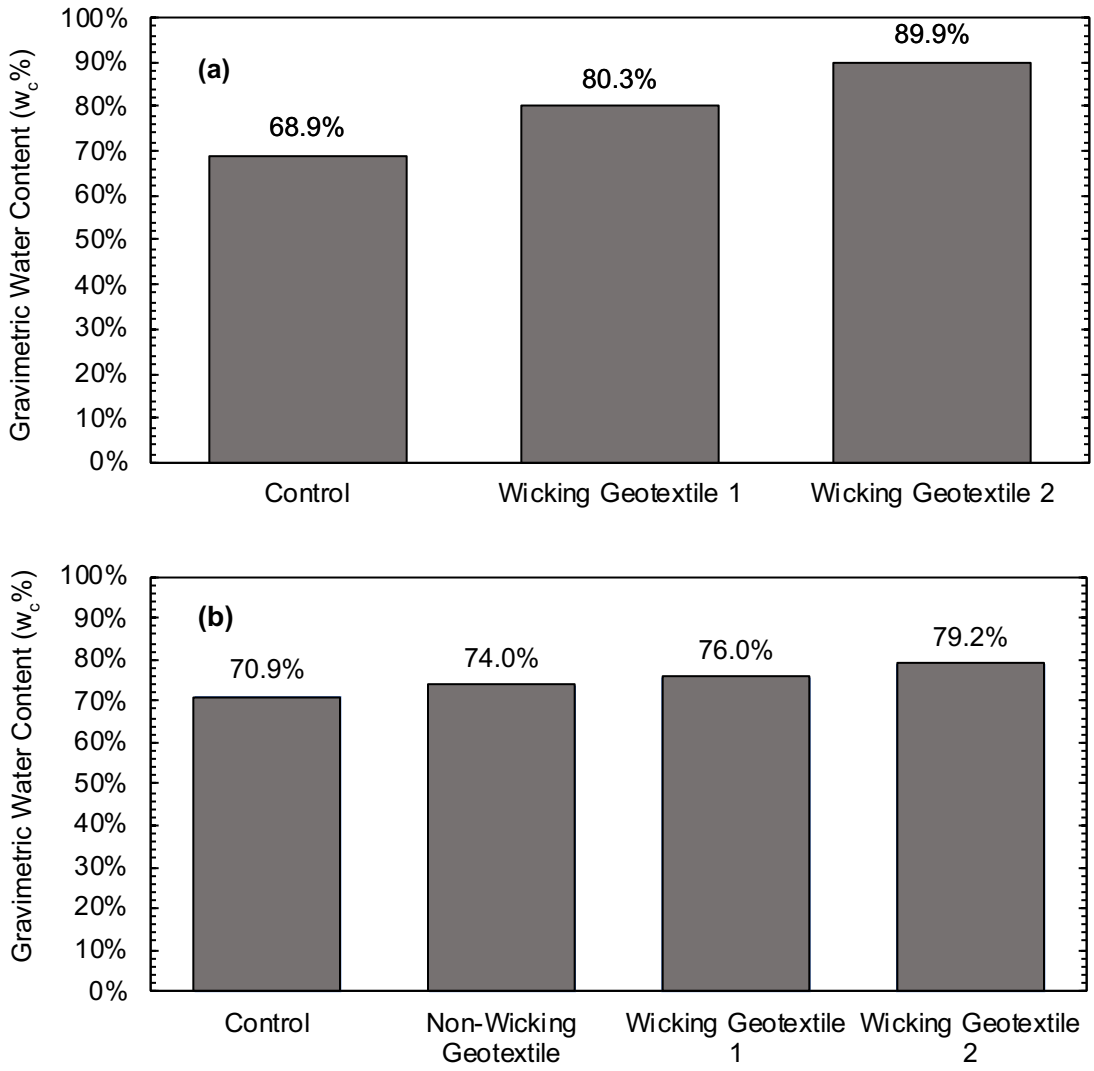

Figure A.4 - Tank experiment water mass losses after 150 days of drying for (a) single-layered and (b) double-layered configurations.

Using the percent of water mass removed is one way to normalize the dewatering of the tank experiments. A second way to normalize the data is to compare the change in solids content throughout the duration of the experiment, as to compare the wicking geotextiles to themselves in varying stratigraphies. The tank experiments were all created at 50% solids contents and the

changes over time are illustrated in Figure A.5. Generally good agreement can be seen in the geotextile 2 data early on.

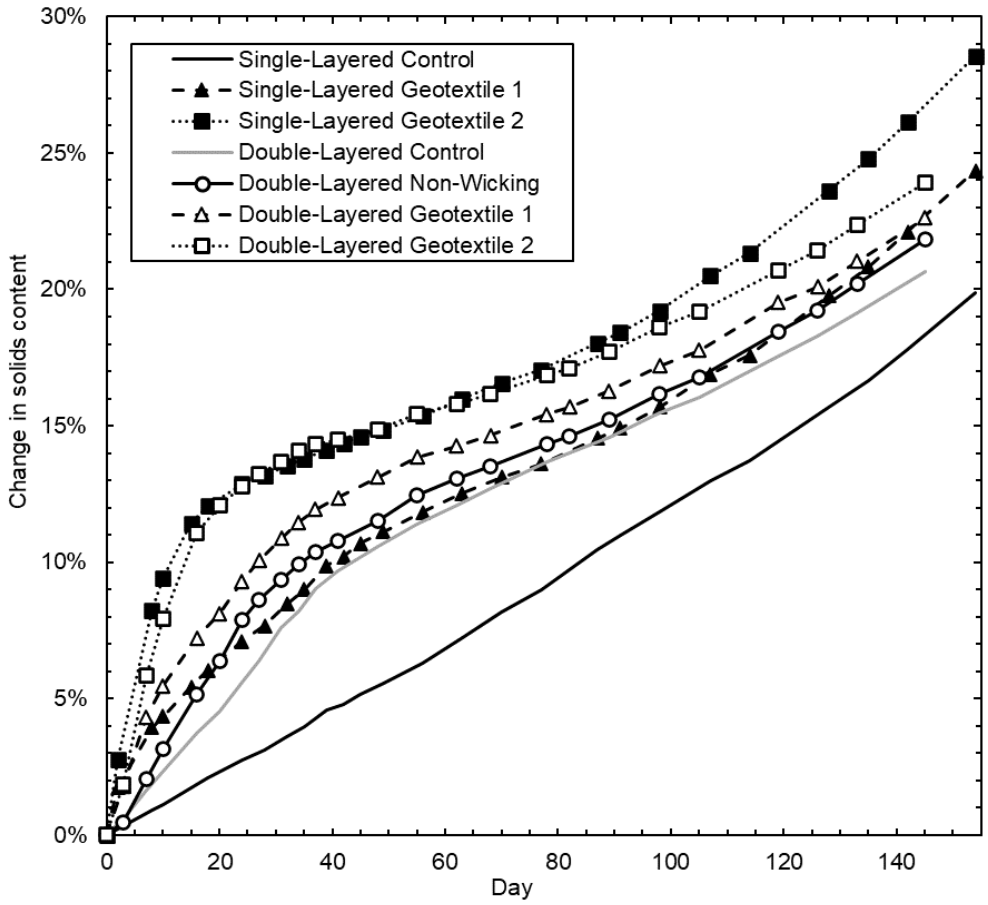

Figure A.5 – Single-layered and double-layered tank experiments change in solids contents.

Water content samples were collected vertically throughout each of the tanks. Figure A.6 is a schematic representation of the water contents seen throughout the layering of the tanks. The schematic shows that the wicking geotextiles removed a greater percentage of water than the control in the single-layered configuration, but a relatively similar amount of water in the double-layered configuration. No water was found in any samples taken from the coarse or fine sand layers throughout.

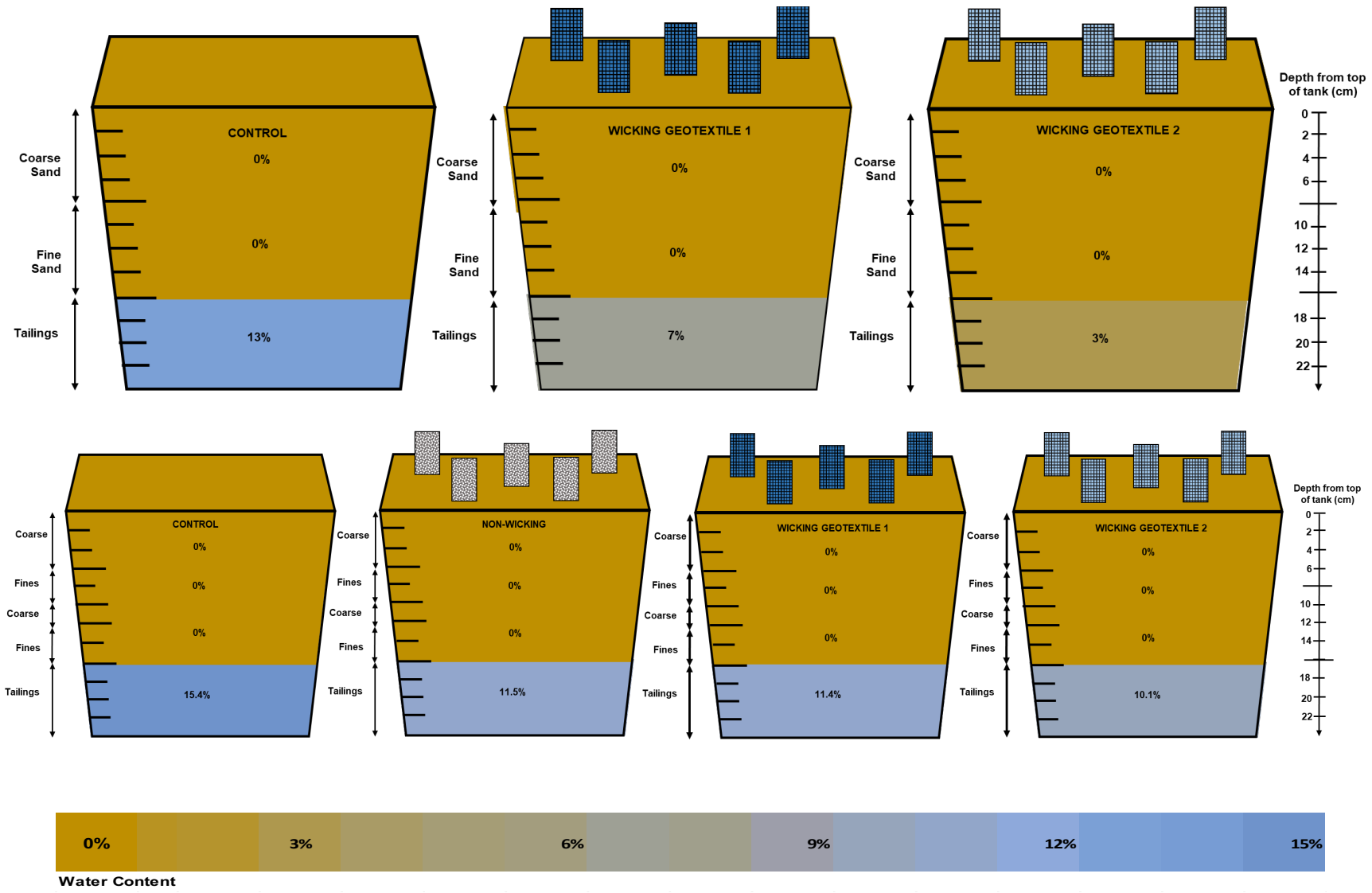

Figure A.6 - Tank experiments schematics representing water content samples versus depth

A.2.2 Radial Capability of Wicking Geotextiles

Gravimetric water content samples were collected during tank experiment deconstruction. Samples were collected at varying radial distances away from the textiles to determine their radius of influence, as well as vertically throughout the tank to create a saturation profile.

Throughout all of the tank experiments, the maximum amount of water recorded in the layers above the tailings (in the coarse- and fine-grained sand layers) was 0.1%. This indicates that water loss within the tailings layers succesfully moved to the surface (due to gravity, evaporation, or via the geotextile strips) and was not retained by the coarser layers. During both rounds of testing, the wicking geotextile tanks had greater amounts of water mass loss than either of the controls or the non-wicking geotextile. The radial water contents for each of the tank experiments is displayed in figure A.7. Generally, the water content samples taken nearest to the geotextile strips had the lowest amonts of water and the outermost edge samples had the greatest, but this generalization does not apply to all the tanks. The single-layered wicking geotextile 2 is signficantly more dewatered than the other two tanks and this is clearly defined by the contrast of browns seen in the schematic. The double-layered tanks show less dramatic differences in water contents between the control and wicking geotextiles.

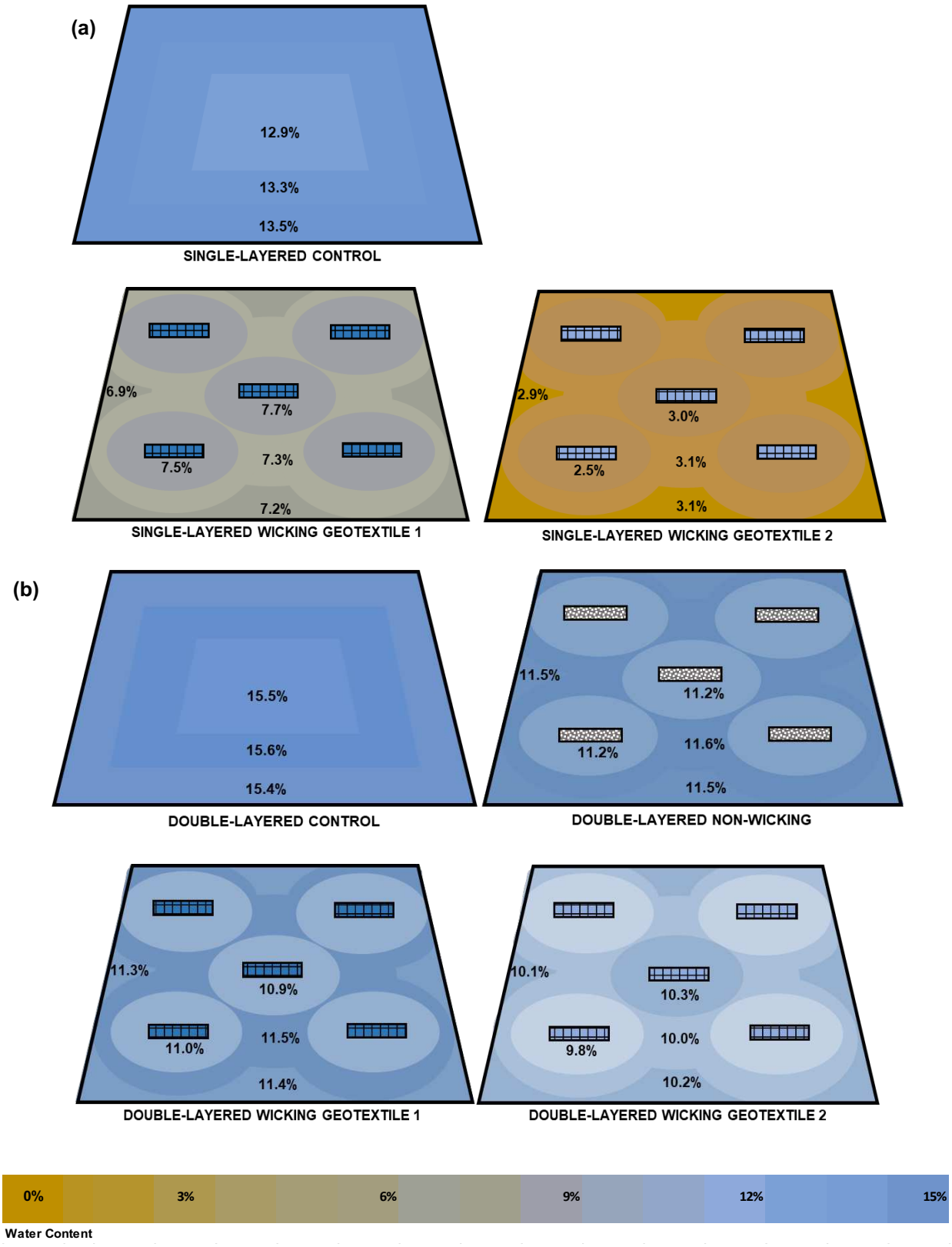

Figure A.7 - Tank concept experiment radial water contents for (a) single-layered and (b) double-layered stratigraphies.

A.3 DISCUSSION AND CONCLUSIONS

The wicking geotextiles effectively removed more water mass than the control and non-wicking tanks in both the single-layered and double-layered experiments. In Figures A.8 and A.9, the wicking geotextiles are shown surpassing the paste tailings boundary weeks before the control does. The success of the tank experiments led to the design and construction of the column experiments, as well as other index testing following test conclusion.

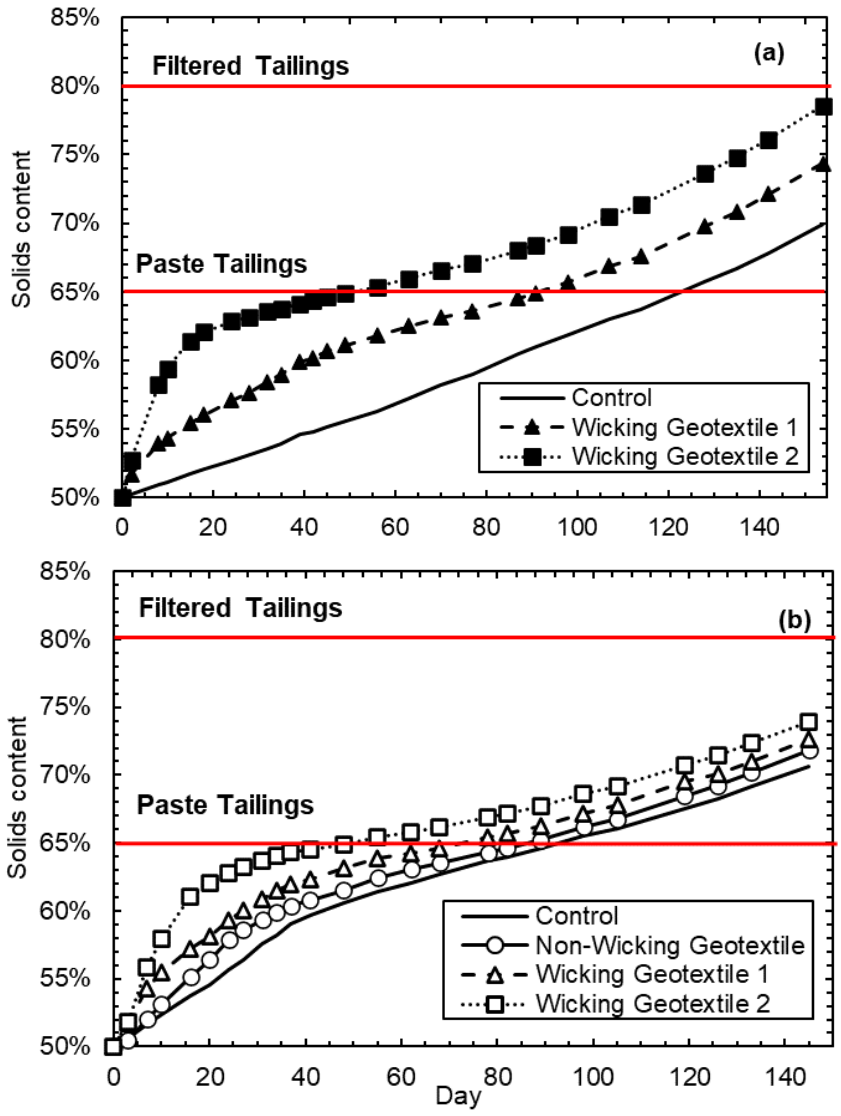

Figure A.8 - Tailings dewatering continuum boundaries on (a) single-layered and (b) double-layered solids contents plots.

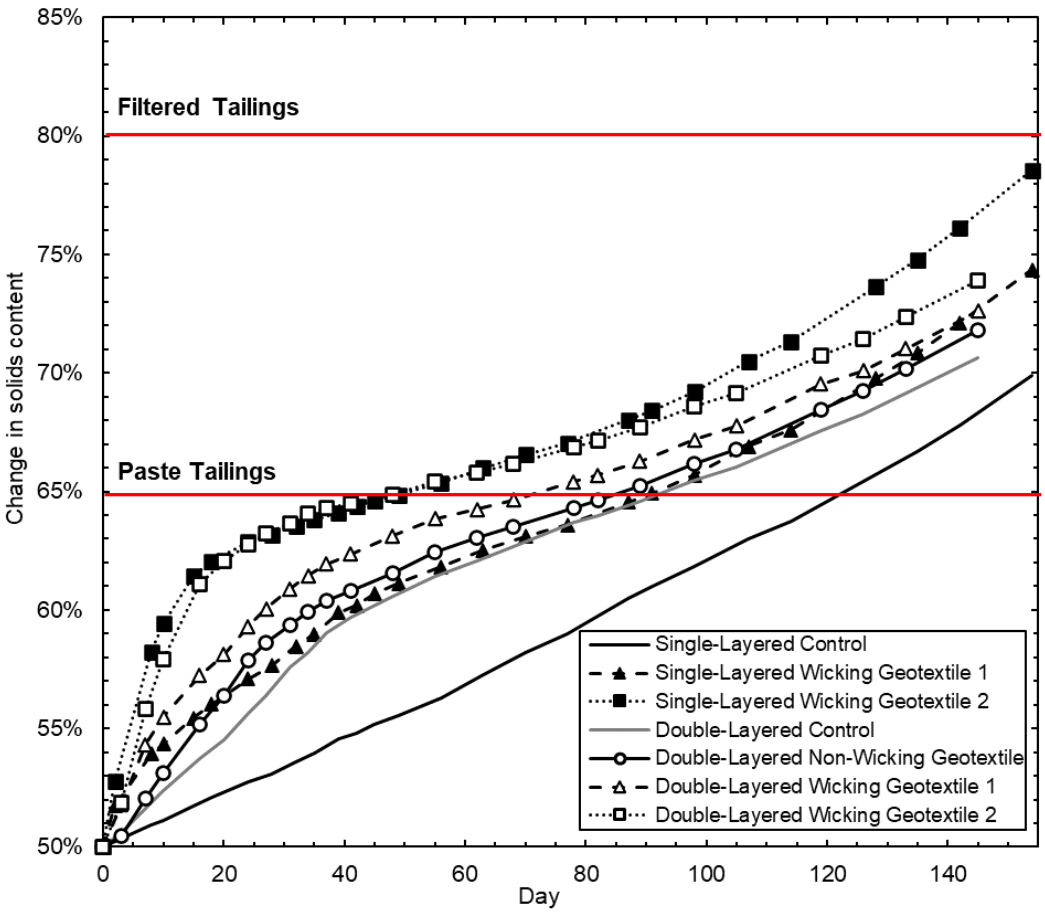

Figure A.9 - Tailings dewatering continuum boundary for all tank experiments.

The transition achieved by dewatered tailings from an undrained to drained state is a significant driver for the implementation of increased practice. Passive methods of dewatering, such as the use of PVDs or capillary geotextiles, offers the ability to retain stronger and more stable tailings with a lower cost and energy input. For legacy TSFs, where limited background is known, a safe assumption would be that there are problematic, saturated fine-grained tailings layers that would benefit from applied dewatering practices.

APPNEDIX B – PHOTO LOG

Figure B.1 - 300 mL tailings beaker experiments aerial view.

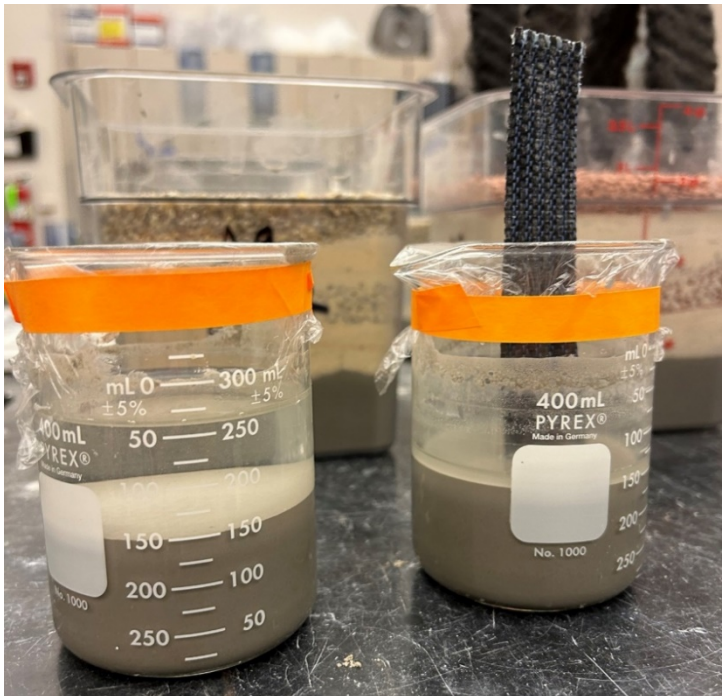

Figure B.2 – Day 17: 300 mL tailings beaker experiments control versus wicking geotextile 1 dewatering visual update.

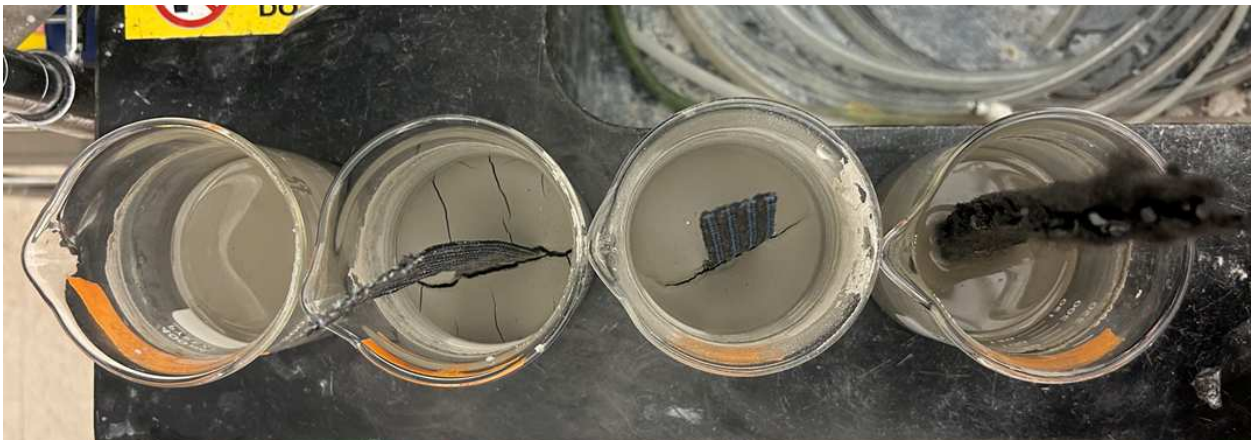

Figure B.3 - Day 24: 300 mL tailings beaker experiments dewatering and desiccation visual update. Left to right: control, wicking geotextile 2, wicking geotextile 1, and non-wicking geotextile.

Figure B.4 - Setting up the tailings column experiments and visually observing immediate drain down into the lower fines layer.

Figure B.5 - Sample collection series from various depths of deconstructed tailings column.

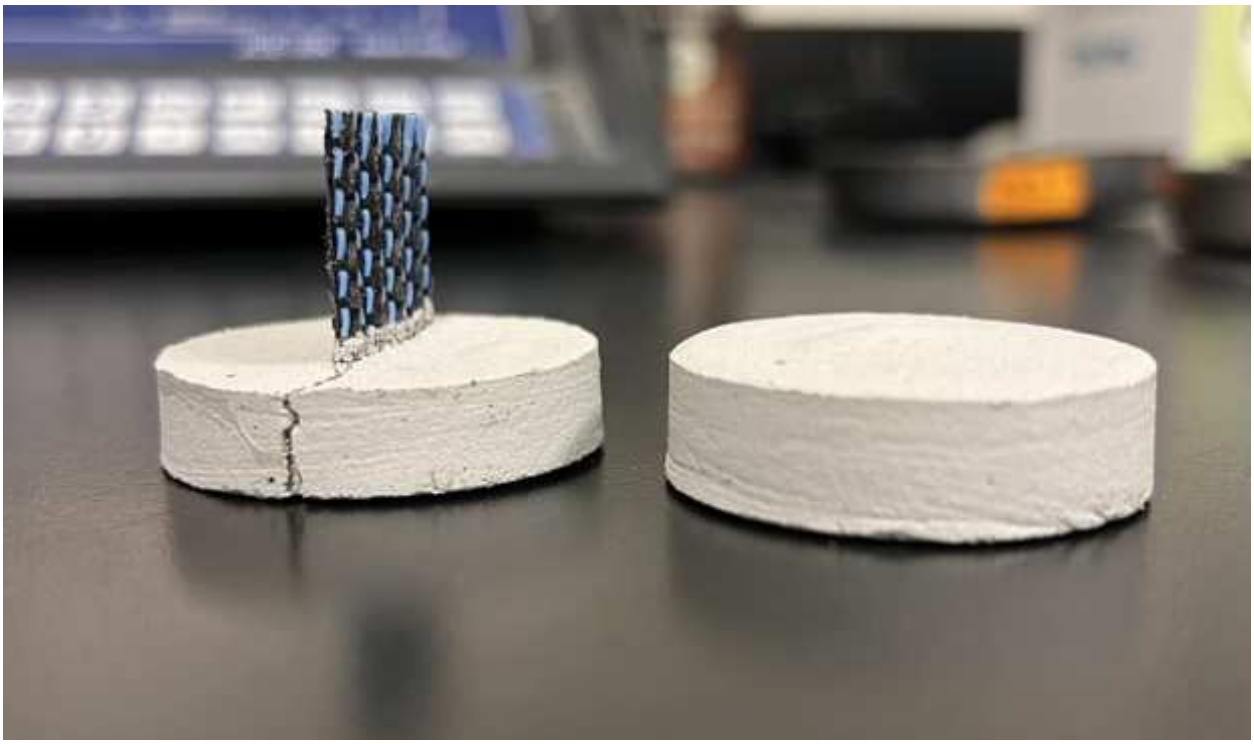

Figure B.6 - Frontal observation of dried tailings control and wicking geotextile 2 pucks from shrinkage testing.

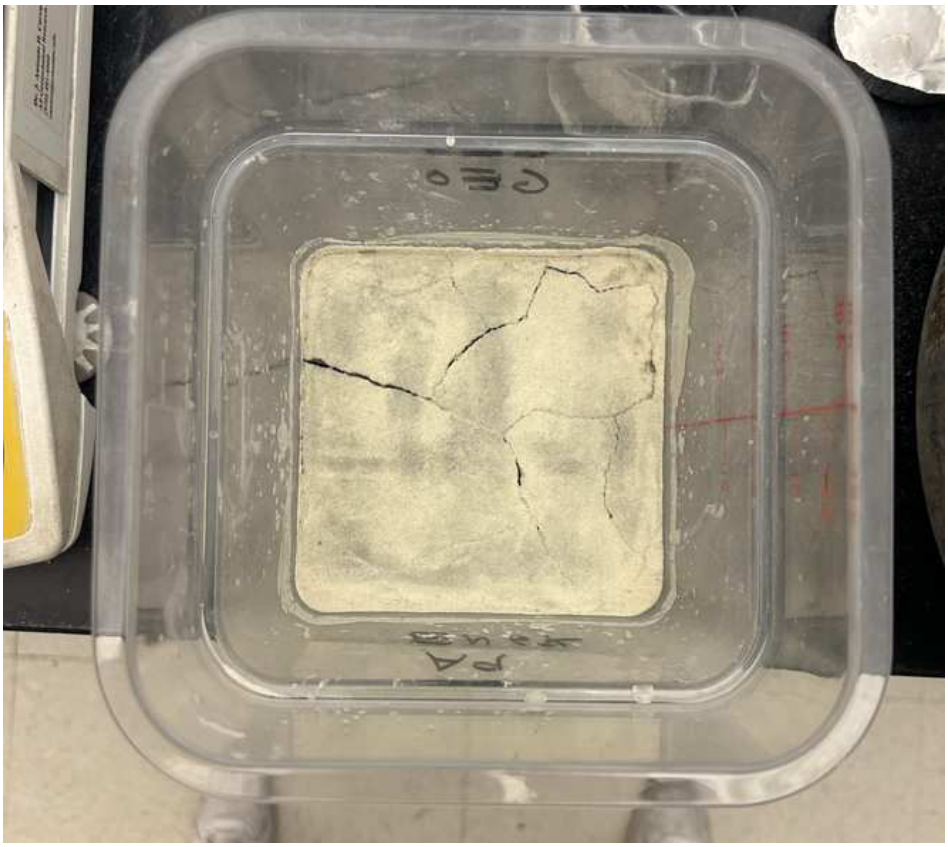

Figure B.7 - Desiccation cracking patterns in control tailings layer underlying fines during deconstruction.

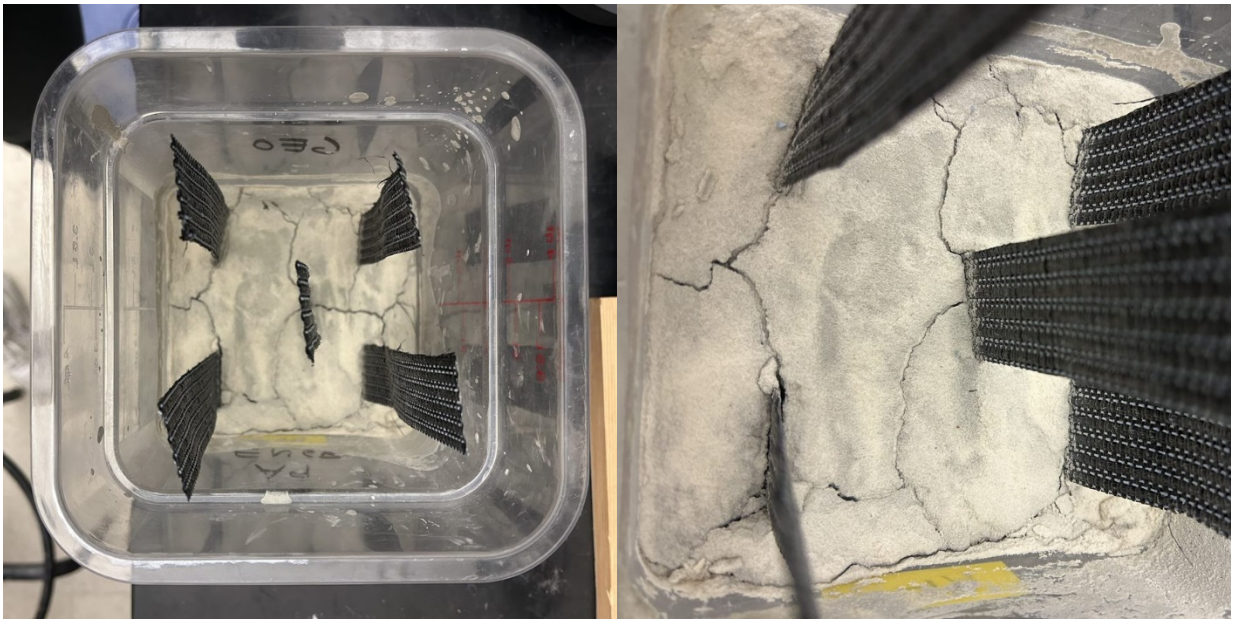

Figure B.8 - Desiccation cracking patterns in wicking geotextile 1 tailings layer underlying fines during deconstruction.

Figure B.9 – Deconstructed tank experiments tailings samples.

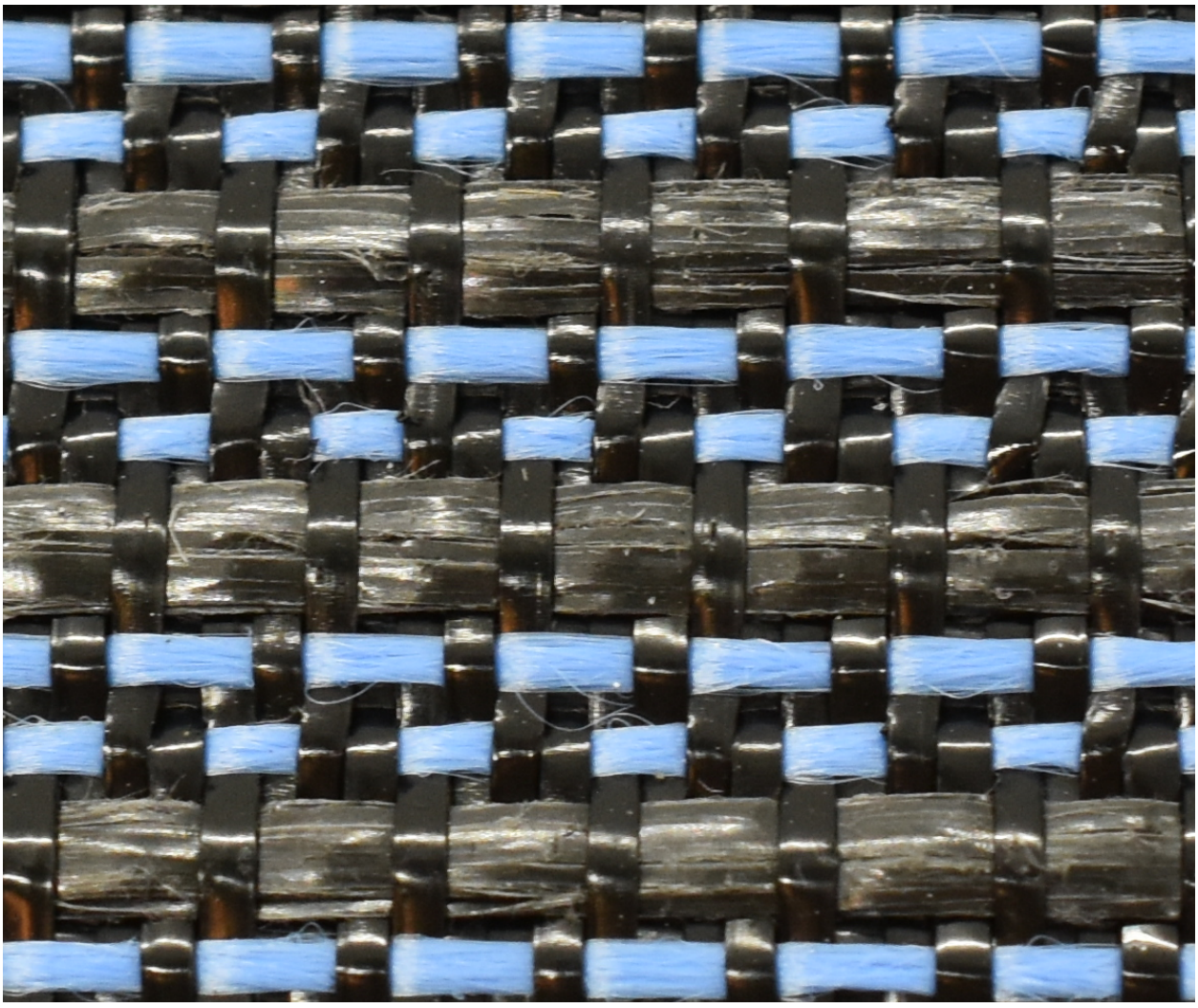

Figure B.10 – Zoomed in aerial view of wicking geotextile 2 fibers.

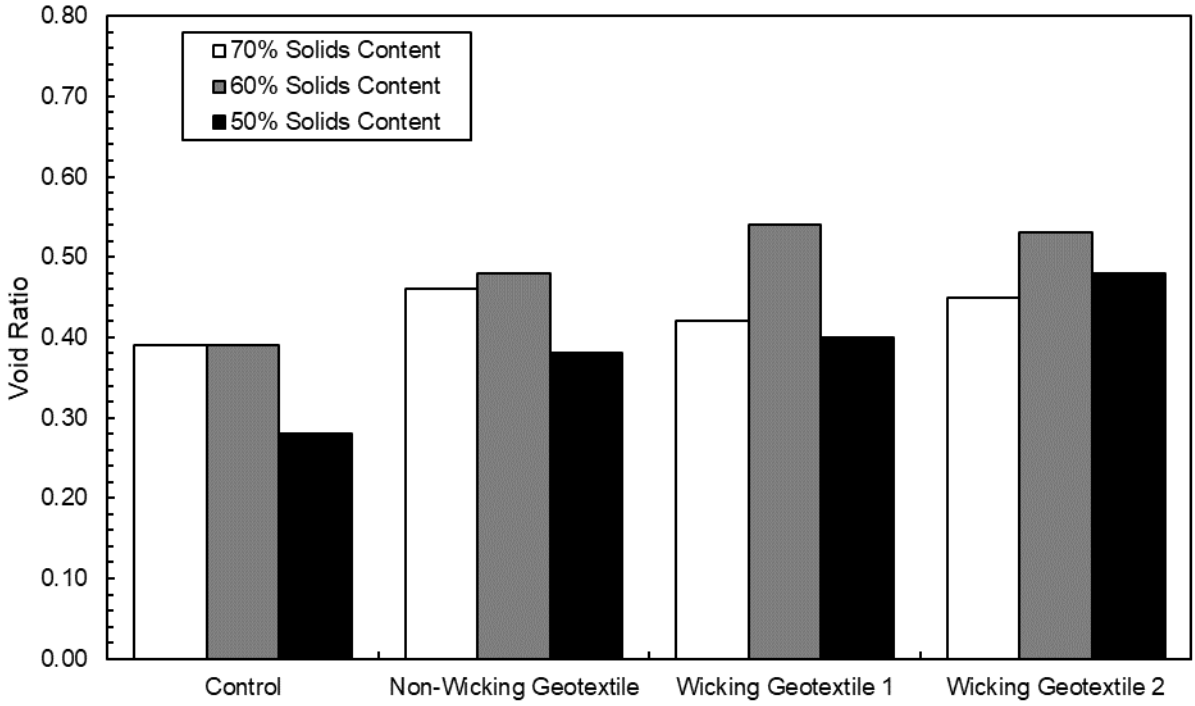

Figure C.1 – Shrinkage ring final averaged void ratios.